Fatigue Analysis of Flexible Riser - Effect of Mean Stress Correction Procedures

Boyang Zhao

Fatigue analysis of Flexible Riser – effect of mean stress correction procedures

Master Thesis   SPRING 2013

Boyang Zhao

6/10/2013

PREFACE

This thesis is for the Master of Science degree in Norwegian University of Science and Technology (NTNU). The Duration of thesis work is about 5 months.

Through this thesis work, basic concepts of flexible pipes are introduced. Plenty of Finite Element Analysis with BFLEX 2010 and RFLEX is finished. The different methods for getting the mean stress correction are compared with each other after doing the fatigue analysis.

I would like to express my sincere gratitude to my supervisor Svein Sævik. Without his advice and unique support this thesis would never had become a reality. Further I would like to thank Mr. Naiquan Ye in MARINTEK for this help on BFLEX and Rui Zhang for helping with the MATLAB to deal with the data.

Boyang Zhao

June 10th, 2013

Trondheim, Norway

Abstract

As the critical part of the oil product system, flexible riser's fatigue life during the normal operating service is more and more significant. Finding the most dangerous point in the flexible riser and using the accurate enough method to do the fatigue analysis are both critical for the safety of the whole riser system. In order to find the critical point's position and lifetime, we execute the dynamic analysis and fatigue analysis on the flexible riser, utilizing the finite element analysis software RIFLEX and BFLEX2010, developed by MARINTEK, in this master thesis.

Chapter 1 shows the literature study on the riser's structure and method's background introduction including the static analysis, dynamic analysis, fatigue analysis, effect of the mean stress and bending curvature. Chapter 2 introduce the mainly structure of the software RFLEX and BFLEX2010. It tells the function and responsibility in this thesis. Chapter 3 has defined the case situation and method to do the whole analytical process. Chapter 4 shows the curvature time series result of the static and dynamic analysis with the RFLEX. The result of rain flow counting process and the fatigue analysis with the BFLEX2010 has been got in Chapter 5. The fatigue damage is given with the formulation as Miner Sum. Chapter 7 has showing the conclusion for the whole thesis. It tells the different methods to do the fatigue analysis with both linear and nonlinear material by comparing the fatigue damage or lifetime. The thesis focuses on the process to finding the dangerous point in the special layer of the flexible riser and the different mean stress correction procedures' influence on calculating the fatigue damage for this dangerous point.

List of symbols

D	Outer diameter
r	Displacement vector
σ	Stress tensor
S	Displacement field
$\sigma_{xx}, \sigma_{yy}, \sigma_{zz}$	Stress along x,y,z axial
Δt	Time increment
$PVDF$	Poly vinylidene floride
$HDPE$	High density polyethylene
$XLPE$	Cross-linked polyethylene
VIV	Vortex induced vibration
n_i	Number of cycle
N_i	Number of cycle to damage
C	Miner Sum
ΔK	The cyclical component
a	Crack length
E_T	tangent modulus
E_S	secant modulus
f_m	Reduction factor

CONTENT

1 Literature study

In this chapter, some useful background knowledge is included. The purpose of this chapter is to show the history of the risers or the pipeline's development. Also some relevant knowledge for the FPS should be included since it is the foundation of the pipeline. What's more, the detail structure, which mainly is the different layers of the flexible risers, is introduced.

1.1 Riser technology

With the development of the technology, the utilized of the flexible is all over the world. And the Gulf of Mexico and North Sea are the mainly place where the flexible riser is used. As the most relatively product in the oil and gas field for subsea technology, it is carried out in 1970s first time. Through 1990s, the concept of Floating Production Systems (FPS) was developed and implemented as a very cost effective way of exploiting offshore oil and gas resources. When the offshore industry approaches deeper water, there are no alternatives due to the large motion of the platform. For marginal fields, the engineering cost may be significantly reduced by using FPS instead of traditional fixed platforms. A floating production system with flexible pipe system is shown in figure 1.
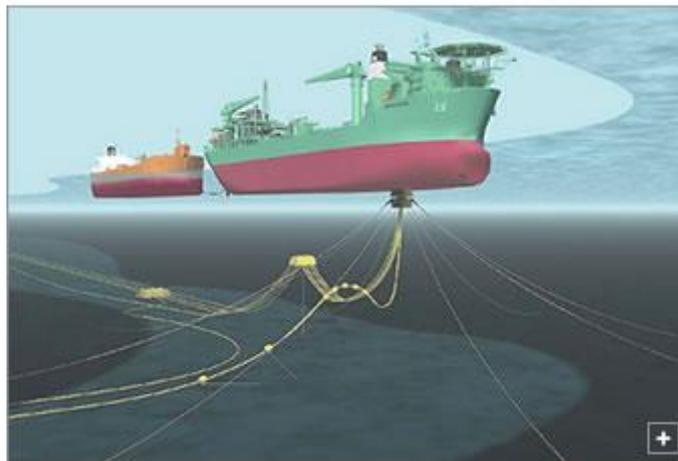
Figure 1-1 Floating Production Systems (FPS)

The flexible pipe system plays a very important and dominant role in FPS. If the flexible pipe fails, the whole system would fail. Flexible pipes connected to the top floater could allow large floater motions induced by wind, current and wave. [I]

[I] http://www.flexirisertest.com/

1.2 Flexible riser's structure in detail

1.2.1 Different layers' structure

However, the most different property to figure out the flexible pipe is the bending moment inside the different of layers of the pipeline. This is achieved through the use of a number of layers of different material in the pipe wall fabrication. These layers are capable of slipping past each other when they are under the influence of external and internal loads.1. The name of different layers in flexible riser is listed in the figure 1-2.
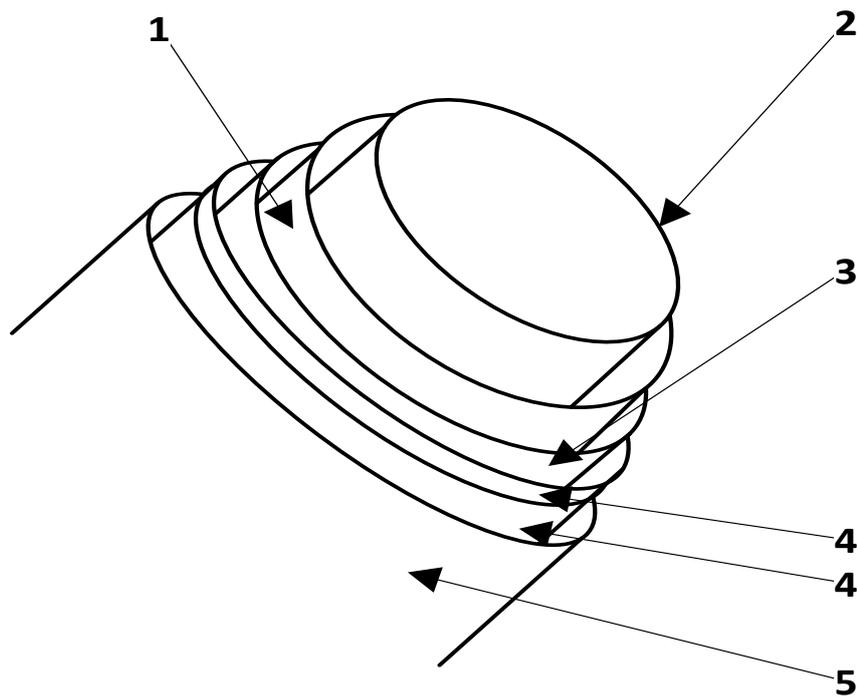
Figure 1-2 Different layers of the flexible riser

1. *Interlocked stainless steel carcass*

2. *Internal pressure sheath*

3. *Zeta spiral (pressure armor)*

4. *Tensile armor (double cross wound armors)*

5. *Outer thermoplastic sheath*

1.2.2 Function and material

1.2.2.1 Zeta pressure spiral / flat spiral

Zeta layer is the most important section in this thesis and should be investigated deeply. The main role of pressure armor is to withstand the stress in the hoop direction which is caused by the internal fluid pressure. The Zeta pressure armor is made of Z-shaped interlocking wires. These wire profiles

allow bending flexibility and control the gap between the armor wires to prevent internal sheath extrusion through the armor layer. It will also provide resistance against external pressure and crushing effects from the tensile armor. In order to best resist the hoop stress in the pipe wall, the pressure armor is wound at an angle of about 89 degree to the pipe longitudinal axis. And the material of pressure armor is rolled carbon steel with tensile strength in the range of 700 – 900 Mpa. Other different profiles of pressure armor are also used in engineering, such as C-clip, Theta shaped pressure armor, X-LiNkt and K-LiNKT, etc. In case of need, in order to satisfy certain operation requirements in engineering, the zeta layer may be reinforced by a flat steel spiral.

In this report, zeta layer is mainly studied to do the fatigue analysis.

1.2.2.2 The layer of the tensile armor

The tensile armor layers are always cross-wound in pairs. As its names implies, the tensile armor layers provide resistance to axial loads and torsion. Most of time, the tensile armor layers are made of flat rectangular wires, which are laid at about 30 °- 55 ° to the longitudinal axis along the flexible riser.

1.2.2.3 The layer of the interlocked carcass

The function of the carcass, as the layer which is inside the pipe to be the first layer, is to direct contact with the fluid in the bore in order to provide the resistance strength against the external hydrostatic pressure. It is made of a stainless steel flat strip that is formed into an interlocking profile .The fluid in the bore is free to flow through the carcass.

1.2.2.4 The layer of the internal pressure sheath

The function of the sheath layer is to provide internal fluid integrity as an extruded polymer layer. So it is used as sealing component, made from a thermoplastic by extrusion over the carcass. The main function is to ensure integrity and sealing. The fluid temperature in the bore is guaranteed by this layer.

- *Polyamid (nylon), PA11 or PA 22*

- *Poly vinylidene floride (PVDF)*

- *High density polyethylene (HDPE) and cross-linked polyethylene (XLPE)*

1.2.2.5 External thermal plastic layer / outer sheath

This is a layer that we could see directly from the outside of flexible riser. It is also called outer sheath. The function of the external thermoplastic layer is to protect the metallic layers against corrosion, abrasion and bind the underlying armor. Also it could separate the steel components and the sea water.

1.2.2.6 Other Layers and Configurations

Flexible pipes could be different with each other, due to the different operation fields. There are still some other layers, just as figure 1-3 shows.

Outer sheath

Outer layer of tensile armor

Anti-wear layer

Inner layer of tensile armor

Anti-wear layer

Back-up pressure armor

Interlocked pressure armor

Internal pressure sheath

carcass
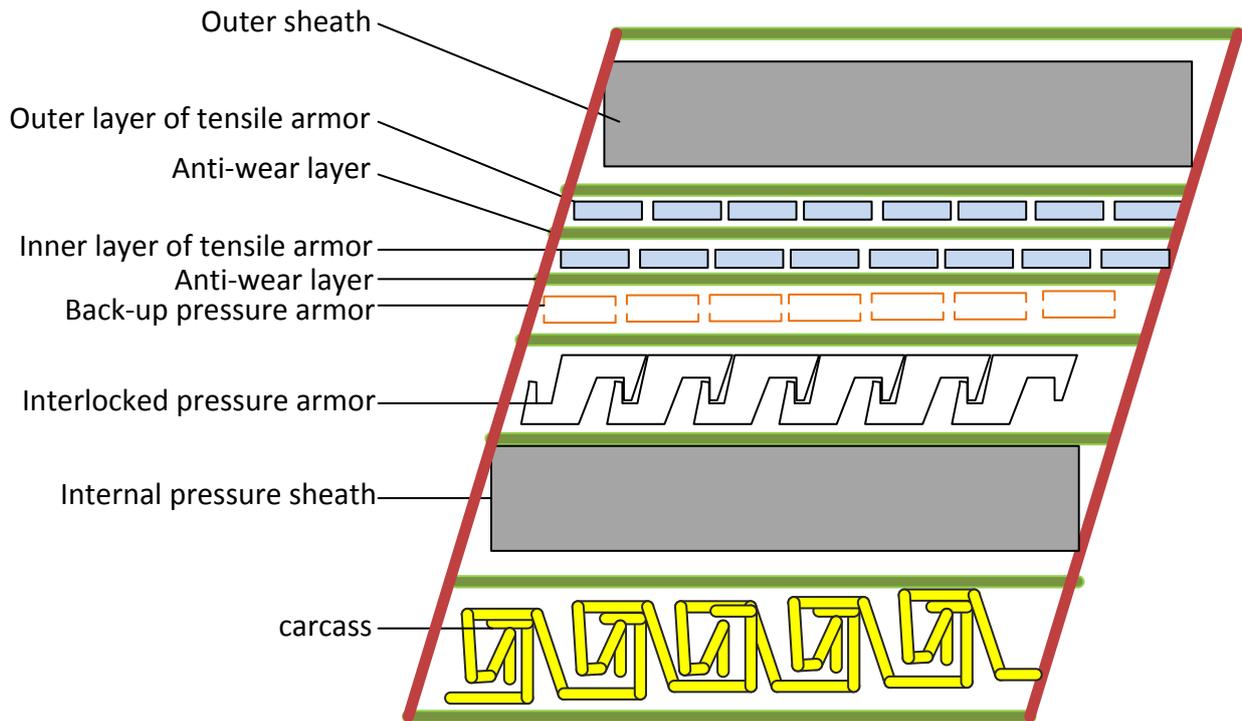
Figure 1-3 Flexible pipeline wall structure

We could see there are several anti-wear layers in figure1-3, for example the anti-wear layer between two tensile armor layers, and the anti-wear layer between inner layer of tensile armor and back-up pressure armor. The purpose of anti-wear layer is to reduce friction and hence wear of the wire layers when they rub past each other as the pipe flexes due to external loads. These tapes ensure that the wires do not twist out of their pre-set configuration. But there exists no anti-wear layer between zeta pressure armor and back-up pressure armor (flat spiral). This is due to the large contact pressure and shear force between these two layers. In fact, if we put the anti-wear layers between them, it would crack very fast. So the anti-wear layers are very important when doing the analysis of fracture.

1.3 Global analysis for both static and dynamic

1.3.1 Static finite element analysis

1.3.1.1 General

The state of the discretized finite element model is completely determined by the nodal displacement vector. The purpose of the static analysis is to determine the nodal displacement vector so that the complete system is in static equilibrium. The static equilibrium configuration is therefore found as the solution of the following system of equations

$$R^s(r) = R^E(r) \tag{1}$$

Where

r: Nodal displacement vector including all degrees of freedom for the system i.e. displacements for a bar model and displacements and rotations for a beam model. Both displacements and rotations are relative to the stress free reference configuration.

$R^s(r)$: Internal structural reaction force vector found by assembly of element contributions. Possible contact forces are also treated as internal reaction forces.

$R^E(r)$: External force vector accounting for specified external forces, rigid body forces for representation of buoys, clump weights etc. and contribution from distributed loading (i.e. weight, buoyancy and current forces) assembled from all elements.[I]

1.3.1.2 Finite element equilibrium iterations

In static analysis it is convenient to distinguish between the following basic load types:

1) Volume forces (weight and buoyancy)

2) Specified displacements (i.e. displacements from stress free configuration to final position of nodal points with specified boundary conditions)

3) Specified forces (nodal point loads)

4) Position dependent forces (current forces)

The incremental loading procedure starting from stress free configuration is organized in a sequence of load conditions where each load condition consists of one or more of the basic load types. Each load condition is applied in a specified (e.g. used defined) number of load increments.[II]

[I] RIFLEX_TheoryManual_40_rev0. Page 1 of 12.

[II] RIFLEX_TheoryManual_40_rev0. Page 5 of 12.

1.3.2 **Dynamic time domain analysis**

1.3.2.1 *General*

The dynamic equilibrium of a spatial discretized finite element system model can in general be expressed as

$$R^I(r, \ddot{r}, t) + R^D(r, \ddot{r}, t) + R^s(r, t) = R^E(r, \dot{r}, t) \tag{2}$$

Where

R^I : Inertia force vector

R^D : Damping force vector

R^s : Internal structural reaction force vector

R^E : External force vector

$r, \dot{r}, \ddot{r}$: Structural displacement, velocity and acceleration vectors.

This is a nonlinear system of differential equations due to the displacement dependencies in the inertia and the damping forces and the coupling between the external load vector and structural displacement and velocity. All force vectors are established by assembly of element contributions and specified discrete nodal forces.

1.3.2.2 *Nonlinear time domain analysis*

Step by step numerical integration of the incremental dynamic equilibrium equations, with a Newton-Raphson type of equilibrium iteration at each time step. This approach allows for a proper treatment of all the described nonlinearities. Nonlinear dynamic analysis is, however, rather time consuming due to repeated assembly of system matrices (mass, damping and stiffness) and triangularisation during the iteration process at each time step.

1.3.3 **Methods for numerical time integration**

The step by step numerical integration of the dynamic equilibrium equations is based on the well known Newmark ß-family including the Wilson θ method considering a constant time step throughout the analysis. Both methods can be applied for nonlinear as well as linearized analysis. These methods apply the following relations between displacements, velocity and acceleration vectors at time t and t+Δt:

$$\dot{r}_{t+\Delta\tau} = \dot{r}_t + (1 - \gamma)\ddot{r}_t\Delta\tau + \gamma\ddot{r}_{t+\Delta\tau}\Delta\tau \tag{3}$$

$$r_{t+\Delta\tau} = r_t + \dot{r}_t\Delta\tau + \left(\frac{1}{2} - \gamma\right)\ddot{r}_t(\Delta\tau)^2 + \beta\ddot{r}_{t+\Delta\tau}(\Delta\tau)^2 \tag{4}$$

where Δτ=θΔ, θ≥1.0

γ, β and θ are parameters in the integration methods defining the functional change in displacement, velocity and acceleration vectors over the time step Δt.[I]

1.4 Fatigue analysis

1.4.1 Failure modes

There were many kinds of fatigue failure modes for the risers. Although different loads were introduced into the damage, we mainly care about the causes of the loads. We can classify the causes into nine items based on the causes as below

- *First order wave loading (wave frequency)*

- *Second order floater motion due to wind, wave and current*

- *Vortex induced vibration (VIV)*

- *Floater vortex induced motion (VIM)*

- *Floater vertical heave induced vibration (HVIV)*

- *Installation fatigue damage*

- *Slugging loads*

- *Transportation*

- *Start up and shut down*

It should be noticed that the first order wave loading was the most significant load contributing to reducing the fatigue life of the risers. After construction of the risers, the loads during transportation and installation should be cared. However, it is difficult to recognize all the loads from the environment easily.
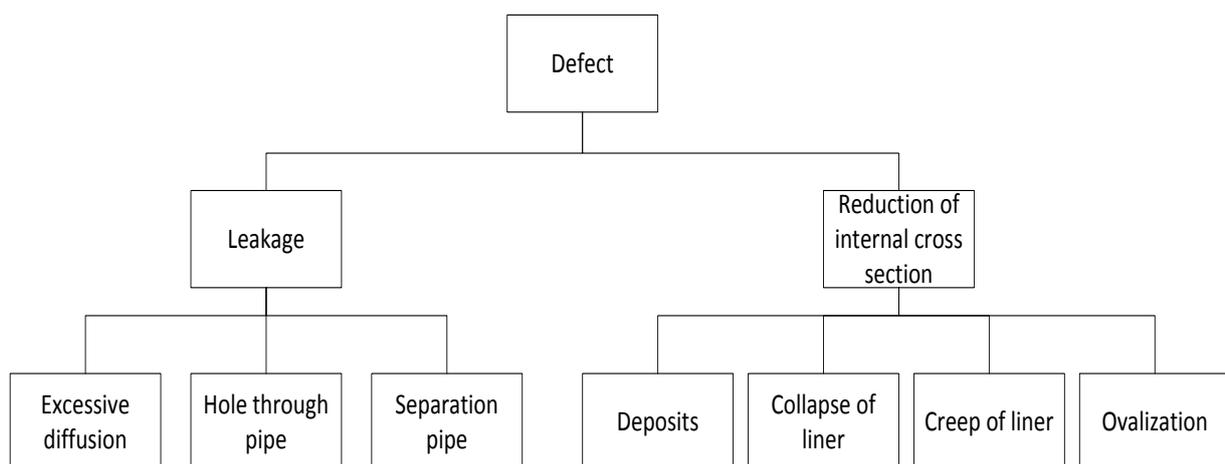
Figure 1-4 Main failure tree for flexible riser

[I] RIFLEX_TheoryManual_40_rev0. Page 3 of 12.

1.4.2 The methods to estimate the lifetime of the riser

It is well known that the estimation of the lifetime of the riser is a difficult question to be figured out because there are so many kinds of loads leading to the damage of the risers. During the period of designing, the S-N curve should be introduced based on the rules to get the fatigue lifetime in a range as small as possible. Then the fatigue test should be done using the real one for a long testing time. Based on the different rules, several of SN curves could be chose whereas the result should be the same more or less.

1.4.3 Miner theory

In 1945, M. A. Miner popularized a rule that had first been proposed by A. Palmgren in 1924. The rule, variously called Miner's rule or the Palmgren-Miner linear damage hypothesis, states that where there are k different stress magnitudes in a spectrum, S_i ($1 \leq i \leq k$), each contributing $n_i(S_i)$ cycles, then if $N_i(S_i)$ is the number of cycles to failure of a constant stress reversal Si, failure occurs when:

$$\sum_{i=1}^{k} \frac{n_i}{N_i} = C \qquad (5)$$

C is experimentally found to be between 0.7 and 2.2. Usually for design purposes, C is assumed to be 1.This can be thought of as assessing what proportion of life is consumed by stress reversal at each magnitude then forming a linear combination of their aggregate. Though Miner's rule is a useful approximation in many circumstances, it has several major limitations:

- *It fails to recognize the probabilistic nature of fatigue and there is no simple way to relate life predicted by the rule with the characteristics of a probability distribution. Industry analysts often use design curves, adjusted to account for scatter, to calculate Ni(Si).*

- *There is sometimes an effect in the order in which the reversals occur. In some circumstances, cycles of low stress followed by high stress cause more damage than would be predicted by the rule. It does not consider the effect of overload or high stress which may result in a compressive residual stress. High stress followed by low stress may have less damage due to the presence of compressive residual stress.*

1.4.4 Paris' Relationship

In Fracture mechanics, Anderson, Gomez and Paris derived relationships for the stage II crack growth with cycles N, in terms of the cyclical component ΔK of the Stress Intensity Factor K2

$$\frac{da}{dN} = C(\Delta K)^m \qquad (6)$$

Where a is the crack length and m is typically in the range 3 to 5 (for metals).

This relationship was later modified (by Forman, 1967[3]) to make better allowance for the mean stress, by introducing a factor depending on (1-R) where R = min stress/max stress, in the denominator.

1.4.5 Goodman and Gerber

In the presence of stresses superimposed on the cyclic loading, the Goodman relation can be used to estimate a failure condition. It plots stress amplitude against mean stress with the fatigue limit and the ultimate tensile strength of the material as the two extremes. Alternative failure criteria include Soderberg and Gerber.[7]

1.5 Rain flow counting

The rain flow counting method, which is also known as the rain flow counting algorithm, is useful in the analysis of fatigue data in order to reduce a spectrum of varying stress into a set of simple stress reversals. During this report, the rain flow counting method is used to recognize the cycle number, range of the amplitude and mean stress. It could be thought that it is also valid and available for analysis the time series of curvature and axial tensile forcing on one point along the flexible riser in one sea state. Its importance is that it allows the application of Miner's rule in order to assess the fatigue life of a structure subject to complex loading. During the analysis of the Bflex2010, it could be seen that the fatigue analysis is based on the Miner sum to get the fatigue life of the riser or some particular part of the flexible riser. So this method is available for both the post dynamic time domain analysis and after post fatigue analysis. The algorithm was developed by Tatsuo Endo and M.Matsuishi in 1968. Though there are a number of cycle-counting algorithms for such applications, the rain flow method is the most popular as from 2008 to now.

The algorithm has the following properties:

1. Reduce the time history to a sequence of (tensile) peaks and (compressive) troughs.

2. Imagine that the time history is a template for a rigid sheet (pagoda roof).

3. Turn the sheet clockwise 90 ° (earliest time to the top).

4. Each *tensile peak* is imagined as a source of water that "drips" down the pagoda.

5. Count the number of half-cycles by looking for terminations in the flow occurring when either:

   ● It reaches the end of the time history

   ● It merges with a flow that started at an earlier *tensile peak*

   ● It flows opposite a *tensile peak* of greater magnitude.

6. Repeat step 5 for *compressive troughs*.

7. Assign a magnitude to each half-cycle equal to the stress difference between its start and termination.

8. Pair up half-cycles of identical magnitude (but opposite sense) to count the number of complete cycles. Typically, there are some residual half-cycles.

Advantages for rain flow counting

1. **Fast Counting**

Fast counting is used when the fatigue study refers to one static study and has only one variable-amplitude event. In this case, the program extracts bins directly from the original record. It then evaluates the damage resulting from each bin at each node and calculates the accumulative damage.

2. **Full Analysis**

When multiple variable-amplitude events are used, the program calculates the stresses at each point in time for each variable-amplitude record at every node. At each node, the program combines the stresses and extracts the Rain flow bins that are then used to evaluate the damage.

Full analysis is also used when a variable amplitude record is associated with more than one study with the different shifts or intervals.[I]

1.6 Excessive bending curvature

When the pipe is subjected to bending, failure may occur in various modes. Buckling capacity may be reduced considerably due to the vocalization of the cross-section. Helices may be overlapped on the compressive side of the pipe that leads to an increase in the pipe stiffness. Excessive gaps between helices on the tensile side may, on the other hand, result in permanent deformation of the plastic sheath in bonded pipes, and extrusion of elastomeric out of the helix layer that corresponds to disbandment in bonded pipes. In general, the failure criterion is based on the bending radius R and follows

$$R - R_{MBR} \leq 0 \tag{7}$$

The minimum bending radius (MBR), R_{MBR}, should account for all the individual MBR values corresponding to each failure mode caused by the excessive bending curvature, and may be further expressed as

$$R_{MBR} = \min(MBR_1, MBR_2 \dots \dots MBR_i) \tag{8}$$

This is a complicated strength parameter and is subject to large model uncertainty. The failure function is generally expressed as

$$g(x) = B_R R - B_{MBR} R_{MBR} \leq 0 \tag{9}$$

AS the curvature Ks = 1/R is related to the bending moment MB by

$$k = \frac{M_B}{EI} \tag{10}$$

[I] http://help.solidworks.com/2012/English/SolidWorks/cworks/Rainflow_Cycle_Counting_Method.htm?id=bdf69c6adda14fa9b8c95ab53f8048a0#Pg0

Different contributions from the functional and environmental load effects can be separated when the failure function is expressed in terms of the curvature

$$g(x) = \frac{1}{B_{MBR}R_{MBR}} - B_{k_E}k_E - B_{k_F}k_F \leq 0 \tag{11}$$

The uncertainty measure for k is

$$B_k = \frac{B_{M_B}}{B_E B_I} \tag{12}$$

1.7 Non-linear finite element techniques introduction

1.7.1 Geometry nonlinear

The geometry nonlinear is a geometry relationship of the structure itself. It could be illustrated in many methods. For structure designing, the stiffness of the structure should be considered. Furthermore, if the structure is a vessel or a riser, the stiffness of the elements, which consist of the whole structure, should be considered for the whole part. For the finite element method, the nodes' or elements' stiffness matrix should be induced to be set as owning nonlinear geometry property. According to the distribution and type of the mesh, the super element and substructure should be considered to modify the result more accurately.

1.7.2 Material nonlinear

The material nonlinear is the property of the material itself. After the yield stress of the material is exceeded, the relationship of the stress and strain is changed as the increase of the stress, which means the stress has it proportionality limit. Usually it is illustrated by Young's modulus. It is changed

To deal with nonlinear material properties, the tangent modulus should be considered.
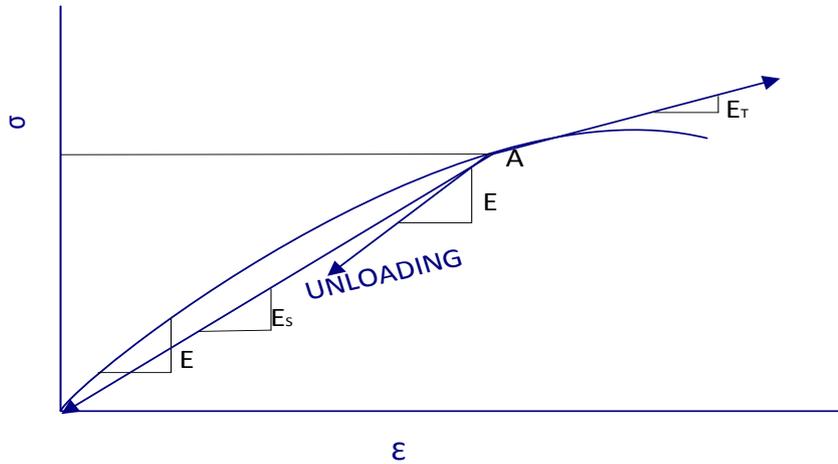
Figure 1-5 Definitions of material properties.

E$_S$ is the *secant modulus*, which depends upon the stress (strain) level. When *loading* is introduced at A, the change of stress, ET can be obtained. ET is the *tangent modulus*.

By *unloading* from A Hooke's law applies:

$$\Delta\sigma = E\Delta\varepsilon (\text{UNLOADING}) \tag{13}$$

The nonlinear property of the material is used in this report.[4]

1.8 Effect of Mean stress correction in BFLEX2010

If part of the stress is in the static of compression, the stress range may be reduced in a relative scale. In order to do the fatigue analysis of the local place of the material, which may not influenced by the residual stress, the reduction is able to be carried out for cut-outs in the base material. The calculated stress range obtained may be multiplied by the reduction factor f$_m$ as obtained from the figure below before carrying on the S-N curve.

The reduction factor can be derived from the following equation[5]

$$f_m = \frac{\sigma_t + 0.6\sigma_c}{\sigma_t + \sigma_c} \tag{14}$$

Where

$$\sigma_t = \text{maximum tension stress}$$

$$\sigma_c = \text{maximum compression stress}$$
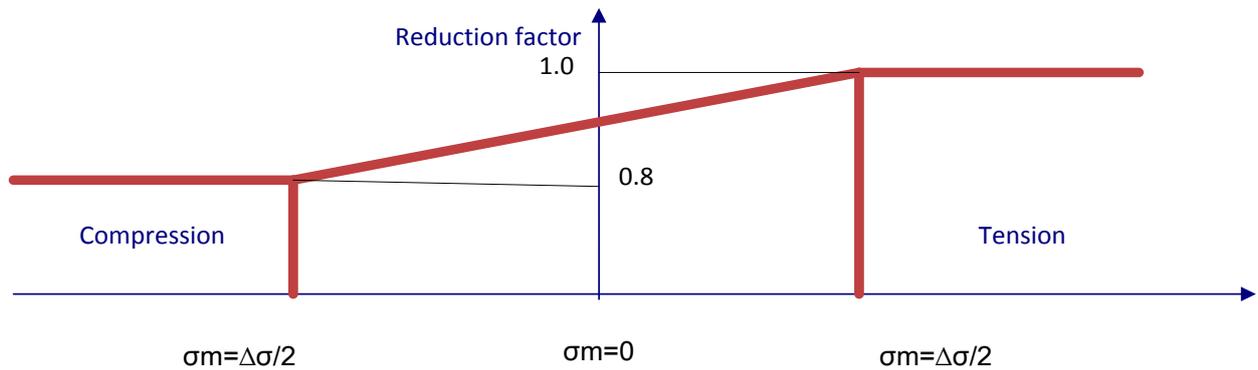
Figure 1-6 Reduction factor

There are eleven methods to calculate the correction of the mean stress as below and the methods for taking the mean stress into account for longitudinal failure mode.

The mean stress correction code is showing in the following

0. No mean stress is taken into account. Stress range calculated considering longitudinal stress range for tensile armor, von Mises for pressure armor.

1. Goodman interpolation mean stress calculated as $\sigma_{xx} + \sigma_{yy} + \sigma_{zz}$ where

    σ_{yy} and σ_{zz} only applies for the pressure armor. Stress range calculated considering longitudinal stress range for tensile armor, von Mises for pressure armor.

2. Gerber interpolation mean stress calculated $\sigma_{xx} + \sigma_{yy} + \sigma_{zz}$ where σ_{yy} and σ_{zz}

    only applies for the pressure armor. Stress range calculated considering longitudinal stress range for tensile armor, von Mises for pressure armor.

3. Goodman interpolation mean stress calculated

    as$\bar{\sigma} = \sqrt{\sigma_{xx}^2 + \sigma_{yy}^2 + \sigma_{zz}^2 - \sigma_{xx}\sigma_{yy} - \sigma_{yy}\sigma_{zz} - \sigma_{zz}\sigma_{xx} + 3\sigma_{xy}^2 + 3\sigma_{yz}^2 + 3\sigma_{xz}^2}$. For

    tensile armor only σ_{xx} applies. Stress range calculated considering longitudinal stress range for tensile armor, von Mises for pressure armor.

4. Gerber interpolation mean stress calculated

    as$\bar{\sigma} = \sqrt{\sigma_{xx}^2 + \sigma_{yy}^2 + \sigma_{zz}^2 - \sigma_{xx}\sigma_{yy} - \sigma_{yy}\sigma_{zz} - \sigma_{zz}\sigma_{xx} + 3\sigma_{xy}^2 + 3\sigma_{yz}^2 + 3\sigma_{xz}^2}$. For

    tensile armor onlyσ_{xx} applies. Stress range calculated considering longitudinal stress range for tensile armor, von Mises for pressure armor.

5. Only valid for pressure armor. Goodman interpolation mean stress calculated as the mean principal stresses in two directions Principle stress ranges calculated for the same directions and mean stress correction respectively applied to the two components. In the transverse direction the material is assumed to start from yield

13

stress. The two reported modes from Life- time will be different, 1= longitudinal mode, 2= transverse mode. $\Delta\sigma = \max(\Delta\sigma_j)$ and $\bar\sigma = \frac{1}{2}(\sigma_j^{max} + \sigma_j^{min}), j = 1,2$

6. Only valid for pressure armor. Gerber interpolation mean stress calculated as the mean principal stresses in two directions. Principle stress ranges calculated for the same directions and mean stress correction respectively applied to the two components. In the transverse direction the material is assumed to start from yield stress. The two reported modes from Lifetime will be different, 1= longitudinal mode, 2= transverse mode. $\Delta\sigma = \max(\Delta\sigma_j)$ and $\bar\sigma = \frac{1}{2}(\sigma_j^{max} + \sigma_j^{min}), j = 1,2$

7. Only valid for pressure armor. Goodman interpolation mean stress calculated as the Von Mises stress. Principle stress ranges calculated for the same directions and mean stress correction respectively applied to the two components. In the transverse direction the material is assumed to start from yield stress. The two reported modes from Lifetime will be different, 1= longitudinal mode, 2= transverse mode. $\Delta\sigma = \max(\Delta\sigma_j)$ and

$$\bar\sigma = \sqrt{\sigma_{xx}^2 + \sigma_{yy}^2 + \sigma_{zz}^2 - \sigma_{xx}\sigma_{yy} - \sigma_{yy}\sigma_{zz} - \sigma_{zz}\sigma_{xx} + 3\sigma_{xy}^2 + 3\sigma_{yz}^2 + 3\sigma_{xz}^2}$$

8. Only valid for pressure armor. Gerber interpolation mean stress calculated as the Von Mises stresses. Principle stress ranges calculated for the same directions and mean stress correction respectively applied to the two components. In the transverse direction the material is assumed to start from yield stress. The two reported modes from Lifetime will be different, 1= longitudinal mode, 2= transverse

mode. $\Delta\sigma = \max(\Delta\sigma_j)$ and $\bar\sigma =$

$$\sqrt{\sigma_{xx}^2 + \sigma_{yy}^2 + \sigma_{zz}^2 - \sigma_{xx}\sigma_{yy} - \sigma_{yy}\sigma_{zz} - \sigma_{zz}\sigma_{xx} + 3\sigma_{xy}^2 + 3\sigma_{yz}^2 + 3\sigma_{xz}^2}$$

21. Assuming the fatigue curve given at constant mean stress. A Goodman interpolation of mean stress is applied as $\bar\sigma = \sqrt{\sigma_{xx}^2 + \sigma_{yy}^2 + \sigma_{zz}^2 - \sigma_{xx}\sigma_{yy} - \sigma_{yy}\sigma_{zz} - \sigma_{zz}\sigma_{xx} + 3\sigma_{xy}^2 + 3\sigma_{yz}^2 + 3\sigma_{xz}^2}$. For tensile armor only σ_{xx}^2 applies. Stress range calculated considering longitudinal stress range for tensile armor, von Mises for pressure armor.

22. Assuming the fatigue curve given at constant mean stress. A Gerber interpolation of mean stress is applied as $\bar\sigma = \sqrt{\sigma_{xx}^2 + \sigma_{yy}^2 + \sigma_{zz}^2 - \sigma_{xx}\sigma_{yy} - \sigma_{yy}\sigma_{zz} - \sigma_{zz}\sigma_{xx} + 3\sigma_{xy}^2 + 3\sigma_{yz}^2 + 3\sigma_{xz}^2}$. For tensile armor only σ_{xx}^2 applies. Stress range calculated considering longitudinal stress range for tensile armor, von Mises for pressure armor.

2 Software introduction on BFLEX2010 and RFLEX

2.1 RFLEX

RIFLEX was developed as a tool for analysis of flexible marine riser systems. It has the function in doing the global analysis for both static and dynamic in this thesis. But is as well suited for any type of slender structure, such as mooring lines, umbilical's, and also for steel pipelines and conventional risers.

These slender structures may be characterized by:

- Small bending stiffness
- Large deflection
- Large upper end motion excitation
- Nonlinear cross section properties
- Complex cross section structure

Due to the complex cross sections typical found for flexible pipes, a global cross section model is applied in RIFLEX. This means that cross section properties such as axial, bending, and tensional stiffness must be specified as input. Furthermore, structural response is always computed as global deformations and stress resultants (axial force, moments). Hence, local strains and stresses in different cross section layers and materials are not considered. Nonlinear cross section behavior is modeled by introducing nonlinear relations between global deformation parameters and stress resultant, i.e. curvature and moment; relative elongation and tension.

The program computes static and dynamic characteristics of the structure.

Static analysis comprises:

- Equilibrium configuration
- Parameter variations of tension or position parameters, current velocity and direction

Dynamic analysis comprises:

- Eigen value analysis, natural frequencies and mode shapes
- Response to harmonic motion and wave excitation
- Response to irregular wave- and motion excitation

The program is based on a nonlinear finite element formulation. The following key features are Included:

- Flexible modelling of simple as well as complex systems
- Nonlinear time domain simulation of riser motions and forces
- Nonlinear cross section properties
- Generalized Morison type of load model Simplified analysis options:
- Static analyses, catenary approximations Linearized time domain simulation
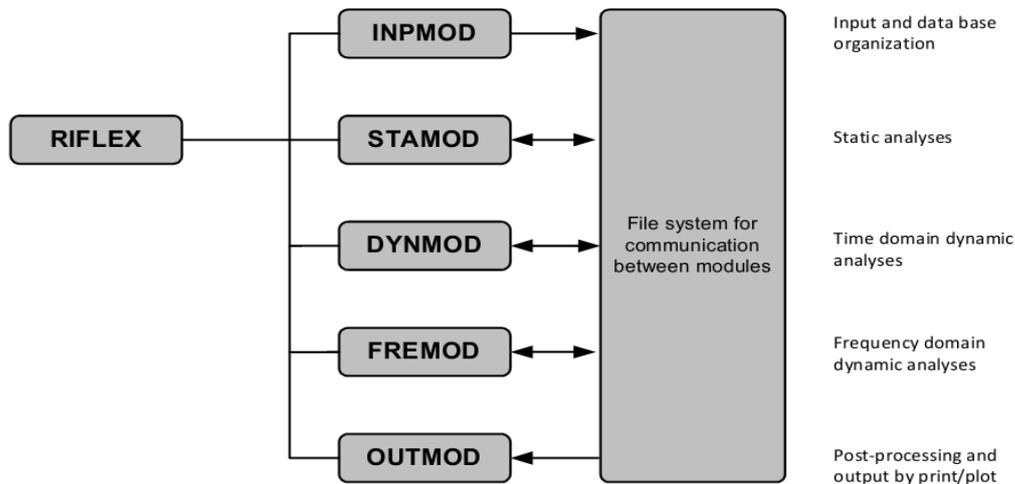
Figure 2-1 Frequency domain analysis

[I]A complete dynamic analysis must include a run of all modules. However, an efficient data base system simplifies the work during a complete study by storing input data and intermediate results. (I.e. problem description, static configurations, wave induced vessel motions and water particle velocities and accelerations).

Each module will be further detailed in the following.

- INPMOD module

The INPMOD module reads most input data and organizes a data base for use during subsequent analyses. Once the INPMOD module has been run, several analyses can be performed by the other modules without rerun of INPMOD.

- STAMOD module

The STAMOD module performs several types of static analyses. The results may be used directly in parameter studies etc., and are also used to define the initial configuration for a succeeding dynamic analysis. Element mesh, stress free configuration and key data for finite element analysis are also generated by STAMOD based on system data given as input to INPMOD.

- DYNMOD module

The DYNMOD module carries out time domain dynamic analyses based on the final static configuration, environment data and data to define motions applied as forced displacements in the analysis. It is possible to perform several dynamic analyses without rerun of INPMOD and STAMOD. Response time series are stored on file for further post processing by OUTMOD and PLOMOD. In addition to dynamic response, natural frequencies and mode shapes can be calculated.

- OUTMOD module

16

OUTMOD performs post processing of selected results generated by STAMOD and DYNMOD. It is possible to store plots on a separate file for graphic output in the PLOMOD module. It is also possible to export time series via a standardized file format for further post processing by general purpose statistical analysis program (STARTIMES).

- PLOMOD module

Interactive plotting module for graphic presentation of plots is generated by OUTMOD. An animation tool is available for visualization of the dynamic behavior of the complete system (mooring lines, risers, vessel and waves).[I]

2.2 **BFLEX2010**

BFLEX2010 has the function to do the stress analysis and fatigue analysis for the different layers in the flexible riser. Although the RFLEX could also do the fatigue analysis for the pipeline, it could find the result much more accurate comparing with the RFLEX since it just could find out the section's fatigue life along the flexible riser without investigating the layers.

The BFLEX computer program was originally developed by SINTEF Civil and Environmental Engineering as part of the project Service Life Analysis of Deep-water Risers which was sponsored by the Test rig JIP (oil companies, 70%) and The Norwegian Re-search Council (30%).The first program version was released in 2001. A Bflex User Group was further established in order to commercialize and maintain the program system. The user group first included Statoil, Norsk Hydro and Seaflex. Since then, several new users have been included and the user group of today additionally includes NKT, Aker and Prysmian.The input and output files' names convention[6]:

Model.bif-The BFLEX2010 Input File (model definition)

Model.bof-The BFLEX2010 Output File (print of result from input data handling plus results)

Model.blf- The BFLEX2010 Log File (print of the iteration status at each load step) or error messages.

Model.2bpi-The BFLEX2010POST Input File

Model.2bpl-The BFLEX2010POST Log File

Model.plf-The PFLEX Log File (print of the iteration status at each load step)

Model.bol-The BOUNDARY Log le (print of the iteration status at each load step)

Model.raf- The BFLEX2010 Result Database File (result presentation) model_blex2010.raf The BFLEX2010 Result Database File generated by BFLEX2010POST for selected parts of the global model. Local post processed by Bflex, BOUND-ARY, LIFETIME and BPOST.

Fatiguedata The BFLEX2010 fatigue data file, which is arbitrarily named by the user(one for each layer type where fatigue analysis is to be carried out)

Model.lif-The LIFETIME Input File

[I] BFLEX2010_usermanual_v307 page 19

Model.lof-The LIFETIME Output File

These files are very useful when doing the batching of all the load cases. In this report, the fatigue analysis will use the model.lif in the last step, which means the batch file could be generated as the quick way to do the analysis for each of the load case in order to save the time.

3 Case definition and method

3.1 Process flow chart

The whole thesis is used to do the fatigue analysis of the riser finally and investigate the mean stress correction's influence on the calculating the fatigue damage. But this part is finished under the condition that the critical point has been found correctly along the flexible riser. So the whole process of the steps is showing in the figure below
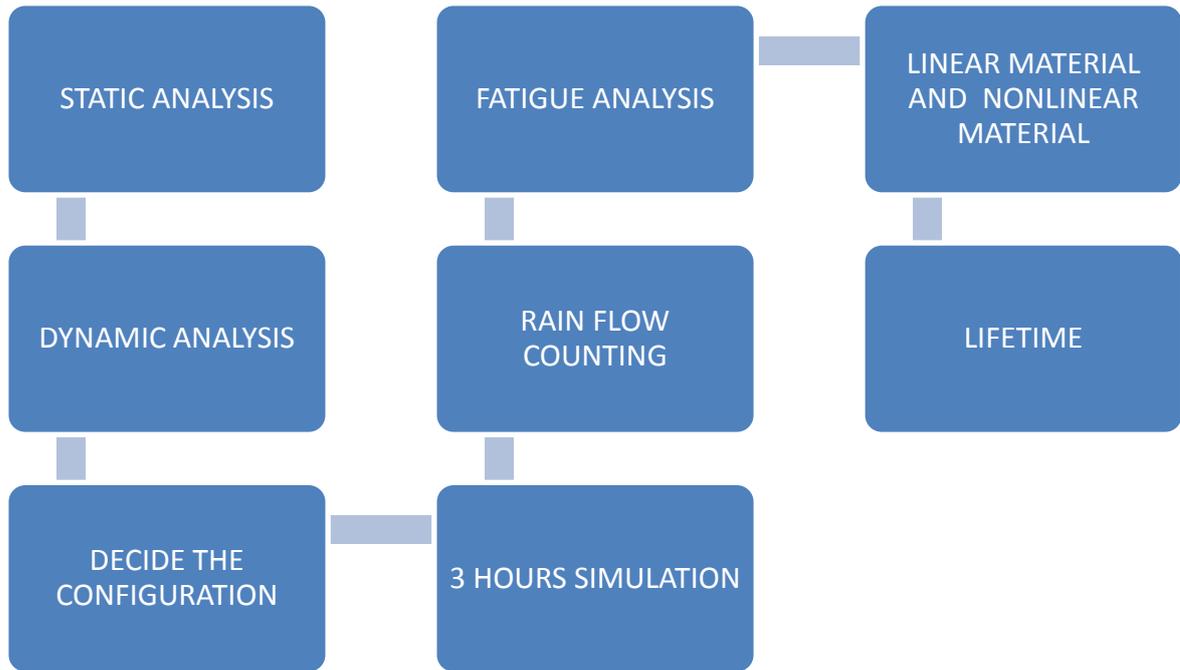
Figure 3-1 process flow chart

3.2 Modeling in RIFLEX

The RIFLEX software has several models to do the different analyses. The following information should be added input file to different calculating model. All the input file should be in *.inp file to edit with the *.txt file. The inpmod.inp has the basic information of the environment including the wave, current and wind. For selection the wave spectrum, the two parameter JONSWAP spectrum should be chosen since the significant wave height and wave period are known for each sea state. The current profile is modified with the depth and scale factors. The wind influence is neglected in this case. The transfer function is also included in this file. The transfer function in this case is provided with a result from the SESAM software and could be used directly in the inpmod.inp file. The two super nodes of both top and end of the riser are connected to the support vessel and seabed separately. The BOP system is neglected in this case. It should be noticed that the RIFLEX is also included in the DEEP-C. So it is quite efficient to use DEEP-C to model the whole part of the riser and the environment. It could generate the input file finally for the RIFLEX model. However, choosing the model of the DEEP-C should be pay attention that only RIFLEX part should be included in the DEEP-C when doing the analysis

3.2.1 **Inpmod.inp**

3.2.1.1 The distribution of the flexible riser

In the inpmod.inp, the basic structure and environment should be set correctly. The riser is set to be only one line in this report. And the boundary condition for the riser is set to connect the support vessel to the sea bed. The boundary condition is set to be fixed for six degree of freedom at the vessel side as the top of the riser and the other side of the riser is set to be simply support at the sea bed. Since the top side of the riser is fixed, the original direction of it should be set as 86.6 degree as the data given in the Table 3-1. In order to avoid the influence of the torsion, the bottom position is set to be with the same y value in

Figure 3-2. And the x value is already found in the Table 4-5, which is 250m. It could also been shown in the Table 3-1.

Name	X(m)	Y(m)	Z(m)	Top angle(degree)	Azimuth angle(degree)
OPR top	51.0	-1.15	21.5	9.5	3.4
OPR bottom	250.0	-1.15	-365.0		

Table 3-1 Power cable and riser departure position and angles

And the distribution of the riser is showing in the

Figure 3-2
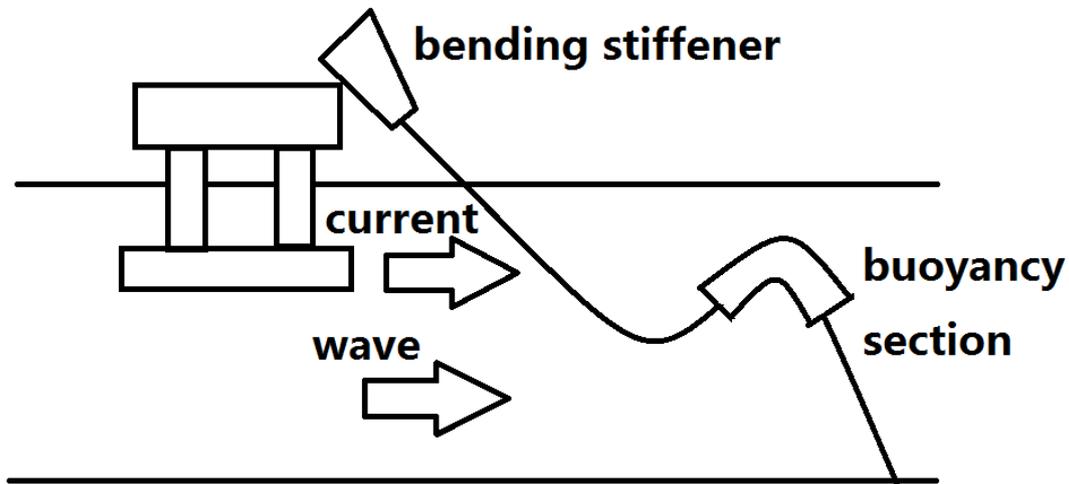
Figure 3-2 Oil production riser configuration

The global accurate geometry for the flexible riser system is shown in

Figure 3-2. The flexible riser is a traditional (lazy wave) configuration with a part of the riser resting on the seafloor in the same way as a catenary. It also should be noticed that the starting point of the riser at the first step in the static analysis should be given in advance. Since the computational procedure is set to be the finite element method based on stress in the stamod.inp file, the stress free

start configuration should be calculated by hand in advance. For this report, the original position of the end side of the riser is kept all the time at the point (250,-1.15,-365). The original position of the top side of the riser is set at the sea bed without the stress inside it and the starting point should be set to the position (-315,-1.15,-365).
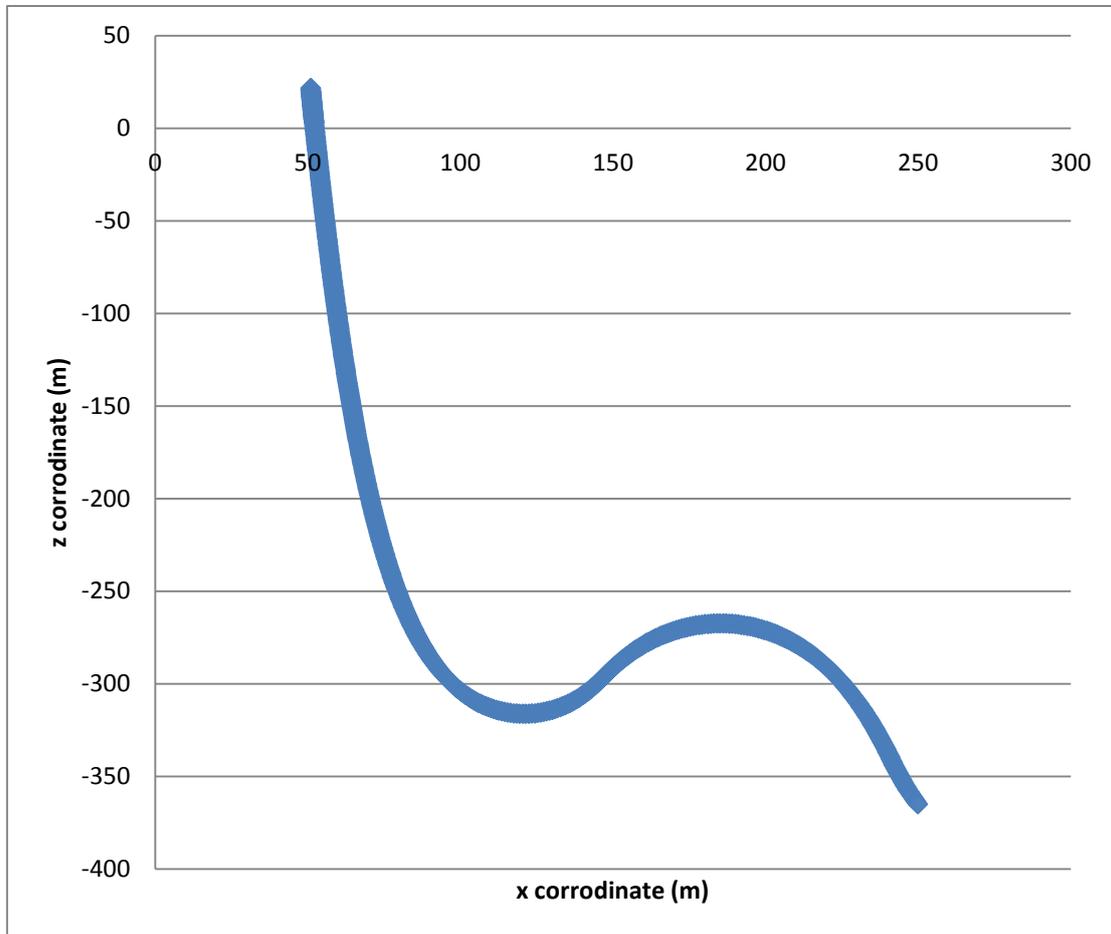
Figure 3-3 Global distribution of the flexible riser

The riser cross-section is uniform and identical. On the buoyant segment (EF section, see Figure 3-2) 150 buoyancy elements are mounted, each with a length of 1m. Hence, the total length of the buoyant segment is 150m. Cross-section data and segment length are given in Figure 3-3.

A Morison type of load model should be used, applying the following equation for tangential drag force to the riser sections of constant cross-section:

$$F_T = \frac{1}{2}\rho C_T \pi d u_T |u_T| \tag{15}$$

And ρ is the density of water, D is diameter, u_T is relative pipe/fluid velocity along the pipe. For the buoyant segment, each participant was free to apply any load model for tangential forces.

The Table 3-3 shows the very important information about the one case for both the static analysis and dynamic analysis valid for flexible riser system. The environmental data are shown in Table 3-5 and Table 3-6. Upper end motions are defined with amplitudes and phase angles relative to the wave according to figure2 and the following equation:

Sea surface elevation

$$\eta(t) = \eta_0 \sin(-kx - \omega t) \qquad \eta_0 = 7.5 \text{ m} \qquad (16)$$

Horizontal motion

$$x(t) = x_a \sin\left(-kx - \omega t + \frac{\pi}{2}\right) \qquad x_a = 4.0\text{m} \qquad (17)$$

Vertical motion

$$y(t) = y_a \sin(-kx_0 - \omega t) \qquad y_a = 6.0\text{m} \qquad (18)$$

With respect to structural damping, it was suggested that a Rayleigh type damping model should be applied with 5% of critical damping at the actual wave frequency.

Lazy wave flexible riser		
Segment AB	8	m
Segment BC	11	m
Segment CD	41	m
Segment DE	330	m
Segment EF	150	m
Segment FG	25	m

Table 3-2 segment length of the riser

Segment	Line length, from to [m]	Marine growth [mm]	property	unit	Oil production riser
A	11(hang-off to 2m above MSL)	0	Mass Outer diameter Axial stiffness Bending stiffness Torsion stiffness Transverse drag coefficient Tangential drag coefficient	Kg/m M MN kNm2 kNm2 [-] [-]	485.0 0.377 1370 596.7 420.1I 1.05 0.01
B	41(2m above MSL to -40m below MSL)	60	Mass Outer diameter Axial stiffness Bending stiffness Torsion stiffness Transverse drag coefficient Tangential drag coefficient	Kg/m M MN kNm2 kNm2 [-] [-]	605.0 0.510 1370 596.7 420.1 1.05 0.01
C	330(from -40m to	30	Mass Outer diameter	Kg/m M	545.0 0.441

I No torsonal stiffness was given by AkerKvaerner

E	buoyancy section) 25(from buoyancy section to tether)		Axial stiffness Bending stiffness Torsion stiffness Transverse drag coefficient Tangential drag coefficient	MN kNm2 kNm2 [-] [-]	1370 596.7 420.1 1.05 0.01
D	150(buoyancy section)	30	Mass Outer diameter Axial stiffness Bending stiffness Torsion stiffness Transverse drag coefficient Tangential drag coefficient	Kg/m M MN kNm2 kNm2 [-] [-]	103.2 0.671 1370 596.7 420.1 1.05 0.01

Table 3-3 flexible riser structure property

Segment number	Segment length (m)	Segment number	Segment length (m)	Segment number	Segment length (m)
32	0.25	9	0.25	22	0.25
33	0.25	10	0.25	24	0.25
34	0.25	11	0.25	25	0.25
35	0.25	13	0.25	26	0.25
36	0.25	14	0.25	27	0.25
2	0.25	15	0.25	28	0.25
3	0.25	16	0.25	29	0.25
4	0.25	17	0.25	30	0.25
5	0.25	18	0.25	1	11
6	0.25	19	0.25	12	41
7	0.25	20	0.25	23	330
8	0.25	21	0.25	31	150
				23	25

Table 3-4 segment and segment length in modeling

The bending stiffness is modeling by 32 segments with different bending stiffness and axial area. The maximum bending stiffness is at the top of the riser and the end of the bending stiffness is the same as the riser part. It is showing in the Figure 4-1 the normalized bending stiffness.

3.2.1.2 The environment

There is only one model in this case. However, there are 17 sea states involved in this case, which is blocked based on the sea state joint density Table 3-7. The principle to block the sea state is that all the sea state in one block should have the same damage to the fatigue life of the flexible riser

comparing to another block sea state. The short term sea state is defined as the 3 hour simulation and the distribution probability should be calculated based on the joint density Table 3-7. In this case, the sea state is found from the north sea part from the sea loads structure of shipbuilding and offshore[I]

The internal fluid of the riser is also taken into consideration and it is set to be the petro with the density of 800 kg/m^3. It has the direction along the flexible riser from the bottom to the top side.

For the environmental control, the water depth is 365m with only one directional irregular wave case. The air density is set to be 1.226 kg/m^3. The water density is set to be 1025kg/m^3. In practice, the kinematic viscosity of water is 0.119E-06 m^2/s. And all these kinds of information could be found in the Table 3-6.

For the irregular wave control, the three parameter JONSWAP spectrum is selected based on the joint density of significant wave heights and wave periods. [II]

Water depth (m)	Current direction (degree)	Current velocity (m/s)
0	0	0.54
-4	**0**	**0.43**
-100	0	0.32
-225	**0**	**0.18**
-265	0	0.11
-365	**0**	**0.00**

<div align="center">Table 3-5 current profile</div>

Water depth (m)	365
Water density (kg/m3)	1025
Air density (kg/m3)	1.226
Water kinematic viscosity (m2/s)	0.119E-06
Air kinematic viscosity (m2/s)	1.824E-05
Oil density (kg/m3)	800

<div align="center">Table 3-6 environmental property</div>

For each of the case, the number of irregular wave case is set to be only one and no regular wave vase should be used. The current state number is also should be set to be one and no wind state data should be input into the inpmod.inp.

For the direction parameters, there should be only one direction for both wave and current. It should be along the x axial in the global coordinate because it will be considered as the most dangerous situation for the flexible system. This will lead to both larger curvature and tensile force when doing the fatigue analysis in theBFLEX2010, but the result will be much more conservative. The direction will be showing in Figure 3-2.

.

[I] sea loads structure of shipbuilding and offshore

[II]Riflex User Manual

3.2.1.3 Three Parameter JONSWAP spectrums

Since the environmental data comes from North Sea state, the JONSWAP spectrum, which is recommended spectrum for limited fetch, should be used in this case. This wave spectrum has including three different input parameters, which are significant wave height, peak period and gamma parameter. The gamma parameter is peakedness parameter giving the ratio of the maximum spectral energy to that of the corresponding Pierson-Moscowitz spectrum. Pierson-Moscowitz spectra is an empirical relationship that defines the distribution of energy with frequency within the ocean[I] For this case, only the significant wave height and peak period should be input and the gamma could be calculated by the inpmod.exe automatically as the default value as the follows

$$\text{Gamma} = e^{5.75 - 1.15} \times \frac{\text{peak period}}{\sqrt{\text{significant wave height}}} \tag{19}$$

$$1.0 \leq \text{Gamma} \leq 5.0$$

The unit for peak period is second and significant owns the unit of meter. [II]

3.2.1.4 Support vessel data

The top side of the flexible riser is connected to the plate form or the support vessel as the boundary condition. All the degrees of freedom for this side are fixed so that it could transfer the transfer function from the vessel (RAO). It also needed to be input into the inpmod.inp file. First the vessel should have the name and the gravity location. In this report, the gravity is set to be as (0,0,0) in the surface of the sea. In the data group F of inpmod.inp, the vessel's RAO data should be written in a special format. The motion transfer function is defined relative to the wave field definition. For this report, the RAO is given by AkerKvaerner.

3.2.2 **Stamod.inp**

The stamod.inp is used for controlling the static analysis with the influence of the gravity force, buoyancy force and the current force and identifies the riser.

The line will be given a name in this control part. The analysis run is used for this part without check it. This is used in order to save analysis time. The choice of the result format could also be decided in this card. The identification of the data used for static analysis is given in this part. This data could be found in the inpmod.inp file. The computational procedure is set to be finite element method based on stress free start configuration.

These loads are defined with the load group data. The number of the load steps and the maximum number of iterations during the application should be input in this part. In this part, the number of load step is set to be 200 normally. The volume forces, specified forces, specified displacements, floater forces, current forces and activate bottom friction forces should be set in this card. And it

---

[I] http://en.wikipedia.org/wiki/Pierson%E2%80%93Moskowitz_spectrum

[II] Bflex2010_usermanual_v307 page 117

should be noticed that the number of load steps should be set a little bit larger for the specified displacement to avoiding the instability for the numerical calculation.

3.2.3 Dynmod.inp

This input file is used for controlling the dynamic analysis in RFLEX. The controlling command of the irregular time series should be set correctly here. The total simulating time is set to be 10800 seconds and the time step is set to be 0.2 seconds. The time step should be smaller than the simulate time. And this information could be extracted from the outmode.res. So the time series of the curvature could be got. For the irregular wave procedure controlling, the kinematics at static position should be chosen. The integration of the wave forces to mean water level should be set as the wave zone. The kinematics at positions selected by the program will be computed here for default kinematics point's procedure. The iteration of the steps will be performed every 1time step and the true Newton-Raphson will be chosen as the type of the iteration. Updating of geometric stiffness from axial force will be considered. Maximum number of iterations for steps with iteration is set to be 10. If the numerical stability is considered, this number should be set a little bit larger.

For storage of the envelop curve, all the data should be included in principle. However, only the data from the bending stiffener is useful according to this report. So only the points from 1 to 32 should be stored in the file finally. And this will represent by the element number, segment number and point number. When doing the 3 hours dynamic analysis, only point 8's information should be stored in order to plot the time history of the curvature.

3.2.4 Outmode.inp

This model is just used to get the result from the analysis with stamod.exe and dynmod.exe. In this report, the dynamic result, time history of the curvature, could be got by every step. The result should be used with the rain flow counting method to analysis in order to do the fatigue analysis.

significant wave height(m)(upper limit of interval)	spectral peak period(s)																			
	3	4	5	6	7	8	9	10	11	12	13	14	15	16	17	18	19	21	22	
1	59	403	1061	1569	1634	1362	982	643	395	232	132	74	41	22	12	7	4	2	2	8636
2	9	212	1233	3223	5106	5814	5284	4102	2846	1821	1098	634	355	194	105	56	30	16	17	32155
3	0	8	146	831	2295	3896	4707	4456	3531	2452	1543	901	497	263	135	67	33	16	15	25792
4	0	0	6	85	481	1371	2406	2960	2796	2163	1437	849	458	231	110	50	22	10	7	15442
5	0	0	0	4	57	315	898	1564	1879	1696	1228	748	398	191	84	35	13	5	3	9118
6	0	0	0	0	3	39	207	571	950	1069	885	575	309	142	58	21	7	2	1	4839
7	0	0	0	0	0	2	27	136	347	528	533	387	217	98	37	12	4	1	0	2329
8	0	0	0	0	0	0	2	20	88	197	261	226	138	64	23	7	2	0	0	1028
9	0	0	0	0	0	0	0	2	15	54	101	111	78	39	14	4	1	0	0	419
10	0	0	0	0	0	0	0	0	2	11	30	45	39	22	8	2	1	0	0	160
11	0	0	0	0	0	0	0	0	0	2	7	15	16	11	5	1	0	0	0	57
12	0	0	0	0	0	0	0	0	0	0	1	4	6	5	2	1	0	0	0	19
13	0	0	0	0	0	0	0	0	0	0	0	1	2	2	1	0	0	0	0	6
14	0	0	0	0	0	0	0	0	0	0	0	0	0	0	1	0	0	0	0	1
15	0	0	0	0	0	0	0	0	0	0	0	0	0	0	0	0	0	0	0	0
sum	68	623	2446	5712	9576	12799	14513	14454	12849	10225	7256	4570	2554	1285	594	263	117	52	45	100001

joint frequency of significant wave height and spectral peak period. Representtive data for the nordern North Sea

Table 3-7 Joint frequency of significant wave height and spectral peak period. Representtive data for the nordern North Sea

3.3 Rain flow counting method

After completed the work above, we got the time series of tensile and curvature separately. There are 17 sea states has been counted for. For each of the blocking result sea state, one worst point belong to the riser should be chosen as the characteristic design position to do the fatigue analysis. There should be one method to be utilized in order to recognize the range of the curvature amplitude and tensile amplitude from the time domain analysis. It is recommended using the rain flow counting method. It will provide the range and mean of each rain flow cycle to aid in fatigue life calculation. In this case, the rain flow counting method will be executed with Microsoft Excel 2010. During the rain flow counting, the following steps should be pay attention

1. Input the time series of curvature or tensile history for each one case

2. Executing the rain flow cycle counting

3. Sorting data into joint density table to develop block cycle test for each sea state.

4. Conclusion for the range and mean value of the curvature and axial force separately.

It should be noted that the data being solved by rain flow counting method should be organized according to the sea state long term distribution function. In this case, the sea states are discrete with the frequency of significant wave height and wave period according to the Table 3-7 Joint frequency of significant wave height and spectral peak period. Representtive data for the nordern North Sea. In generally, each of cycle should be timed with its long term probability in order to consider the variability of the distribution of the significant wave height and wave period, which have the influence on its number of cycles.

3.4 Modeling in BFLEX2010

3.4.1 Case basic information

Since the critical point is already found from the result of RFLEX, the fatigue analysis should be done in the BFLEX2010 in order to find the fatigue damage in some particular layer. The bending stiffness is also neglected and only the riser inside should be focused since this report is for doing the fatigue analysis of the flexible riser.

3.4.1.1 Structure information

The basic structure detail information for the riser is showing in the Table 3-8

Inside diameter	228.6 mm	Service	Sour dynamic	Max Fluid Temp	130.0 ^{o}C	
Design pressure	50.07 MPa	Conveyed Fluid	Oil	Water Depth (m)	300.0 m	
Layer	Material	Strength(MPa)	I.D. (mm)	Thick(mm)	O.D. (mm)	Weight(kg/m)
Carcass	Steel	689	228.60	7.00	242.60	23.786

Antiwear	PVDF		242.60	3.99	248.60	4.097
Barrier	PVDF		248.60	12.00	272.60	17.389
Antiwear	PVDFc		272.60	1.02	274.63	0.873
Z-spiral	Carbon Steel	758	274.63	12.00	298.63	68.762
Flat spiral	CarbonSteel	758	298.63	5.99	310.62	40.835
Antiwear	PA11(nylon)		310.62	1.52	313.67	1.569
Tensile_armour_1	Carbon Steel	758	313.67	5.99	325.66	43.049
Antiwear	PA11(nylon)		325.66	0.41	326.47	0.425
Antiwear	PA11(nylon)		326.47	1.52	329.52	1.649
Tensile_armour_2	Carbon Steel	758	329.52	5.99	341.51	45.400
Antiwear	PA11(nylon)		341.51	0.41	342.32	0.445
Antiwear	PA11(nylon)		342.32	1.52	345.37	1.729
Tensile_armour_3	Carbon Steel	758	345.37	5.99	357.36	46.991
Antiwear	PA11(nylon)		357.36	0.41	358.17	0.466
Antiwear	PA11(nylon)		358.17	1.52	361.22	1.808
Tensile_armour_4	Carbon Steel	758	361.22	5.99	373.21	49.265
Antiwear	PA11(nylon)		373.21	0.41	374.02	0.487
Antiwear	PA11(nylon)		374.02	0.41	374.83	0.319
Protective sheath	PA11(nylon)		374.83	12.00	398.83	15.312

Table 3-8 flexible riser's structure data

Layer	Dimension (mm)	Pitch (mm)	Wires	Angle (o)	Filled (%)
Carcass	55 × 1.4	-	-	-	-
Z-sprial	26.8 × 12	-	-	-	-
Flar spiral	16 × 6	-	1	-	-
Tensile_armour_ 1	12 × 6	1039.9	54	44	91.3
Tensile_armour_ 2	12 × 6	1091.5	57	44	91.8
Tensile_armour_ 3	12 × 6	1225.9	61	42	90.7
Tensile_armour_ 4	12 × 6	1281.2	64	42	91.0

Table 3-9 flexible riser's detail information on the geometry

Densities to be based on data sheet values using the combined weight and thickness values provided. The overall pipe mass in empty condition is 364.65 kg/m. During operation (oil filled condition – oil density = 800 kg/m^3) the mass increases to 399.1 kg/m^3. In the laboratory test condition, the mass will be 407.7 kg/m^3 . The buoyancy mass to be calculated based on the external diameter and a sea water density of 1025 kg/m^3.

The geometry of the carcass can be handled according to an example input provided and the basic principles outlined in below figure utilizing the layer thickness and the thin plate (dimension 1.4*55 mm) used to form the carcass.

Mechanical properties are given below.

Material	Young's modulus (MPa)	Poisson's ratio (-)
Steel	2e5	0.3
Plastic layers	300	0.4

Table 3-10 mechanical properties

Since the mainly job of this report is fatigue analysis, the structure is very simply modeled in order to save time. All the information was provided by MARINTEK.

The structure is simplified as the zeta layer, carcass layer and four tensile armor layers. The spiral layer is not included. The most important part in this report is the zeta layer, which is shown as the figure below. The length of the riser is 0.5m.
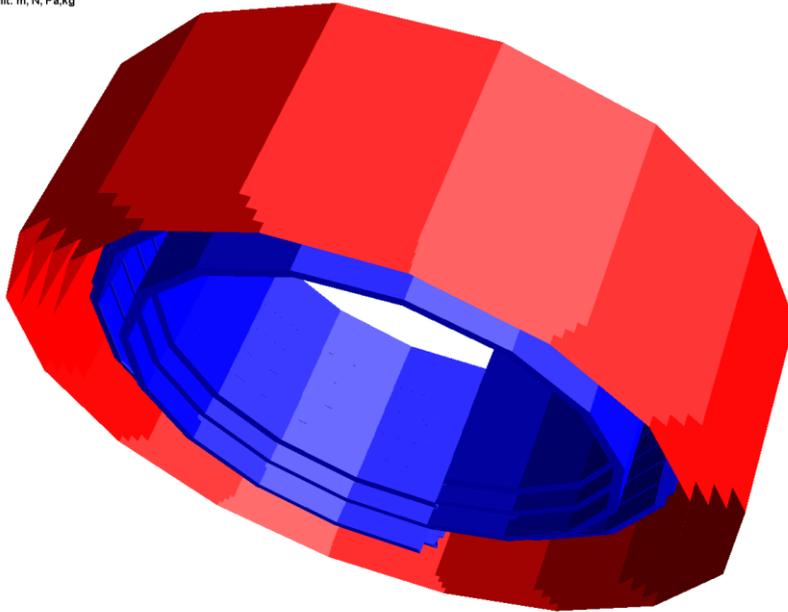
Figure 3-4 flexible riser's whole section in BFLEX2010
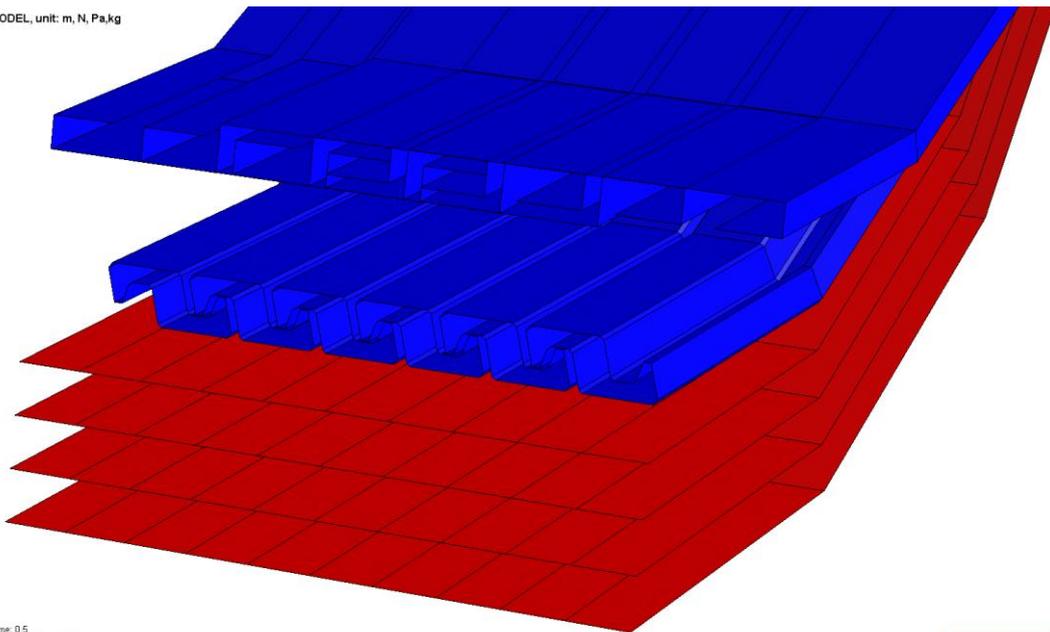
The cross section of the riser is showing in the Figure 3-5. All the layers are the steel layers without the plastic layers. The inner blue layer is the carcass and the outer blue layer is zeta spiral layer. All the red layers are the tensile armor layers.
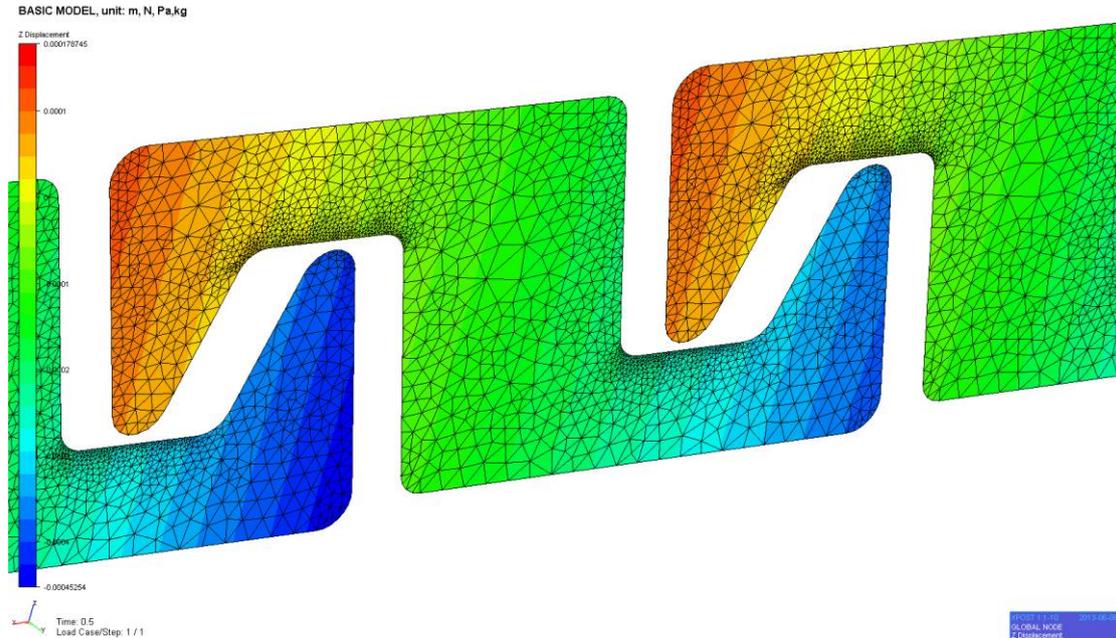
Figure 3-6 cross section of the zeta spiral layer

The mainly section need to be considered is the zeta spiral layer, which is showing in the Figure 3-6. The different color is showing the displacement on the z direction.

3.4.1.2 Material property

This thesis will compare the influence of the mean stress correction with the linear and nonlinear material. The material property is showing in the

3.4.1.2.1 Linear material

Layer	Number	Poisson's ratio	Density(kg/m3)	Young's modulus(MPa)	Transvere Young's modulus(MPa)
Zeta	1	0.3	7700	205000.00	205000.00
Tensile armor	4	0.3	7860	210000.00	210000.00
Tape	13	0.4	1800	370.24	370.24

Table 3-11 Linear material property

The material was chosen as the normal steel. It could be seen that the young's module is constant for each layer. The transverse young's modulus are the same so that the material is isotropic in both directions.

3.4.1.2.2 Nonlinear material

Layer	Number	Poisson's	Density(kg/m3)	Temperature	Thermal	Heat

		ratio		elongation coeff	conductivity(EL-1TE-1)	capacity(E-1TE-1M-1)
Zeta	1	0.3	7850	1.17e-5	50.00	800

Table 3-12 Nonlinear material property

The difference between the linear and nonlinear material in BFLEX2010 is just the zeta layer, which this report mainly studies. The temperature elongation coefficient, thermal conductivity and the heat capacity are also included to show the result much more reality in practice.

Strain start point	Stress(MN/m2)
0	**0**
3.000E-03	**545.0**
5.000E-03	**720.0**
8.000E-03	**800.0**

Table 3-13 Nonlinear material of Strain-stress points' relationship for zeta layer

The material's nonlinear property is changed by illustrating the relationship of the strain and stress. It could be seen that only material nonlinear property is considered in this report. The relation could be shown like the curve in figure 10.
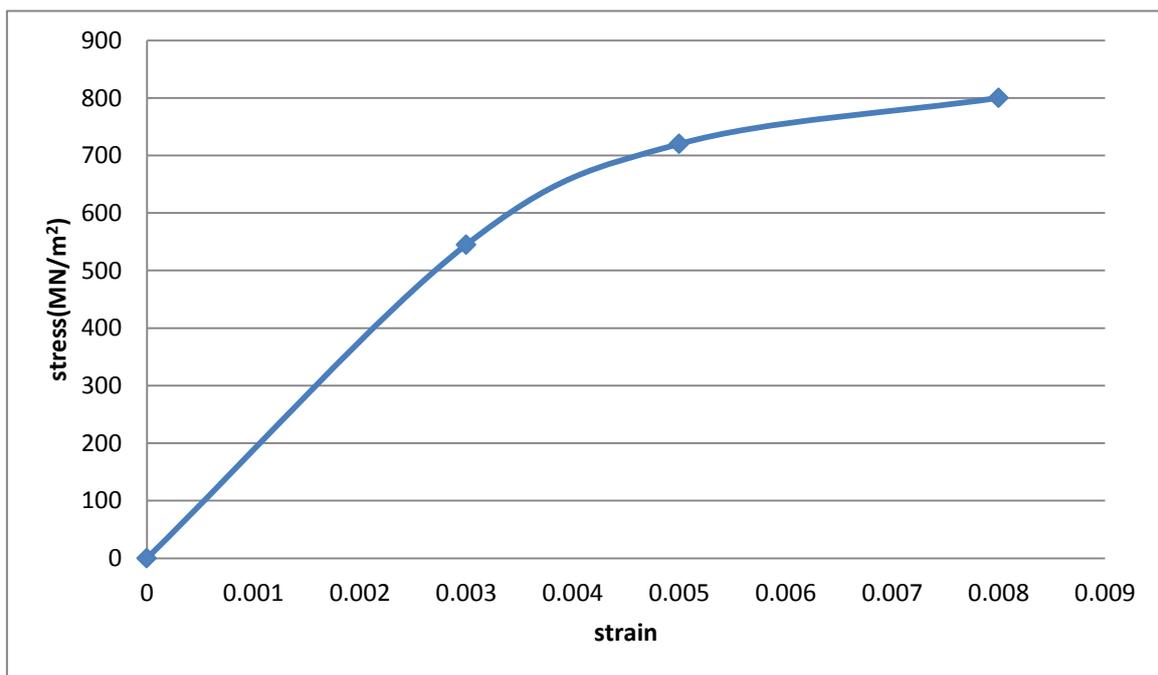
Figure 3-7 Nonlinear material of strain-stress curve for zeta layer

The nonlinear material was considered in this report and had been modified to put into the BFLEX.

3.4.1.2.3 S-N curve

The SN curve is shown as the very important part of the fatigue analysis for the riser. In this report, the S-N curve is shown as the DNV-RP-C20. This is the S-N curve for high strength steel.

32
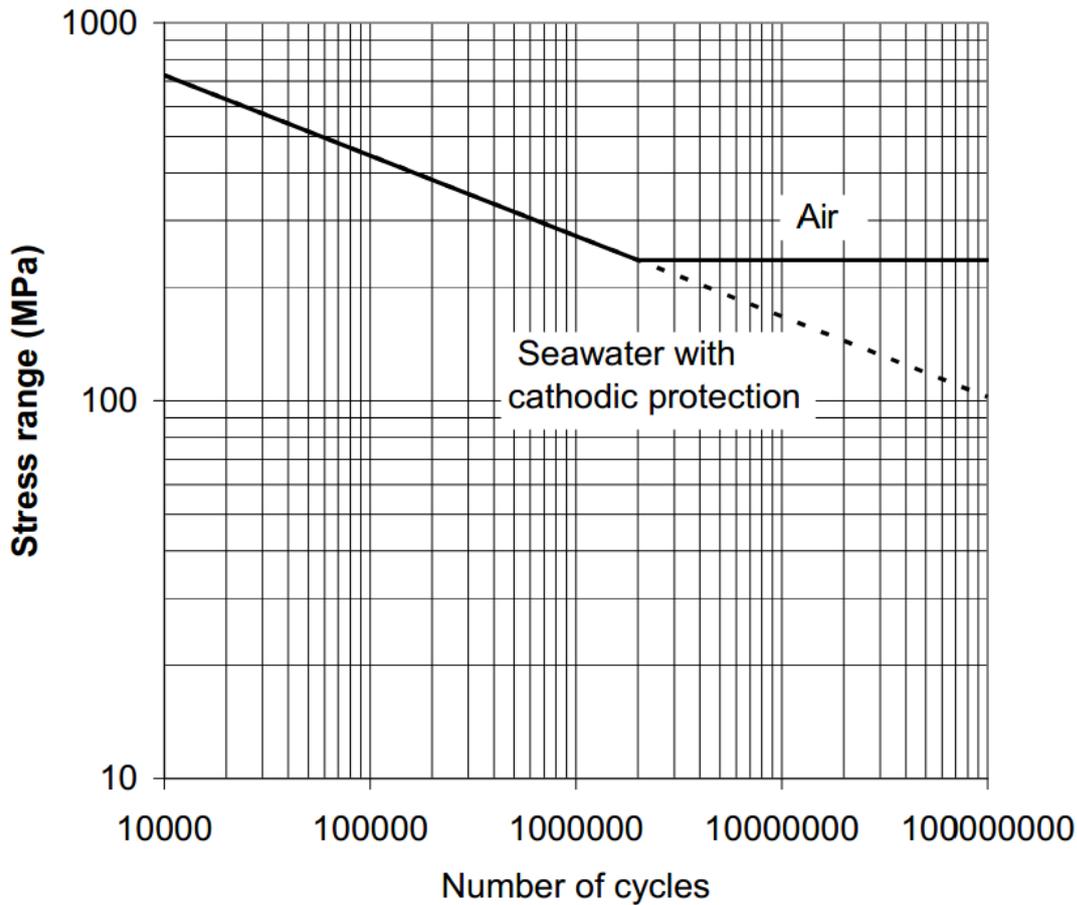
Figure 3-8 S-N curve for high strength steel

3.4.1.3 Boundary conditions

In practice, the flexible riser should be connected to the tensile lines on the top of the platform. It located in the middle of the platform and fixed. On the other side of the riser, it should be fixed inside the BOP and connect to the device under the seabed. So the boundary condition should be fixed on the seabed side, while it should be free on the topside, which only provides the tensile. What's more, the large deviating displacement of the top side of the riser is not permitted so it should be simulated as the spring to be more accurate. However, in this report, the purpose is to do the fatigue analysis of the riser, which means the boundary condition should be as simple as possible in order to regardless other influence. Since only bending moments are induced to this model as the angles range to do the fatigue analysis, it is better to set the simply support boundary condition on both side, which means the rotation freedom around the y-axial should not be limited. What's more, the tensile should be permit in order to simulate the pretension on the top side of the riser in the platform, which means one freedom along the x-axial should not be limited. The simply boundary condition could be illustrated as the figure 11.

Figure 3-9 Boundary condition of the riser

3.4.1.4 Steps for modeling

The FlexEdit is the first step to do the modeling in the Bflex. Before all the structure and loads detail being inputted in the FlexEdit, be pay more attention in order to avoid the programs from being stopped, i.e. the accurate digit should be taken care of in the order line. The unit should be defined previously in the beginning of the report, which specified by using [] to identify optional parameters.

It included almost all kinds of the detail information about the whole structure, which could be concluded as follows

- *Structure details*

- *Loading conditions*

- *Boundary conditions*

- *Define the time and step*

- *Material propertiesI*

- *Contact elementsII*

Note that during a restart all input data that do not influence the element and node definitions may be changed[7]. So it is necessary to restore the result after a reasonable steps' calculation. This is also included in the modeling part of the Bflex.

After this step, the global stresses and tensile amour stress analysis are completed.

The BFLEX2010POST module[III]

This step is mainly to generate the results for further analysis of arbitrary parts of the global model. The input files are necessary in order to get the different results for MATRIXPLOT (.mpf) and for Bflex POST processing. This step generates the *-BFLEX2010.raf to provide the necessary information to PLEX, BOUNDARY and LIFETIME modules calculations. Accordingly, each of the

---

[I] Material properties can be changed of the number of points in material curves are kept unchanged, Bflex2010-usermanual, page14.

[II] This report doesn't have any contact element due to the type of the element PIPE52 being chosen.

[III] For the fatigue analysis, the module should run once for each load case separately

load cases, for fatigue analysis, should create one load case per cycle load condition, which is easy for calculating the fatigue result by adding the numbers of cycles in total.

After this step, the new link between the new modeling features represented by BFELX2010 and other modules is completed.

The BOUNDARY module[I]

After the *.raf files have been generated by BFLEX2010POST, the BOUNDARY module should be used. The input file includes the node having the largest stress from the BFLEX analysis for INOD typically, which means the node position has to be found during the first step analysis.

After this step, the transverse stress analysis of the pressure spirals is completed.

The PFLEX module[II]

The node position for the PFLEX model and the Local deformation parameter should be found to input this step. What's more, the user could get different positions in the BFLEX2010 model without having to perform a new run by BFLEX2010.

After this step, the beam stress analysis of the pressure spirals is completed.

The LIFETIME module

The input file *.lif should be created by user. This includes the SN cure data and the mean stress correction type, which is the important part of this report. This module uses the result of the BFLEX2010POST to do the fatigue analysis[III]. All the load cases should be inputted in the *.lif file, which includes the numbers of cycles for each load case. What's more, the start step and end step for the whole load step process should be included in this part completely.

After this step, the fatigue analysis of the whole structure is completed. The results, such as global coordinate, stress range, modified stress, mean stress, damage and accumulating damage for every unique node, are found in the *.lof file.

3.4.2 Cases and result

All the detail data for inputting into the BFLEX2010 will be included in this section. The result which includes the fatigue damage for both each load case and each method is shown as well.

[I] The BOUNDARY should run before the PFLEX once for each load case separately

[II] The PFLEX should run after the BOUNDARY once for each load case separately

[III] The SN curve should be invoked during the LIFETIME module for fatigue analysis

3.4.3 **Load case condition**

The load case is divided based on the tensile and bending moment, which is added to the boundary of the riser. The direction change of the bending moment should be slow enough in order to avoid the dynamic influence to the result.

3.5 **Find the relationship between prescribed displacement value and curvature**

Since the model has been set in BFLEX finally, the control load should be decided and be put into the control card. The command PDISP is used for controlling the prescribed displacement for the pipe. It is known that the model should be created with the beam element in order to do the static analysis with finite element method. The relationship between the angle at the boundary and the curvature, which position is at the middle of the riser particularly, should be found with the function below

$$k = \frac{1}{R} = \frac{2\theta}{l} \qquad (20)$$

k:curvature

R:radiu of the beam

Θ:the angle at the boundary

l : the length of the beam

l=0.1m in this report. However, the riser has been modeled with many layers and elements. The relationship of the angle and curvature is not exactly as the function above described. But it should be linear relationship since the material is linear type. So the new function should be set with the introducing factor A. And the function should be like this

$$k = \frac{1}{R} = A\frac{2\theta}{l} \qquad (21)$$

Add the mean tension and inner pressure in advance to get the right condition, which is calculated before. Then it should set the angle to be 1e-05 and the time load factor to be 1.0 at the load step 28, the curvature is showing in the
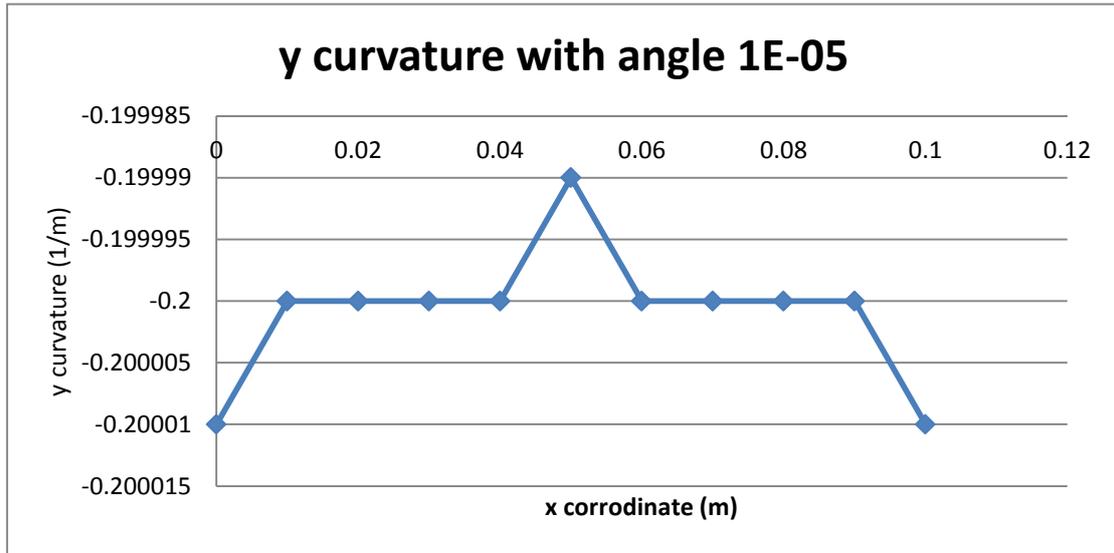
Figure 3-10 y curvature with angle 1e-05

The result in Figure 3-10 is showing that the value is around 0.2 (1/m). So the factor A should be

$$A = \frac{k \times l}{2\theta} = \frac{0.2 \times 0.1}{2 \times (1e - 05)} = 1000 \qquad (22)$$

So the input data for the angle should be multiplied with the factor 1/A for getting the given curvature and the result is showing in the Table 5-3 Input angle for BFLEX in the chapter 5. The load time factor is the factor multiplied by the angle at the time step. It is used to simulate the mean value of the curvature and the range of the curvature. It could be got in the function as below

$$factor = 1 \pm \frac{k_{range} \times 0.5}{k_{mean}} \qquad (23)$$

k_{range} : curvature range

k_{mean}: mean curvature

And the loading process should be controlled in the following process
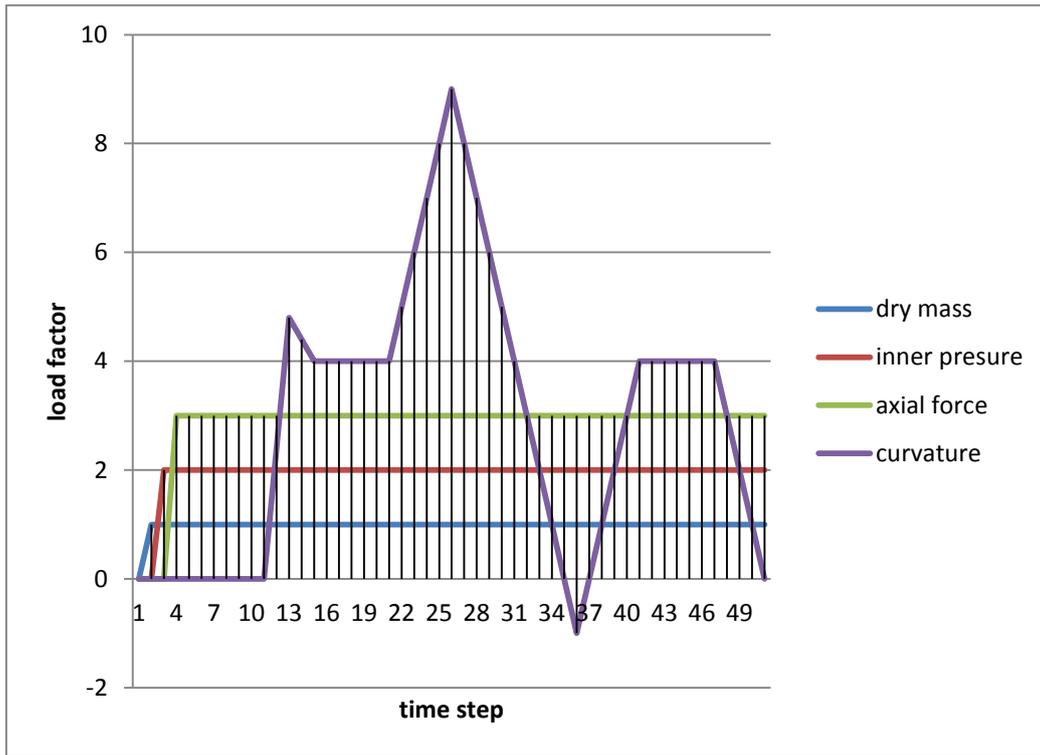
Figure 3-11 load step process

For each of the case, the corresponding mean angle with both positive and negative factor should be set correctly. It also should has the name with the correct cycle number in the fatigue analysis in *.lif file.

4 Result for Global dynamic analysis for the flexible riser

4.1 Static analysis

The model was created in the RIFLEX software and the environment was set including the current and wave impact. The wind influence was not included. The static distribution is showing in the Figure 3-3 Global distribution of the flexible riser. The aim of the figure is to illustrate the configuration of the flexible riser and the surface of the water is at z=0. The result is mainly showing in the chapter 3-case definition. The reason for doing the static analysis is to find out the right bottom position of the flexible riser and critical point along the bending stiffener. Then the configuration of the riser could be made sure finally.

4.1.1 Decide the position of the flexible riser's bottom side on the seabed.

Since the most dangerous distribution is taken into consideration, the wave and current direction is just set to transfer along the x axial in the global coordinate. So it is only needed to decide the x value of the bottom point of the riser on the seabed. It is necessary to do the static analysis with the calculation model "inpmod.exe" and "stamod.exe" in RIFLEX. The "inpmod.exe" has the responsibility to input the structural and environmental condition, while the "stamod.exe" is for doing static analysis for the riser.

Use the length of the riser 565m, water depth 365m and air gap 21m of the support vessel to calculate the largest value of x use the function

$$x = \sqrt{565^2 - (365 + 21)^2} \qquad (24)$$

The result is 412.59m, which is the maximum riser's bottom position along x axial. Then the right value should be estimated by several cases with different x value, which is larger than 0m and smaller than 412.59m. In this case, there are 14 cases which have the x values from 250m to 380m being taken into consideration for the static analysis.

According to the information of bending stiffener, the normalized bending stiffness is showing in the Figure 4-1.
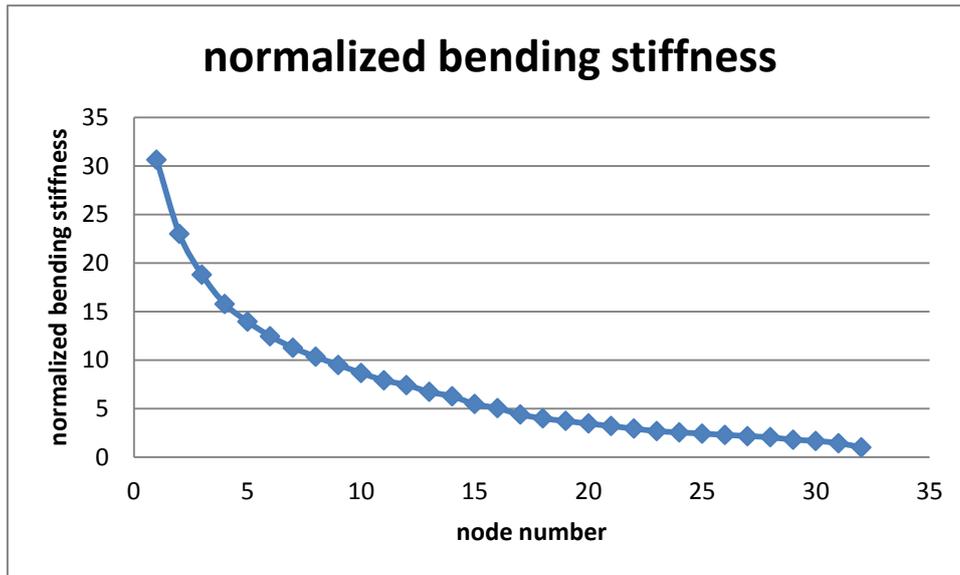
Figure 4-1 the normalized bending stiffness

It could seen from the figure that the maximum value is about 31.5 (normalized EI=31.5 at distance from root of 1m) times larger than the minimum value (normalized EI=1 at distance from root of 8m). It could be set as the role for finding the right position of the riser's bottom position, which means that the largest bending moment at the top should be about 31 times larger than the minimum value at the end side of the bending stiffener.

The bending moment for the bending stiffener is got from the static analysis for 14 cases as showing in the Figure 4-2
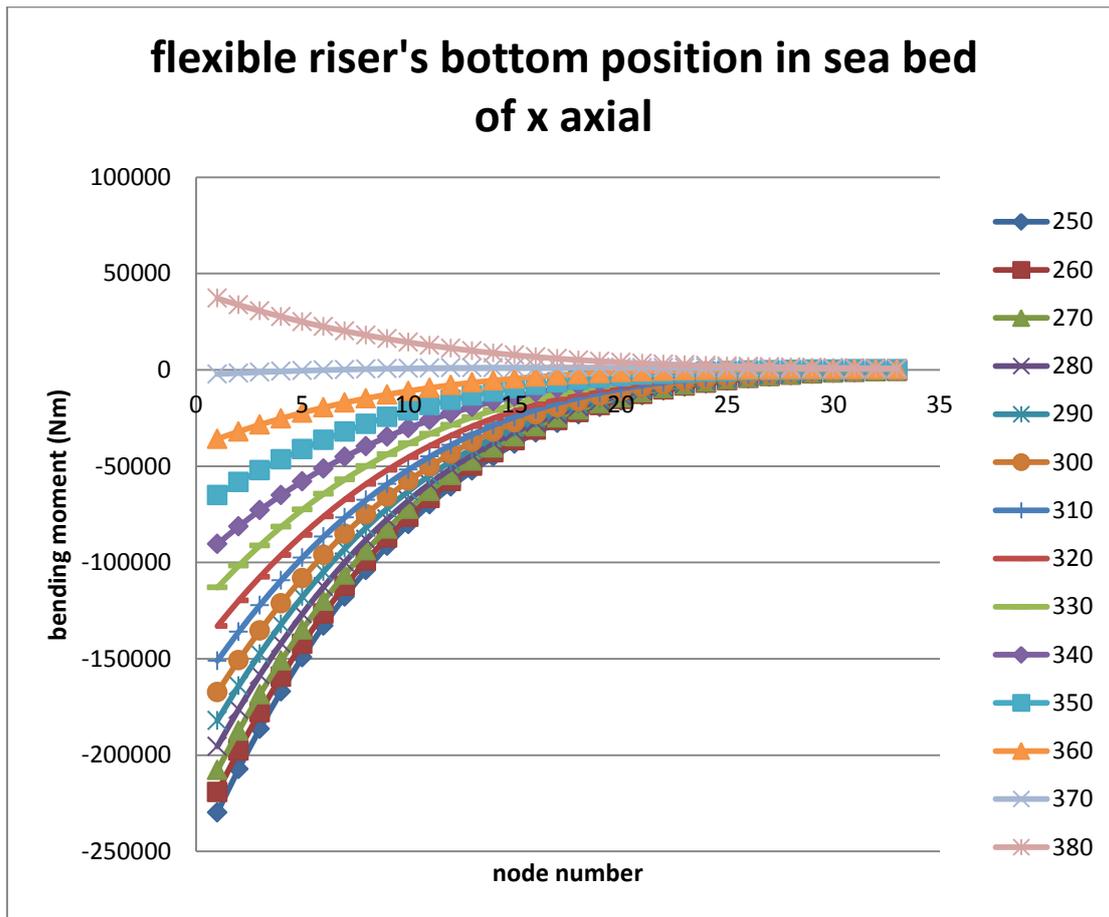
Figure 4-2 flexible riser's bottom position in sea bed of x axial

The series line has the meaning of x value for the point of the riser in the seabed. The unit is m. It could be seen that x=360m, x=370m and x=380m is reasonable result with the maximum value is around 30 times larger than the minimum value.

However, this position is the result from the static analysis, which means there is no current and wave's influence. Since this report considers the most dangerous situation, in which the current and wave have the same direction to take action on the riser, it should be find a reasonable riser's position in the seabed. With the increasing of the current and wave, the bending moment will increase from negative value to positive value. So the bending moment should be as large as possible at the top of the riser and it should be negative value. The other rule to chose the bottom position is to compare the value of bending moment at the end side of the bending stiffener. It could be showing in the Table4-1 It should be noted that Table 4-1 is the result only from the sea state number 8, which is the middle case during the 17 sea states.

Bending moment for sea state 8 with several seabed position (KN*m)			
	node number		
bottom position	**1**	**32**	**33**
250m	-61643.4	-40.7008	14.57347
260m	**-50950.4**	**30.71962**	**71.77819**
270m	-39382.4	107.5335	133.284

280m	**-26816.9**	**190.3642**	**199.5833**
290m	-13106.3	279.927	271.24
300m	**-13106.3**	**279.927**	**271.24**
310m	1928.245	377.0408	348.8977
320m	**18505.38**	**482.6396**	**433.2878**
330m	36894.82	597.7798	525.2336
340m	**57432.49**	**723.6395**	**625.6472**
350m	80541.02	861.5015	735.512
360m	**106759**	**1012.707**	**855.8407**
370m	136782.9	1178.557	987.5892
380m	**171530.4**	**1360.122**	**1131.493**
390m	212240.5	1557.894	1287.772

Table 4-1bending moment for sea state 8 with several seabed position

The point 1 is the top side of the riser and point 32 is the end of the bending stiffener. The point 33 is the beginning point of the flexible riser. It could be seen from the bending moment value that the nude number 32 has turning to be the negative at the position of 250m for the first time, which means nude number 32 has the minimum absolute value when the bottom position is locating at the 250m on the seabed. It could be thought that the bending moment changes the direction at this position. And the reason to consider the absolute value is that the negative value is just the opposite direction for bending of the bending stiffener. So the position of 250m should be chosen as the right position. The result could be found from the Table 4-3 dynamic analysis with bending stiffener's curvatures for all sea states in chapter 6.

4.2 Dynamic analysis with time domain

4.2.1 How to decide the critical point along the bending stiffener.

As the result showing above, the right position of the riser is already been found in the seabed. It should be estimated the damage much more accurately with considering the properties of all the sea states.

After simulating of the 17 sea states, the distributions of the mean value of resultant curvature along the whole flexible riser are shown in Figure 4-3. The results are stored in the dynmod.res file and both dynamic mean value and static value could be found in this file. The standard deviation also is included in this value. Only y axial curvature is included in Figure 4-3. It is because there is not any current and wave along the z axial direction. For the resultant curvature, it shows the same result as the absolutely value of the y axial curvature so it should not be got to do the fatigue analysis because the rain flow counting method could be executed wrongly when counting the value of resultant curvature since all the values are positive alone the time series line.
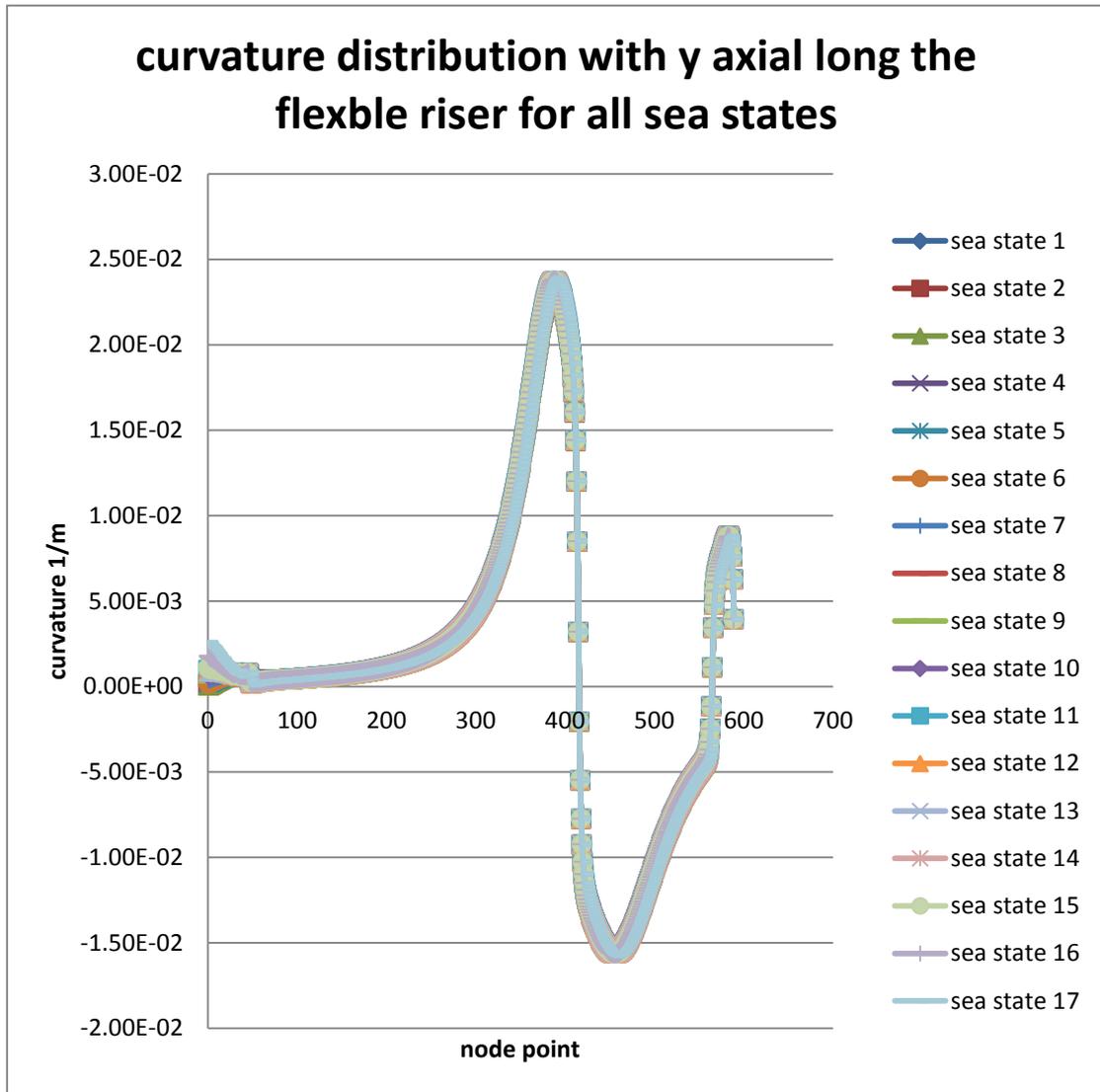
Figure 4-3 Curvature distribution for the whole flexible riser.

It could be seen that there will be large curvature in the buoyancy part and at the end of the flexible riser. However, the top part should be considered significantly because the maximum axial force is in the top part of the flexible riser. Also the support vessel will have the influence with the top side of the riser with the RAO.

Element number	Axial force	Axial elong.	Torsion moment	Torsion deform	xz-proj angle	xy-proj angle	yz-proj angle
1	8.66E+05	6.32E-04	0	0	176.6	0	-90
2	8.65E+05	6.31E-04	0	0	176.6	0	-90
3	8.64E+05	6.31E-04	0	0	176.6	0	-90
4	8.63E+05	6.30E-04	0	0	176.6	0	-90
5	8.62E+05	6.29E-04	0	0	176.6	0	-90
6	8.61E+05	6.29E-04	0	0	176.6	0	-90
7	8.60E+05	6.28E-04	0	0	176.6	0	-90
8	8.59E+05	6.27E-04	0	0	176.6	0	-90
9	8.58E+05	6.26E-04	0	0	176.6	0	-90

10	8.57E+05	6.26E-04	0	0	176.6	0	-90
11	8.56E+05	6.25E-04	0	0	176.6	0	-90
12	8.55E+05	6.24E-04	0	0	176.6	0	-90
13	8.54E+05	6.23E-04	0	0	176.6	0	-90
14	8.53E+05	6.23E-04	0	0	176.6	0	-90
15	8.52E+05	6.22E-04	0	0	176.6	0	-90
16	8.51E+05	6.21E-04	0	0	176.6	0	-90
17	8.50E+05	6.20E-04	0	0	176.6	0	-90
18	8.49E+05	6.20E-04	0	0	176.6	0	-90
19	8.48E+05	6.19E-04	0	0	176.6	0	-90
20	8.47E+05	6.18E-04	0	0	176.6	0	-90
21	8.46E+05	6.17E-04	0	0	176.6	0	-90
22	8.45E+05	6.17E-04	0	0	176.6	0	-90
23	8.44E+05	6.16E-04	0	0	176.6	0	-90
24	8.43E+05	6.15E-04	0	0	176.6	0	-90
25	8.42E+05	6.14E-04	0	0	176.6	0	-90
26	8.41E+05	6.14E-04	0	0	176.6	0	-90
27	8.40E+05	6.13E-04	0	0	176.6	0	-90
28	8.39E+05	6.12E-04	0	0	176.6	0	-90
29	8.38E+05	6.12E-04	0	0	176.6	0	-90
30	8.37E+05	6.11E-04	0	0	176.6	0	-90
31	8.36E+05	6.10E-04	0	0	176.6	0	-90
32	8.35E+05	6.09E-04	0	0	176.5	0	-90

Table 4-2 axial force along the bending stiffener

In principle, both the axial force and curvature should be taken into consideration for fatigue analysis. It will take much more time to do the simulation and rain flow counting in usual. However, the axial force, which is showing in the Table 4-2, ranges so small that it could be consider the axial force is the same along the 8 meter's bending stiffener. The largest axial force is 866 KN and the smallest axial force is 835 KN. The largest one is the smallest one 1.037 times. While considering the curvature value in the Figure 4-7, it could be seen that the largest curvature is from sea state 10 with 1.6E-04 1/m and the smallest value is 1E-05 1/m or almost zero. The largest value is as 16 times as larger than the smallest value. So the change of the curvature is much more important. So the curvature value is the major control cause in the fatigue analysis when choosing the point along the flexible riser.
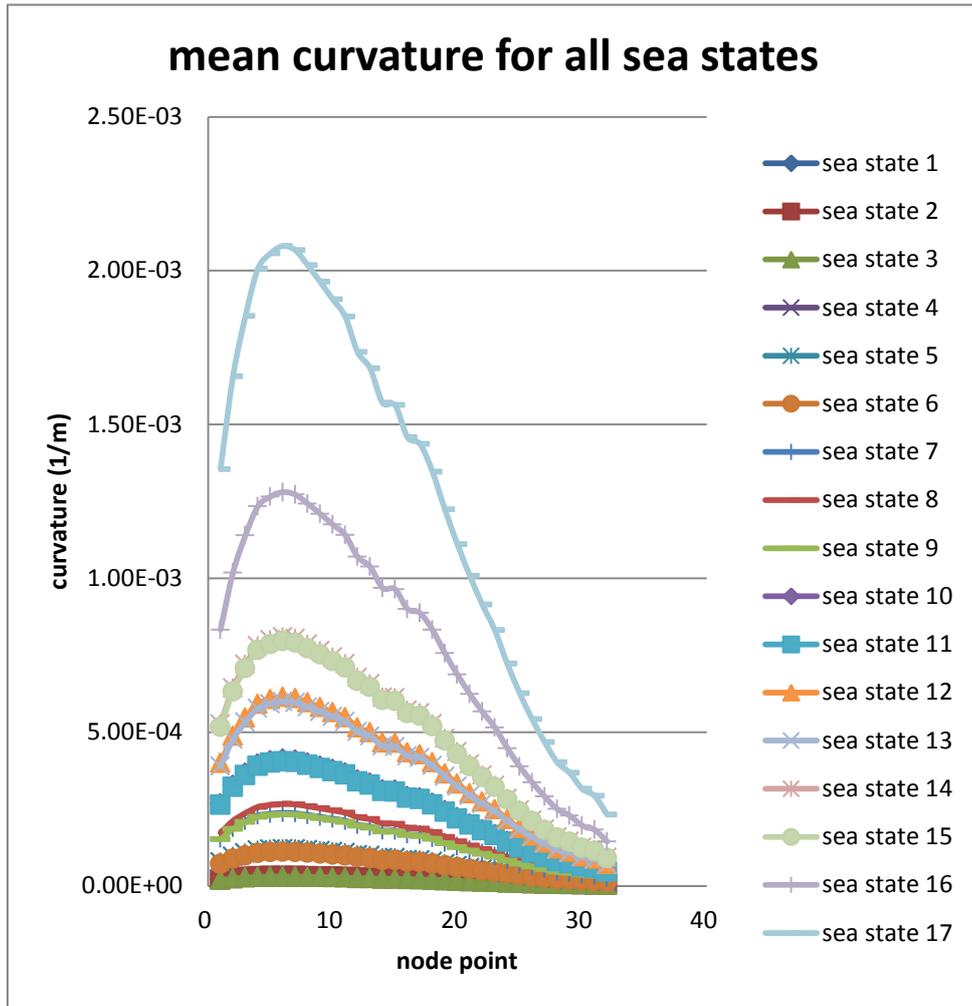
Figure 4-4 mean curvature for all sea states

The mean curvature for all sea states is showing in the Figure 4-4. This is the dynamic analysis result. They are the absolute value of the curvature. The sea state 17 is the worst sea state and it gives the highest value. This is reasonable because the worst sea state could cause the largest bending moment.
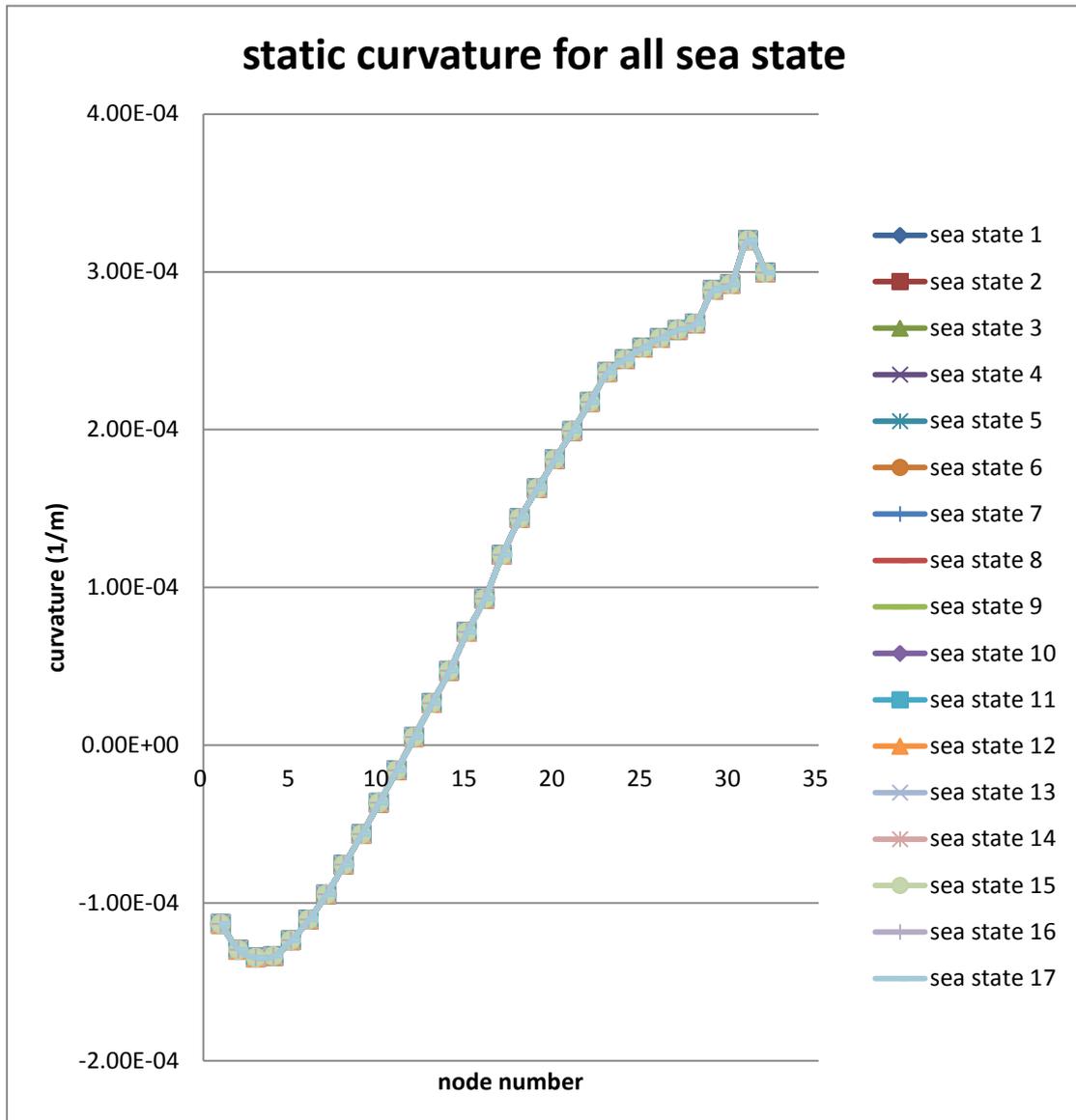
Figure 4-5 Static curvature for all sea state

The static value is the same for all the sea states. It is the result with the current speed. This distribution is used to be modeling in the worst situation, which wave and current direction is the same, since all the current profile is the same for the 17 sea states. The end of the bending stiffener has the largest value around 3.00E-04. The curvature changes the direction at the point 10, which means that the bending moment change the direction at the point 10. So the static value is not the right value for doing the static analysis.
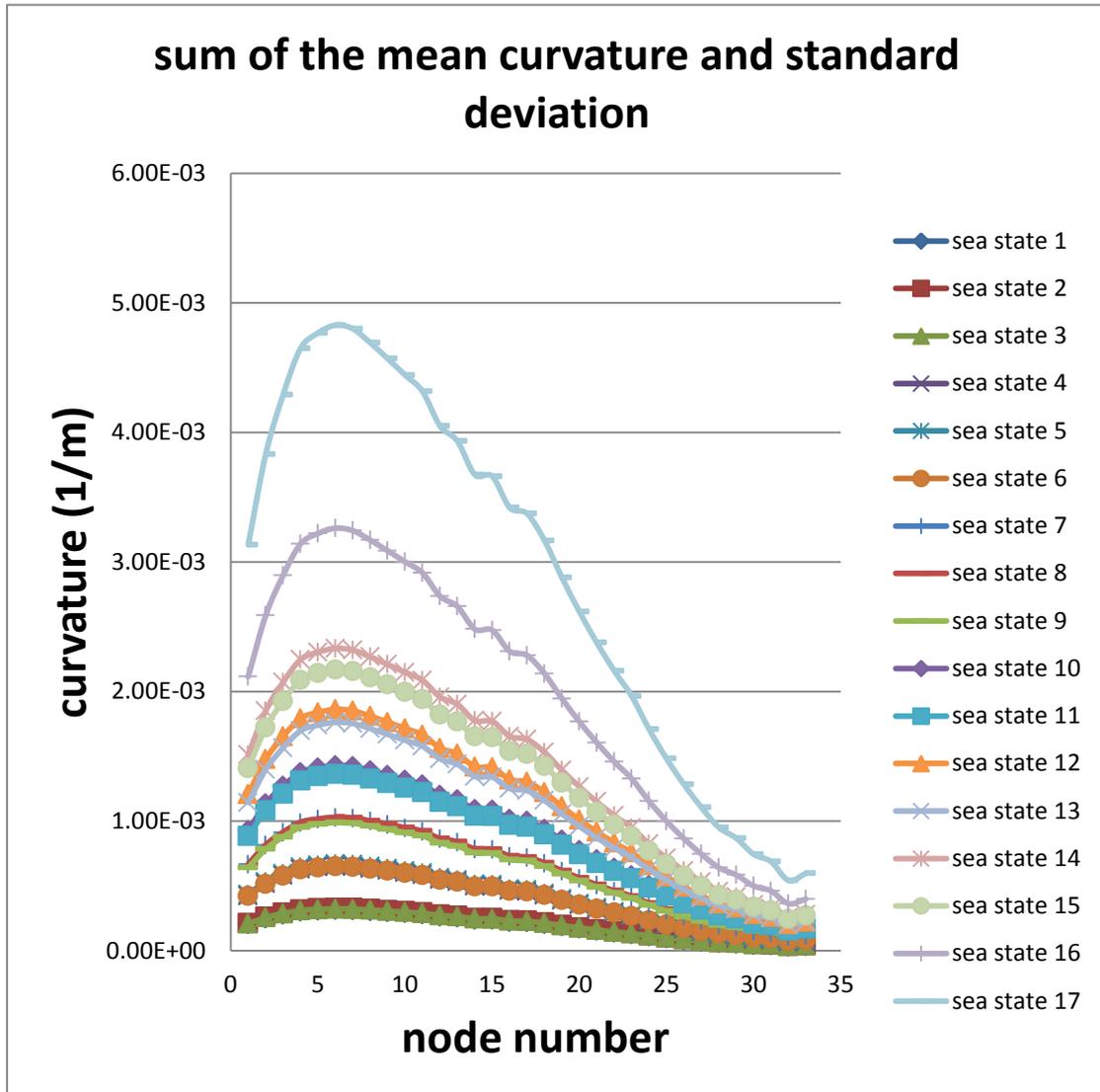
Figure 4-6 Sum of the mean curvature and standard deviation

This is the result by adding the mean curvature and standard deviation. It should be the largest result without the static analysis. It could be used as the range of the curvature and tells us the largest range of the curvature. And the worst sea state 17 has the largest curvature. However, this result is the just used for finding the critical point along the flexible riser. What's more, the static result is also needed to be considered.

Since all the 17 sea states have been simulated during the 3 hours, it should be noted that the curvatures of the 17 cases has the distributions from point number 1 to point number 32 according to the Figure 4-7
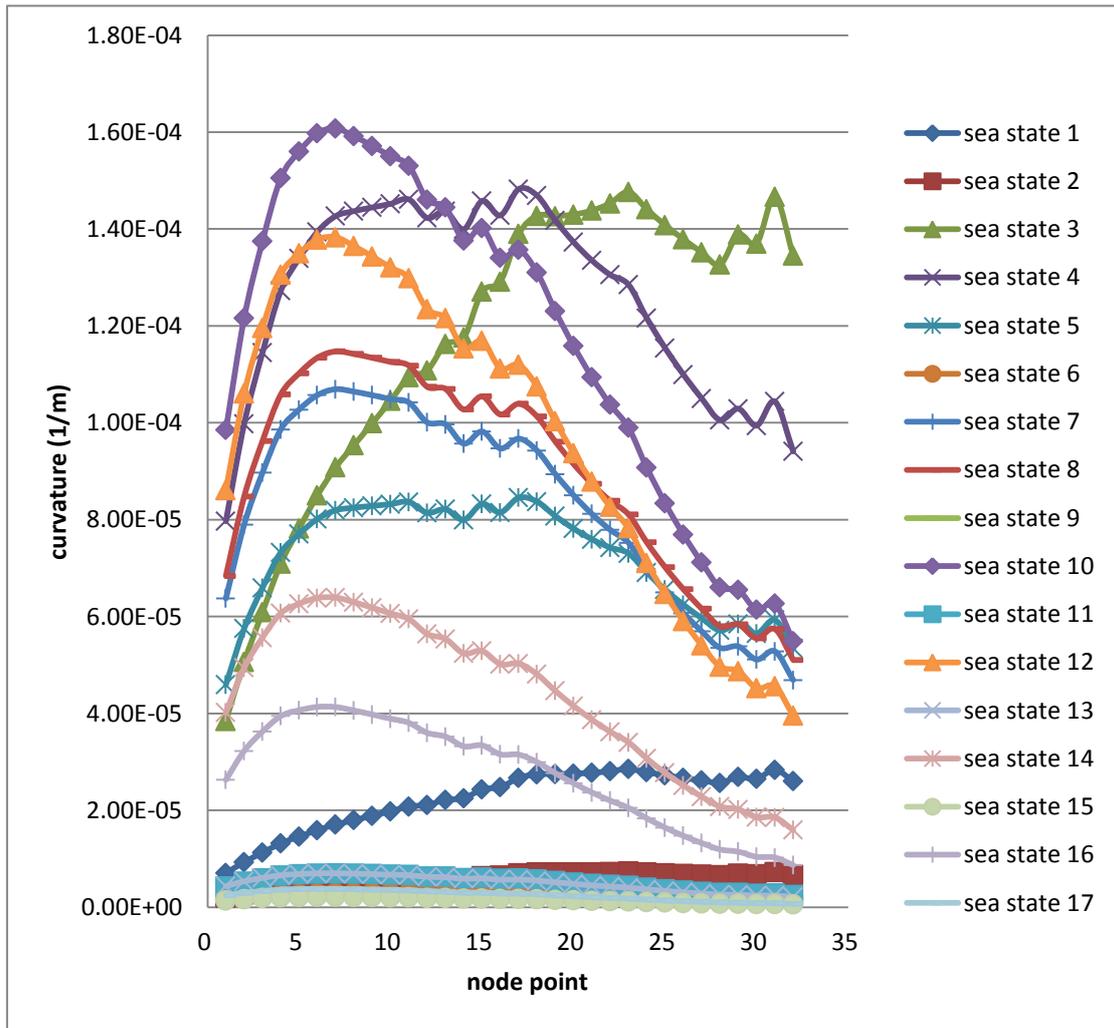
Figure 4-7 curvatures distribution of dynamic analysis along the flexible riser for top part of the riser (node 1 to node 32) in all 17 seat states

It could be seen that it is so difficult the estimate the critical point along the flexible riser. In principle, every point should be included to do the fatigue analysis and find the maximum damage along the bending stiffener. And the data is showing in the Table 4-3 dynamic analysis with bending stiffener's curvatures for all sea states

	sea state 1	sea state 2	sea state 3	sea state 4	sea state 5	sea state 6	sea state 7	sea state 8	sea state 9	sea state 10	sea state 11	sea state 12	sea state 13	sea state 14	sea state 15	sea state 16	sea state 17
	Dynamic analysis with bending stiffener's curvatures for all sea states																
1	8.91E-05	1.01E-04	9.61E-05	3.10E-04	3.21E-04	3.08E-04	5.52E-04	5.54E-04	5.28E-04	8.14E-04	7.71E-04	1.09E-03	1.03E-03	1.40E-03	1.29E-03	2.00E-03	3.02E-03
2	1.18E-04	1.33E-04	1.27E-04	3.89E-04	4.02E-04	3.86E-04	6.84E-04	6.87E-04	6.55E-04	1.00E-03	9.52E-04	1.35E-03	1.27E-03	1.72E-03	1.59E-03	2.46E-03	3.70E-03
3	1.43E-04	1.59E-04	1.52E-04	4.46E-04	4.61E-04	4.43E-04	7.77E-04	7.80E-04	7.44E-04	1.14E-03	1.08E-03	1.52E-03	1.43E-03	1.94E-03	1.79E-03	2.76E-03	4.15E-03
4	1.67E-04	1.85E-04	1.77E-04	4.95E-04	5.12E-04	4.92E-04	8.54E-04	8.58E-04	8.19E-04	1.24E-03	1.18E-03	1.66E-03	1.56E-03	2.11E-03	1.95E-03	3.01E-03	4.52E-03
5	1.85E-04	2.03E-04	1.95E-04	5.22E-04	5.38E-04	5.18E-04	8.90E-04	8.94E-04	8.53E-04	1.29E-03	1.22E-03	1.72E-03	1.62E-03	2.18E-03	2.02E-03	3.10E-03	4.64E-03
6	2.02E-04	2.20E-04	2.13E-04	5.43E-04	5.60E-04	5.40E-04	9.16E-04	9.20E-04	8.79E-04	1.32E-03	1.25E-03	1.75E-03	1.65E-03	2.22E-03	2.06E-03	3.15E-03	4.72E-03
7	2.16E-04	2.35E-04	2.27E-04	5.55E-04	5.72E-04	5.52E-04	9.26E-04	9.30E-04	8.90E-04	1.33E-03	1.26E-03	1.76E-03	1.66E-03	2.23E-03	2.06E-03	3.15E-03	4.71E-03
8	2.28E-04	2.46E-04	2.38E-04	5.59E-04	5.76E-04	5.57E-04	9.22E-04	9.26E-04	8.86E-04	1.32E-03	1.25E-03	1.73E-03	1.64E-03	2.19E-03	2.03E-03	3.09E-03	4.62E-03
9	2.39E-04	2.57E-04	2.50E-04	5.62E-04	5.79E-04	5.60E-04	9.16E-04	9.20E-04	8.81E-04	1.30E-03	1.24E-03	1.71E-03	1.61E-03	2.15E-03	2.00E-03	3.03E-03	4.51E-03
10	2.51E-04	2.68E-04	2.61E-04	5.65E-04	5.81E-04	5.63E-04	9.09E-04	9.13E-04	8.75E-04	1.28E-03	1.22E-03	1.68E-03	1.59E-03	2.11E-03	1.96E-03	2.96E-03	4.41E-03
11	2.63E-04	2.80E-04	2.74E-04	5.69E-04	5.84E-04	5.67E-04	9.03E-04	9.07E-04	8.70E-04	1.26E-03	1.21E-03	1.65E-03	1.56E-03	2.07E-03	1.92E-03	2.90E-03	4.30E-03
12	2.67E-04	2.83E-04	2.77E-04	5.54E-04	5.69E-04	5.52E-04	8.67E-04	8.71E-04	8.37E-04	1.21E-03	1.15E-03	1.57E-03	1.49E-03	1.96E-03	1.83E-03	2.74E-03	4.06E-03
13	2.81E-04	2.97E-04	2.91E-04	5.59E-04	5.74E-04	5.58E-04	8.63E-04	8.68E-04	8.34E-04	1.19E-03	1.14E-03	1.55E-03	1.46E-03	1.93E-03	1.80E-03	2.68E-03	3.96E-03
14	2.85E-04	3.00E-04	2.94E-04	5.45E-04	5.59E-04	5.44E-04	8.29E-04	8.33E-04	8.02E-04	1.14E-03	1.09E-03	1.47E-03	1.39E-03	1.82E-03	1.70E-03	2.53E-03	3.72E-03
15	3.08E-04	3.23E-04	3.18E-04	5.68E-04	5.82E-04	5.67E-04	8.51E-04	8.55E-04	8.24E-04	1.16E-03	1.11E-03	1.49E-03	1.41E-03	1.84E-03	1.72E-03	2.55E-03	3.73E-03
16	3.14E-04	3.28E-04	3.23E-04	5.56E-04	5.69E-04	5.55E-04	8.20E-04	8.25E-04	7.96E-04	1.11E-03	1.06E-03	1.41E-03	1.34E-03	1.75E-03	1.63E-03	2.40E-03	3.51E-03
17	3.38E-04	3.52E-04	3.47E-04	5.77E-04	5.91E-04	5.77E-04	8.38E-04	8.43E-04	8.15E-04	1.12E-03	1.08E-03	1.42E-03	1.36E-03	1.75E-03	1.64E-03	2.40E-03	3.49E-03

18	3.48E-04	3.61E-04	3.57E-04	5.72E-04	5.85E-04	5.72E-04	8.17E-04	8.21E-04	7.95E-04	1.08E-03	1.04E-03	1.37E-03	1.30E-03	1.67E-03	1.57E-03	2.28E-03	3.31E-03
19	3.48E-04	3.61E-04	3.57E-04	5.52E-04	5.64E-04	5.53E-04	7.74E-04	7.79E-04	7.56E-04	1.02E-03	9.80E-04	1.27E-03	1.22E-03	1.56E-03	1.46E-03	2.11E-03	3.04E-03
20	3.49E-04	3.61E-04	3.57E-04	5.35E-04	5.46E-04	5.36E-04	7.37E-04	7.42E-04	7.20E-04	9.57E-04	9.24E-04	1.19E-03	1.14E-03	1.45E-03	1.36E-03	1.95E-03	2.80E-03
21	3.52E-04	3.63E-04	3.60E-04	5.20E-04	5.31E-04	5.22E-04	7.03E-04	7.08E-04	6.89E-04	9.04E-04	8.74E-04	1.12E-03	1.07E-03	1.35E-03	1.27E-03	1.81E-03	2.58E-03
22	3.56E-04	3.66E-04	3.63E-04	5.08E-04	5.19E-04	5.11E-04	6.75E-04	6.80E-04	6.63E-04	8.57E-04	8.31E-04	1.05E-03	1.01E-03	1.26E-03	1.19E-03	1.68E-03	2.38E-03
23	3.62E-04	3.72E-04	3.69E-04	5.00E-04	5.10E-04	5.03E-04	6.52E-04	6.57E-04	6.42E-04	8.18E-04	7.95E-04	9.94E-04	9.57E-04	1.19E-03	1.12E-03	1.56E-03	2.20E-03
24	3.53E-04	3.62E-04	3.60E-04	4.73E-04	4.83E-04	4.77E-04	6.05E-04	6.11E-04	5.98E-04	7.50E-04	7.30E-04	9.03E-04	8.72E-04	1.07E-03	1.01E-03	1.40E-03	1.95E-03
25	3.45E-04	3.54E-04	3.52E-04	4.49E-04	4.58E-04	4.53E-04	5.63E-04	5.69E-04	5.58E-04	6.89E-04	6.73E-04	8.22E-04	7.96E-04	9.66E-04	9.20E-04	1.25E-03	1.73E-03
26	3.38E-04	3.46E-04	3.45E-04	4.28E-04	4.36E-04	4.32E-04	5.26E-04	5.32E-04	5.23E-04	6.36E-04	6.23E-04	7.51E-04	7.29E-04	8.75E-04	8.36E-04	1.12E-03	1.54E-03
27	3.32E-04	3.39E-04	3.38E-04	4.09E-04	4.17E-04	4.14E-04	4.93E-04	5.00E-04	4.92E-04	5.88E-04	5.78E-04	6.87E-04	6.69E-04	7.95E-04	7.62E-04	1.01E-03	1.37E-03
28	3.25E-04	3.32E-04	3.32E-04	3.92E-04	3.99E-04	3.97E-04	4.64E-04	4.70E-04	4.64E-04	5.46E-04	5.38E-04	6.31E-04	6.17E-04	7.23E-04	6.97E-04	9.08E-04	1.22E-03
29	3.41E-04	3.48E-04	3.47E-04	4.01E-04	4.08E-04	4.07E-04	4.66E-04	4.73E-04	4.68E-04	5.41E-04	5.36E-04	6.20E-04	6.07E-04	7.04E-04	6.81E-04	8.73E-04	1.16E-03
30	3.36E-04	3.43E-04	3.42E-04	3.87E-04	3.94E-04	3.93E-04	4.43E-04	4.50E-04	4.46E-04	5.07E-04	5.04E-04	5.75E-04	5.65E-04	6.46E-04	6.28E-04	7.92E-04	1.04E-03
31	3.60E-04	3.66E-04	3.67E-04	4.06E-04	4.14E-04	4.14E-04	4.58E-04	4.66E-04	4.63E-04	5.18E-04	5.16E-04	5.80E-04	5.73E-04	6.46E-04	6.31E-04	7.81E-04	1.01E-03
32	3.30E-04	3.36E-04	3.36E-04	3.66E-04	3.73E-04	3.73E-04	4.06E-04	4.14E-04	4.12E-04	4.54E-04	4.54E-04	5.03E-04	4.99E-04	5.55E-04	5.45E-04	6.62E-04	8.41E-04

Table 4-3 dynamic analysis with bending stiffener's curvatures for all sea states

However, a simple way to estimate the damage could be done with simple calculation first in order to save the time.

It could be thought that the larger curvature has the larger damage during each time of the cycle. So time the curvature with the probability of the sea state each correspondingly and it could get the estimated damage results. It could be done with the function below

$$\text{estimated damage} = \sum_{i=1}^{17} \text{point's curvature per sea state} \times \text{probability for the sea state (i)}$$

The result is showing in the Table 4-4 dynamic analysis with bending stiffener's curvatures considering the probabilities for all sea states and estimated damage result

Dynamic analysis with bending stiffener's curvatures considering the probabilities for all sea states and estimated damage result

No.	sea state 1	sea state 2	sea state 3	sea state 4	sea state 5	sea state 6	sea state 7	sea state 8	sea state 9	sea state 10	sea state 11	sea state 12	sea state 13	sea state 14	sea state 15	sea state 16	sea state 17
1	7.03E-06	2.01E-06	3.84E-05	7.97E-05	4.60E-05	1.63E-06	6.37E-05	6.84E-05	1.78E-06	9.85E-05	4.27E-06	8.61E-05	4.35E-06	4.02E-05	1.37E-06	2.63E-05	2.43E-06
2	9.31E-06	2.63E-06	5.06E-05	9.98E-05	5.75E-05	2.04E-06	7.90E-05	8.48E-05	2.21E-06	1.22E-04	5.27E-06	1.06E-04	5.36E-06	4.94E-05	1.68E-06	3.23E-05	2.98E-06
3	1.13E-05	3.16E-06	6.09E-05	1.14E-04	6.59E-05	2.34E-06	8.97E-05	9.62E-05	2.51E-06	1.37E-04	5.96E-06	1.20E-04	6.05E-06	5.57E-05	1.89E-06	3.63E-05	3.34E-06
4	1.32E-05	3.67E-06	7.10E-05	1.27E-04	7.32E-05	2.60E-06	9.86E-05	1.06E-04	2.76E-06	1.51E-04	6.53E-06	1.31E-04	6.61E-06	6.07E-05	2.06E-06	3.95E-05	3.63E-06
5	1.46E-05	4.03E-06	7.82E-05	1.34E-04	7.71E-05	2.74E-06	1.03E-04	1.10E-04	2.88E-06	1.56E-04	6.77E-06	1.35E-04	6.83E-06	6.26E-05	2.13E-06	4.06E-05	3.74E-06
6	1.59E-05	4.37E-06	8.50E-05	1.39E-04	8.01E-05	2.85E-06	1.06E-04	1.13E-04	2.96E-06	1.60E-04	6.94E-06	1.38E-04	6.98E-06	6.38E-05	2.17E-06	4.14E-05	3.80E-06
7	1.71E-05	4.66E-06	9.08E-05	1.43E-04	8.19E-05	2.92E-06	1.07E-04	1.15E-04	3.00E-06	1.61E-04	6.99E-06	1.38E-04	7.01E-06	6.39E-05	2.18E-06	4.13E-05	3.79E-06
8	1.80E-05	4.88E-06	9.54E-05	1.44E-04	8.25E-05	2.94E-06	1.06E-04	1.14E-04	2.99E-06	1.59E-04	6.92E-06	1.36E-04	6.92E-06	6.30E-05	2.15E-06	4.06E-05	3.71E-06
9	1.89E-05	5.11E-06	9.99E-05	1.44E-04	8.28E-05	2.96E-06	1.06E-04	1.13E-04	2.97E-06	1.57E-04	6.84E-06	1.34E-04	6.82E-06	6.18E-05	2.11E-06	3.98E-05	3.63E-06
10	1.98E-05	5.33E-06	1.05E-04	1.45E-04	8.32E-05	2.97E-06	1.05E-04	1.13E-04	2.95E-06	1.55E-04	6.75E-06	1.32E-04	6.71E-06	6.06E-05	2.07E-06	3.89E-05	3.55E-06
11	2.08E-05	5.57E-06	1.09E-04	1.46E-04	8.37E-05	2.99E-06	1.04E-04	1.12E-04	2.93E-06	1.53E-04	6.67E-06	1.30E-04	6.60E-06	5.95E-05	2.03E-06	3.81E-05	3.46E-06
12	2.11E-05	5.63E-06	1.11E-04	1.42E-04	8.14E-05	2.92E-06	1.00E-04	1.07E-04	2.82E-06	1.46E-04	6.37E-06	1.23E-04	6.28E-06	5.64E-05	1.93E-06	3.60E-05	3.26E-06
13	2.22E-05	5.90E-06	1.16E-04	1.44E-04	8.22E-05	2.95E-06	9.97E-05	1.07E-04	2.81E-06	1.44E-04	6.31E-06	1.22E-04	6.19E-06	5.54E-05	1.90E-06	3.52E-05	3.19E-06
14	2.25E-05	5.95E-06	1.18E-04	1.40E-04	8.00E-05	2.87E-06	9.57E-05	1.03E-04	2.70E-06	1.38E-04	6.02E-06	1.15E-04	5.88E-06	5.24E-05	1.80E-06	3.32E-05	2.99E-06
15	2.43E-05	6.42E-06	1.27E-04	1.46E-04	8.33E-05	2.99E-06	9.82E-05	1.05E-04	2.78E-06	1.40E-04	6.14E-06	1.17E-04	5.96E-06	5.29E-05	1.82E-06	3.34E-05	3.00E-06
16	2.48E-05	6.52E-06	1.29E-04	1.43E-04	8.15E-05	2.93E-06	9.47E-05	1.02E-04	2.68E-06	1.34E-04	5.88E-06	1.11E-04	5.68E-06	5.02E-05	1.72E-06	3.15E-05	2.83E-06
17	2.67E-05	7.00E-06	1.39E-04	1.48E-04	8.45E-05	3.05E-06	9.67E-05	1.04E-04	2.75E-06	1.36E-04	5.96E-06	1.12E-04	5.73E-06	5.03E-05	1.73E-06	3.15E-05	2.81E-06
18	2.75E-05	7.18E-06	1.43E-04	1.47E-04	8.37E-05	3.02E-06	9.43E-05	1.01E-04	2.68E-06	1.31E-04	5.76E-06	1.07E-04	5.50E-06	4.81E-05	1.66E-06	3.00E-05	2.66E-06

19	2.75E-05	7.17E-06	1.43E-04	1.42E-04	8.08E-05	2.92E-06	8.94E-05	9.61E-05	2.55E-06	1.23E-04	5.42E-06	1.00E-04	5.14E-06	4.47E-05	1.54E-06	2.77E-05	2.45E-06
20	2.76E-05	7.18E-06	1.43E-04	1.37E-04	7.82E-05	2.83E-06	8.50E-05	9.15E-05	2.43E-06	1.16E-04	5.11E-06	9.38E-05	4.82E-06	4.15E-05	1.44E-06	2.56E-05	2.25E-06
21	2.78E-05	7.21E-06	1.44E-04	1.34E-04	7.60E-05	2.76E-06	8.12E-05	8.74E-05	2.32E-06	1.09E-04	4.84E-06	8.79E-05	4.52E-06	3.87E-05	1.34E-06	2.37E-05	2.07E-06
22	2.81E-05	7.27E-06	1.45E-04	1.31E-04	7.42E-05	2.70E-06	7.79E-05	8.39E-05	2.23E-06	1.04E-04	4.60E-06	8.27E-05	4.26E-06	3.62E-05	1.26E-06	2.20E-05	1.91E-06
23	2.85E-05	7.38E-06	1.48E-04	1.29E-04	7.31E-05	2.66E-06	7.52E-05	8.11E-05	2.16E-06	9.90E-05	4.40E-06	7.82E-05	4.04E-06	3.40E-05	1.19E-06	2.05E-05	1.77E-06
24	2.79E-05	7.20E-06	1.44E-04	1.22E-04	6.91E-05	2.52E-06	6.98E-05	7.53E-05	2.01E-06	9.07E-05	4.04E-06	7.10E-05	3.68E-06	3.07E-05	1.07E-06	1.84E-05	1.57E-06
25	2.72E-05	7.03E-06	1.41E-04	1.15E-04	6.56E-05	2.39E-06	6.50E-05	7.02E-05	1.88E-06	8.34E-05	3.73E-06	6.47E-05	3.36E-06	2.77E-05	9.72E-07	1.64E-05	1.40E-06
26	2.67E-05	6.87E-06	1.38E-04	1.10E-04	6.25E-05	2.28E-06	6.07E-05	6.57E-05	1.76E-06	7.69E-05	3.45E-06	5.91E-05	3.08E-06	2.51E-05	8.84E-07	1.47E-05	1.24E-06
27	2.62E-05	6.73E-06	1.35E-04	1.05E-04	5.97E-05	2.18E-06	5.70E-05	6.16E-05	1.66E-06	7.12E-05	3.20E-06	5.41E-05	2.83E-06	2.28E-05	8.05E-07	1.32E-05	1.10E-06
28	2.57E-05	6.60E-06	1.33E-04	1.01E-04	5.71E-05	2.10E-06	5.36E-05	5.80E-05	1.56E-06	6.60E-05	2.98E-06	4.97E-05	2.61E-06	2.08E-05	7.36E-07	1.19E-05	9.81E-07
29	2.69E-05	6.91E-06	1.39E-04	1.03E-04	5.85E-05	2.15E-06	5.38E-05	5.84E-05	1.58E-06	6.55E-05	2.96E-06	4.87E-05	2.57E-06	2.02E-05	7.19E-07	1.15E-05	9.31E-07
30	2.65E-05	6.81E-06	1.37E-04	9.94E-05	5.65E-05	2.08E-06	5.11E-05	5.55E-05	1.50E-06	6.14E-05	2.79E-06	4.52E-05	2.39E-06	1.86E-05	6.64E-07	1.04E-05	8.34E-07
31	2.84E-05	7.28E-06	1.47E-04	1.04E-04	5.93E-05	2.18E-06	5.28E-05	5.74E-05	1.56E-06	6.27E-05	2.85E-06	4.56E-05	2.42E-06	1.86E-05	6.66E-07	1.03E-05	8.11E-07
32	2.60E-05	6.68E-06	1.35E-04	9.41E-05	5.35E-05	1.97E-06	4.69E-05	5.10E-05	1.39E-06	5.49E-05	2.51E-06	3.96E-05	2.11E-06	1.59E-05	5.75E-07	8.70E-06	6.77E-07

Table 4-4 dynamic analysis with bending stiffener's curvatures considering the probabilities for all sea states and estimated damage result

Then add all the damage for every nude in the bending stiffener to get the large damage position in the riser. The result could be got in the Figure 4-8 estimate damage.
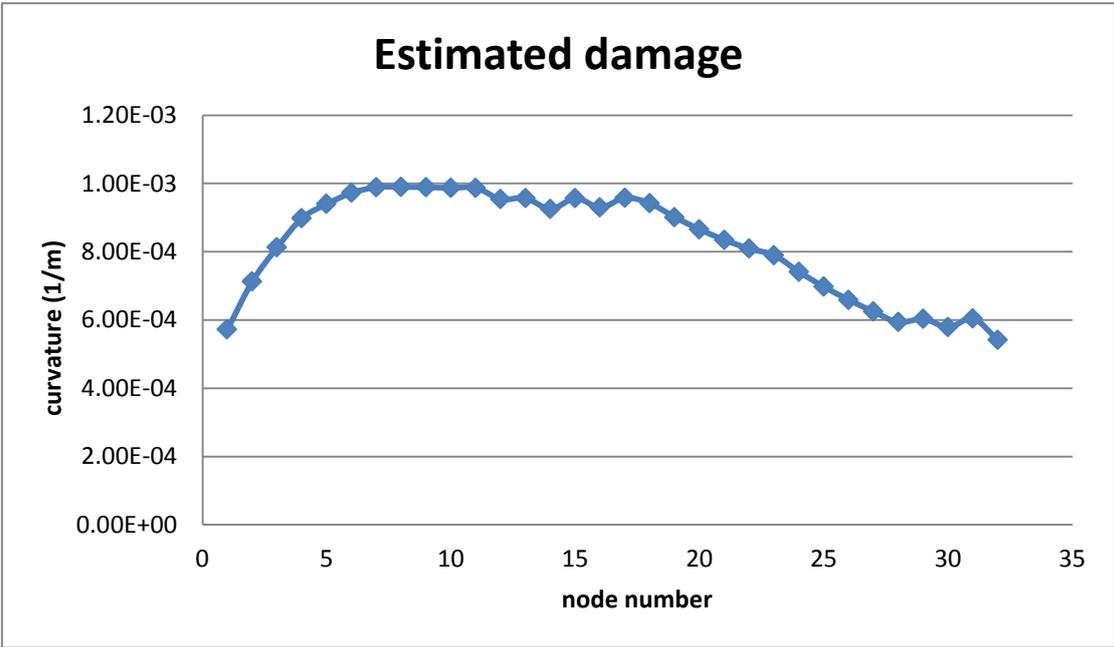
Figure 4-8 estimate damage

It could be seen from the Figure 4-8 that the points from 5 to 14, point 15 and point 17 has the larger value than other points in the riser. They are in the top part of the bending stiffener. The reason is that the distribution of the bending stiffness and bending moment owning the different decrease speed.
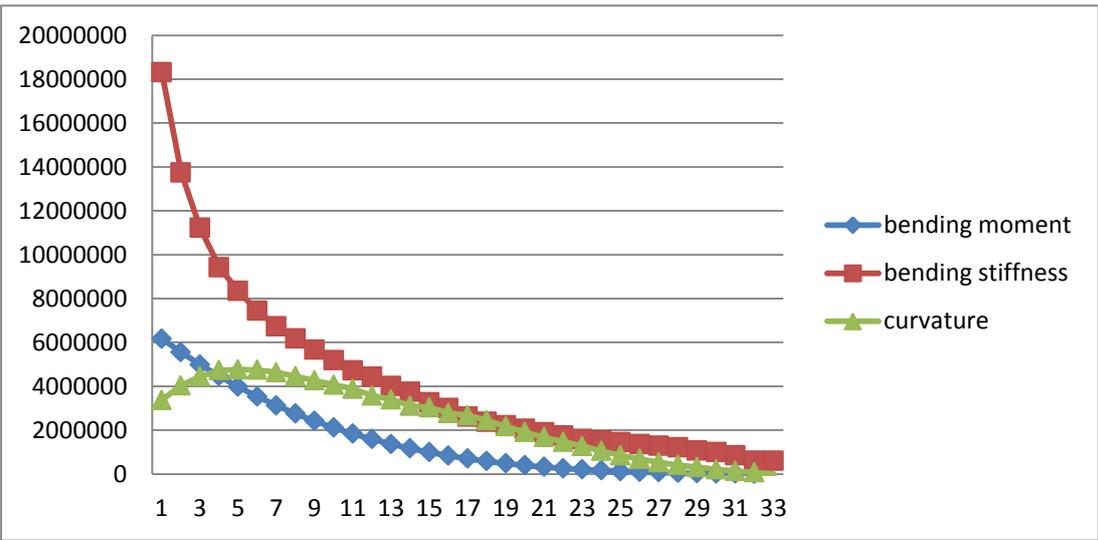
Figure 4-9 distribution of the bending moment, bending stiffness and curvature

54

Multiply the curvature with -1000000000 and bending moment with -100, the final result is showing in the

Figure 4-9. It could be seen that the node point 5 has the large curvature. However, this is the result from the static analysis.

The data result of all the result could be found in the Table 4-4. And the damage for each of the point is showing in the Table 4-5. The yellow line is showing the largest value and red lines illustrate the distribution of the estimated damage

nude number	Estimated damage
1	5.7220E-04
2	7.1251E-04
3	8.1274E-04
4	8.9820E-04
5	9.4002E-04
6	9.7251E-04
7	9.8901E-04
8	9.8988E-04
9	9.8874E-04
10	9.8723E-04
11	9.8679E-04
12	9.5422E-04
13	9.5687E-04
14	9.2519E-04
15	9.5674E-04
16	9.2989E-04
17	9.5772E-04
18	9.4150E-04
19	9.0115E-04
20	8.6533E-04
21	8.3439E-04
22	8.0885E-04
23	7.8953E-04
24	7.4069E-04
25	6.9734E-04
26	6.5881E-04
27	6.2443E-04
28	5.9353E-04
29	6.0307E-04
30	5.7865E-04
31	6.0386E-04
32	5.4112E-04

Table 4-5 total estimate damage for bending stiffener

It could be seen that the largest damage is happening at the point 8 at the top part of the bending stiffener. So the point 8 has been chosen as the critical point to do the local fatigue analysis in BFLEX.

It also should be noticed that the other points beside the point number 8 are also having a considerable large value comparing with the result of point number 8. It should also be analyzed if much more investigation required to be done.

What's more, the curvature in the Figure 4-7 is the resultant mean curvature with the mean value of both y axial and z axial. The following formulation should be applied to get the resultant mean curvature

$$k = \sqrt{k_y^2 + k_z^2} \qquad (25)$$

k is the resultant mean curvature, k_y is the mean curvature for the local y axial, k_z is the mean curvature for the local z axial. The sea surface is around node number 46 and it could be shown that the distribution of the curvature decreases separately based on different sea states with different maximum and decreasing speed. It should be noticed that the signal for both y axial and z axial should be included in order to do the rain flow counting. It is encouraged to use the formula below to find the resultant curvature.

$$k = k_y\sqrt{1 + \alpha^2}$$
$$k_y = \alpha k_z \qquad (26)$$

The series number 17 is the worst sea state among all the sea states so that it has the largest curvature in the water at the top part of the flexible riser. However, the bending stiffness part should be focused because it is under the large tensile compared with the other part of the risers.

4.2.2 Do the short term analysis simulation

Since the critical point in the riser has been found, the simulation for this point in the dynamic analysis should be executed. The irregular wave parameters, which are significant wave and wave period, are set with the 17 sea states. The total time for each of the sea state is 3 hours and the time step is set to be 0.2 seconds. It is possible to have small step to simulate the wave process accurately. It should be noticed that the time step should be as small as possible, but the arrays stored in the result file is limited. For example, it will beyond the stored arrays in the result file when the time

step is set to be less than 0.15 second in three hours' calculation. So the curvature history of time series could be found in the Figure 4-10.
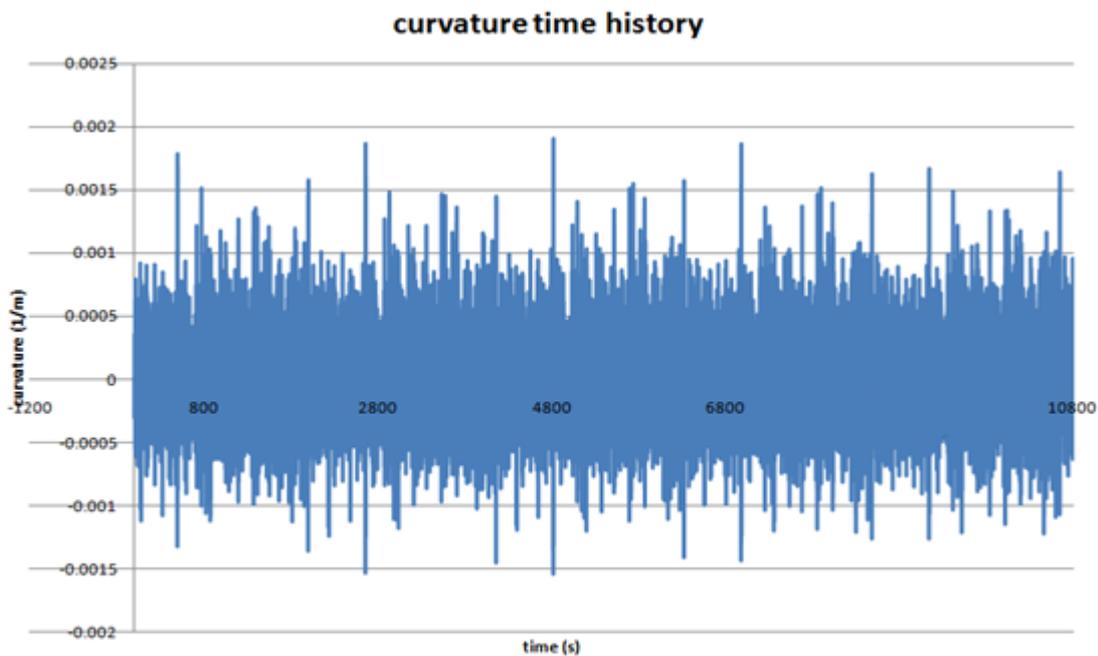
Figure 4-10 curvature time history for sea state 1

This result is showing the time series of the curvature. It could be showing that the curvature range is mainly changing from -0.0005 to 0.001. The range is almost the same as the result showing in the Figure 4-6. The rain flow counting method is just to find the range and mean value of this time history. And the result could be found in the next section. What's more, the finally fatigue damage is the also based on the result here, which is simulated during 3 hours in RFLEX. This is only the data from sea state 1, which is the safest sea state. Each of the sea state should have one curvature time history in order to do the rain flow counting. So 17 sea state blocking data are found based on the 17 curvature history series lines in total.

5 Result for Local fatigue analysis for the stub model for the cross-section of the flexible riser

5.1 Rain flow counting result

The rain flow counting is used to find the cycle number of the curvature. Both mean value of the curvature and curvature range are found for the cycle number each.
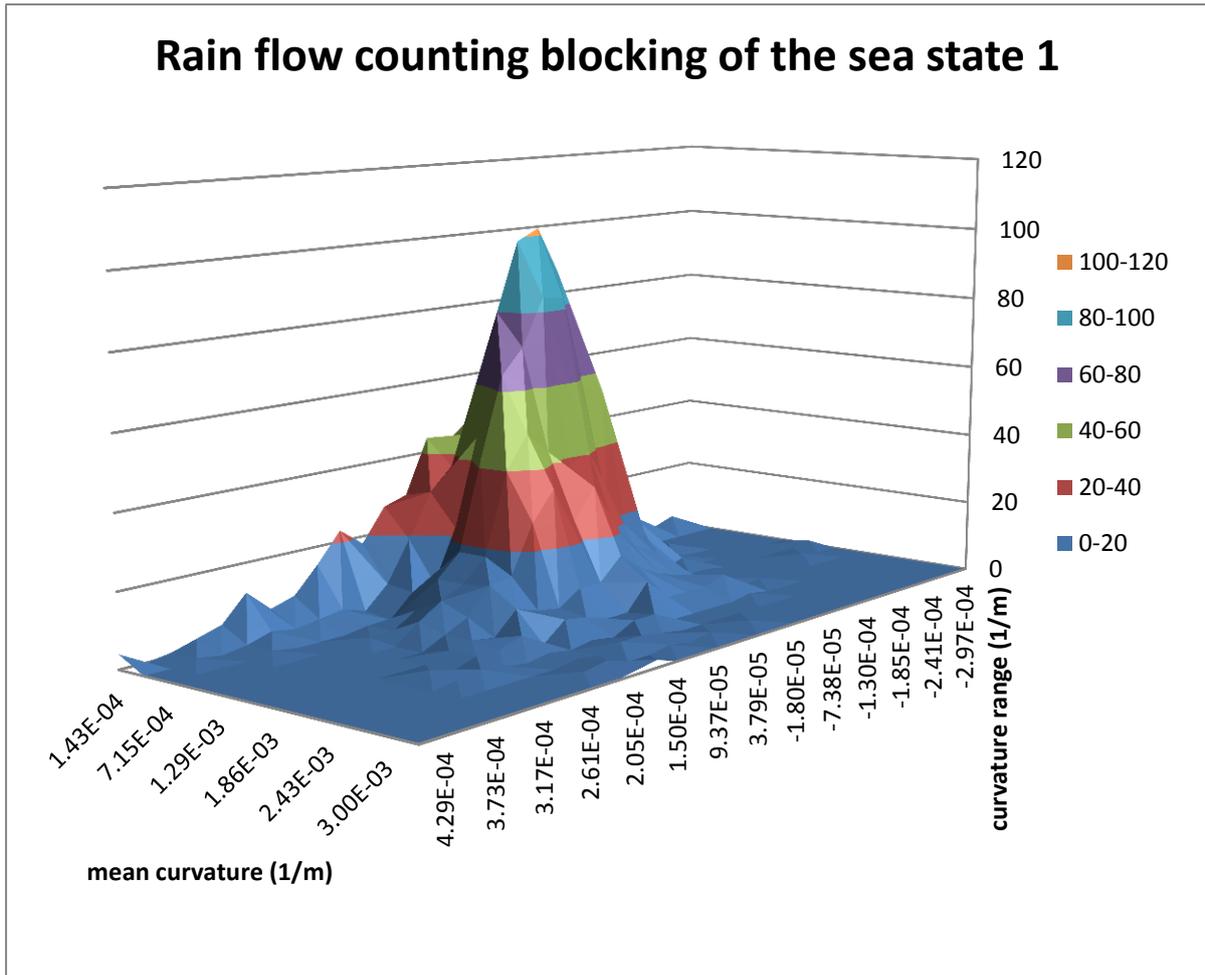
Figure 5-1 rain flow counting data blocking chart

Since the simulation result is based on the 3 hours, the probability of the sea state should be taken into consideration in the curvature range. For each of the sea state, the finally result, which is considered the probability of the sea state, should be calculated with the function following

$$N = n(i) \times \frac{24\ hours \times 365\ days \times P(i)}{3\ hours} \tag{27}$$

N : real number of cycle for sea state i per year

P(i) : probability of sea state i

n(i) : number of cycle counted form the rain flow counting method

The aiming of this step is to find the real cycle number with the combination of the mean curvature and curvature range. It is also needed to consider the probability of the sea state leading to the final cycle number. Generally, the distribution during the single range of the blocking result is considered as the linear distribution or average distribution. And the distance between each of the intersection for both the range and mean value is also be set as the same. This is also another reason leading to the final blocking shape in the Table 5-1 sea state probability. The most important thing is that the error of this kind of method is not very large for the fatigue analysis. Because only the whole distribution of the mean curvature and curvature range should be considered at the same time and the distribution of these is not varying with the little change of the mean curvature and the curvature range.

The sea state probability is showing in Table 5-1 sea state probability.

Significant wave height m	Wave period s	frequency	probability
1	6	1569	0.07892
1	11	395	0.01987
1	17	12	0.00060
2	7	5106	0.25684
2	11	2846	0.14316
2	17	105	0.00528
3	7	2295	0.11544
3	12	2452	0.12334
3	18	67	0.00337
4	9	2406	0.12103
4	17	110	0.00553
5	10	1564	0.07867
5	17	84	0.00423
6	10	571	0.02872
6	18	21	0.00106
8	13	261	0.01313
11	15	16	0.00080
sum		19880	1

Table 5-1 sea state probability

It could be seen that the distribution of the sea state is not linear distribution. But the worst sea state and the most safety sea state have the lower probability. The modest sea state has the high probability. There is also some very low probability or frequency in these sea state. It is mainly because the blocking of North sea state based on the fatigue damage.

blocking of the data from rain flow counting			curvature range (1/m)												sum
			2.31E-09 to 2.58E-03	2.58E-03 to 5.16E-03	5.16E-03 to 7.74E-03	7.74E-03 to 1.03E-02	1.03E-02 to 1.29E-02	1.29E-02 to 1.55E-02	1.55E-02 to 1.81E-02	1.81E-02 to 2.07E-02	2.07E-02 to 2.32E-02	2.32E-02 to 2.58E-02	2.58E-02 to 2.84E-02	2.84E-02 to 3.10E-02	
curvature mean value (1/m)	-2.36E-03	to	-1.65E-03	1078	0	0	0	0	0	0	0	0	0	0	0	1078
	-1.65E-03	to	-9.38E-04	7645	0	0	0	0	0	0	0	0	0	0	0	7645
	-9.38E-04	to	-2.29E-04	223829	10	0	0	0	10	0	0	0	0	0	0	223850
	-2.29E-04	to	4.80E-04	3872046	628891	23116	389	0	21	0	0	0	0	0	0	4524464
	4.80E-04	to	1.19E-03	379178	276920	114661	12548	379	31	31	0	0	0	0	0	783747
	1.19E-03	to	1.90E-03	62817	20343	33529	21535	5607	2091	168	335	31	0	0	0	146457
	1.90E-03	to	2.61E-03	15359	397	1742	6869	3013	1947	753	0	168	0	10	0	30258
	2.61E-03	to	3.31E-03	4499	168	10	421	1981	533	202	10	21	0	0	10	7855
	3.31E-03	to	4.02E-03	1280	10	0	188	10	188	21	31	21	10	0	21	1779
	4.02E-03	to	4.73E-03	376	10	0	0	0	0	31	10	10	0	0	0	438
	4.73E-03	to	5.44E-03	31	0	0	0	0	0	0	10	10	10	0	0	62
	5.44E-03	to	6.15E-03	10	0	0	0	0	10	0	0	0	0	0	0	21
sum				4.57E+06	9.27E+05	1.73E+05	4.19E+04	1.10E+04	4.83E+03	1.20E+03	3.97E+02	2.60E+02	2.05E+01	1.03E+01	3.08E+01	5.728E+06

Table 5-2 Blocking all the 17 sea states using the combination with curvature mean value and curvature range

Case number	Cycle number	mean angle (degree)	curvature angle (degree)	positive factor	negative factor
1	3872046	2.50E-06	2.58E-05	6.2	-4.2
2	628891	2.50E-06	7.74E-05	16.5	-14.5
3	379178	1.67E-05	2.58E-05	1.8	0.2
4	276920	1.67E-05	7.74E-05	3.3	-1.3
5	223829	-1.17E-05	2.58E-05	-0.1	2.1
6	114661	1.67E-05	1.29E-04	4.9	-2.9
7	62817	3.09E-05	2.58E-05	1.4	0.6
8	33529	3.09E-05	1.29E-04	3.1	-1.1
9	23116	2.50E-06	1.29E-04	26.8	-24.8
10	21535	3.09E-05	1.81E-04	3.9	-1.9
11	20343	3.09E-05	7.74E-05	2.3	-0.3
12	15359	4.50E-05	2.58E-05	1.3	0.7
13	12548	1.67E-05	1.81E-04	6.4	-4.4
14	7645	-2.58E-05	2.58E-05	0.5	1.5
15	6869	4.50E-05	1.81E-04	3.0	-1.0
16	5607	3.09E-05	2.32E-04	4.8	-2.8
17	4499	5.92E-05	2.58E-05	1.2	0.8
18	3013	4.50E-05	2.32E-04	3.6	-1.6
19	2091	3.09E-05	2.84E-04	5.6	-3.6
20	1981	5.92E-05	2.32E-04	3.0	-1.0
21	1947	4.50E-05	2.84E-04	4.2	-2.2
22	1742	4.50E-05	1.29E-04	2.4	-0.4
23	1280	7.34E-05	2.58E-05	1.2	0.8
24	1078	-4.00E-05	2.58E-05	0.7	1.3
25	753	4.50E-05	3.36E-04	4.7	-2.7
26	533	5.92E-05	2.84E-04	3.4	-1.4
27	421	5.92E-05	1.81E-04	2.5	-0.5
28	397	4.50E-05	7.74E-05	1.9	0.1
29	389	2.50E-06	1.81E-04	37.1	-35.1
30	379	1.67E-05	2.32E-04	8.0	-6.0
31	376	8.76E-05	2.58E-05	1.1	0.9
32	335	3.09E-05	3.87E-04	7.3	-5.3
33	202	5.92E-05	3.36E-04	3.8	-1.8
34	188	7.34E-05	1.81E-04	2.2	-0.2
35	188	7.34E-05	2.84E-04	2.9	-0.9
36	168	5.92E-05	7.74E-05	1.7	0.3
37	168	3.09E-05	3.36E-04	6.4	-4.4
38	168	4.50E-05	4.39E-04	5.9	-3.9

Table 5-3 Input angle for BFLEX

The mean angle means the angle needs to be set in the boundary of the flexible riser to simulate the curvature to be the mean curvature value. It could be calculated with the function in the following

$$\theta = l \times k \qquad\qquad (28)$$

Which for

θis the rotation angle relative to the curvature for the chosed element.

 L is the length of the element.

 K is the curvature got from the result of riflex.

And the curvature angle is also calculated by this way. However, the value of the curvature angle is no longer important in BFLEX since the loading control factor induced. It is the factor multiplied with the load value or the angle value as the real loading condition when calculating the result. the positive factor and the negative factor should be found with the value of curvature divided by mean curvature. It should be the same for curvature angle divided by mean angle.

Neglect the cycle number smaller than 100 and input the data into the BFLEX2010. The 38 cases have the different loading case under the same condition.
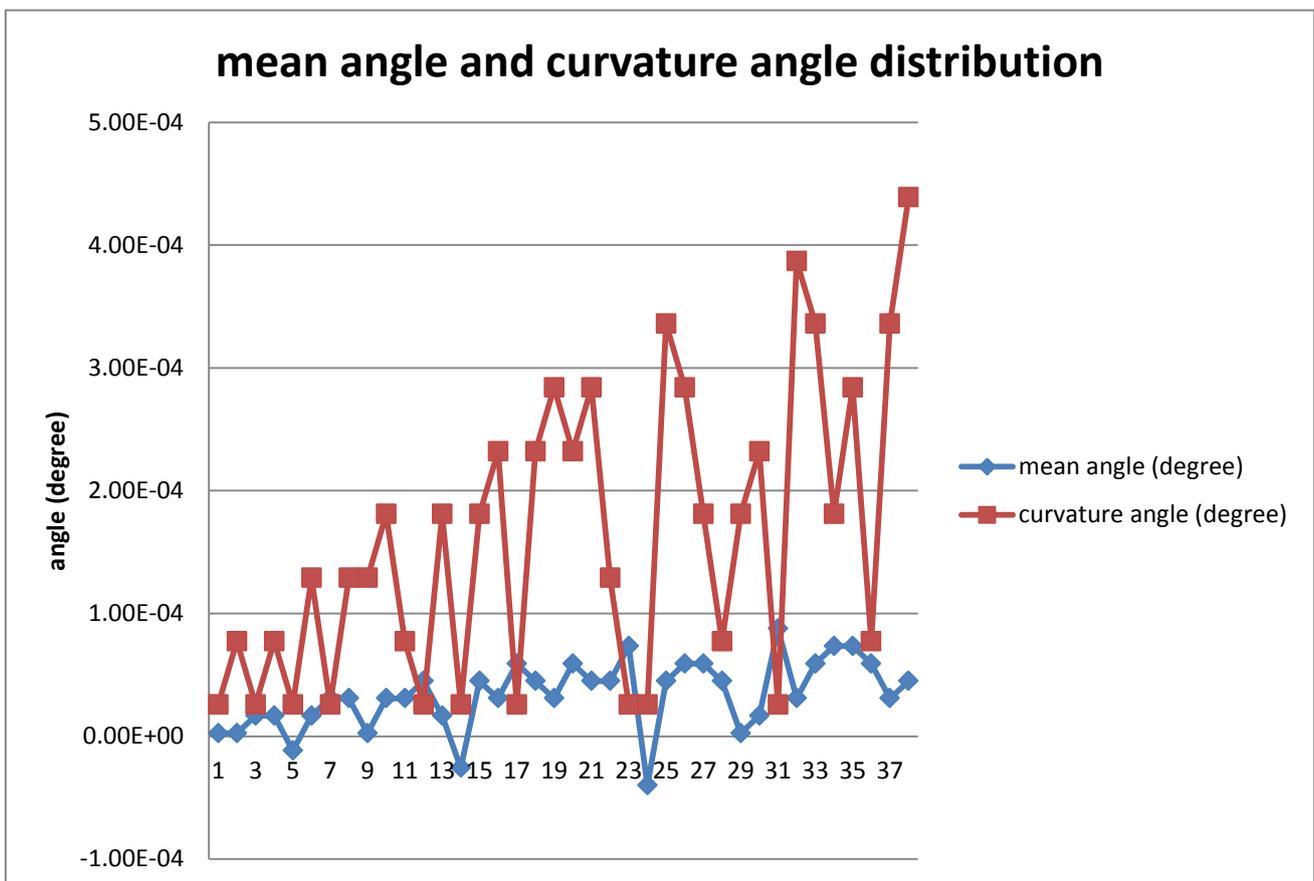
Figure 5-2 mean angle and curvature angle distribution

The case is ranged based on the number of cycles. The mean value is almost the same with the number of cycles' decreasing. It just increases a little bit. However the curvature angle is increasing significantly comparing with the mean angle. This is because the large curvature has small cycle

number in usual. This is the reasonable result from the rain flow counting method. And each of the case should be input into the *.2bif file in BLFEX2010. Then change the mean stress correction code in the BFLEX2010 in the lifetime model. It is necessary to consider the linear and nonlinear material with these cases. If the linear material is used, there is no need to do the mean stress correction. If the nonlinear material is used, the mean stress correction should be considered. The result is showing in the Figure 5-3 damage comparison with or without mean stress correction. It could seen that for large range curvature with small number of cycle has the less fatigue damage than the small range of the curvature with the large number cycles. The linear material has the larger damage than the nonlinear material with the mean stress correction. However, more detail data should be investigated in the following parts in order to compare the different mean stress correction's influence on the fatigue damage since the fatigue analysis's condition is different with or without the mean stress correction.

case number	linear material with no mean stress correction	nonlinear material with mean stress correction
	damage	damage
1	1.45E-04	2.44E-06
2	1.71E-03	9.09E-05
3	3.05E-05	6.56E-07
4	2.77E-25	2.77E-25
5	8.00E-05	2.51E-06
6	1.15E-25	1.15E-25
7	5.64E-06	1.24E-07
8	3.35E-26	3.35E-26
9	1.42E-07	6.34E-10
10	2.15E-26	2.15E-26
11	2.03E-26	2.03E-26
12	1.59E-06	1.54E-26
13	1.25E-26	1.25E-26
14	6.55E-07	1.42E-08
15	6.87E-27	6.87E-27
16	5.61E-27	5.61E-27
17	5.99E-07	4.50E-27
18	3.01E-27	3.01E-27
19	2.09E-27	2.09E-27
20	1.98E-27	1.98E-27
21	1.95E-27	1.95E-27
22	1.74E-27	1.74E-27
23	1.64E-05	1.20E-06
24	1.20E-07	2.79E-09
25	7.53E-28	7.53E-28
26	5.33E-28	5.33E-28
27	4.21E-28	4.21E-28
28	3.97E-28	3.97E-28
29	7.26E-07	3.51E-08
30	3.79E-28	3.79E-28
31	1.14E-07	3.40E-09
32	3.35E-28	3.35E-28

33	2.02E-28	2.02E-28
34	1.88E-28	1.88E-28
35	1.88E-28	1.88E-28
36	1.68E-28	1.68E-28
37	1.68E-28	1.68E-28
38	1.68E-28	1.68E-28
accumulative damage	1.99E-03	9.79E-05

Figure 5-3 damage comparison with or without mean stress correction

5.2 Fatigue damage calculation result

The fatigue damage should be found based on the critical point in the zeta layer. Usually, zeta layer has the highest probability to failure and it is the layer which is holding the inner pressure in the flexible riser. This could be found in the Figure 5-4 Fatigue damage for the part of flexible riser. This is one case of the 38 cases. In order to see it clearly, the riser's cross section is cut out and the blue part owning the fatigue damage with 5.3E-24. It could be seen that only the zeta cross section has the larger fatigue damage within the whole riser.

According to the Figure 5-5 the selected critical point in zeta layer, it could be seen that the edge of
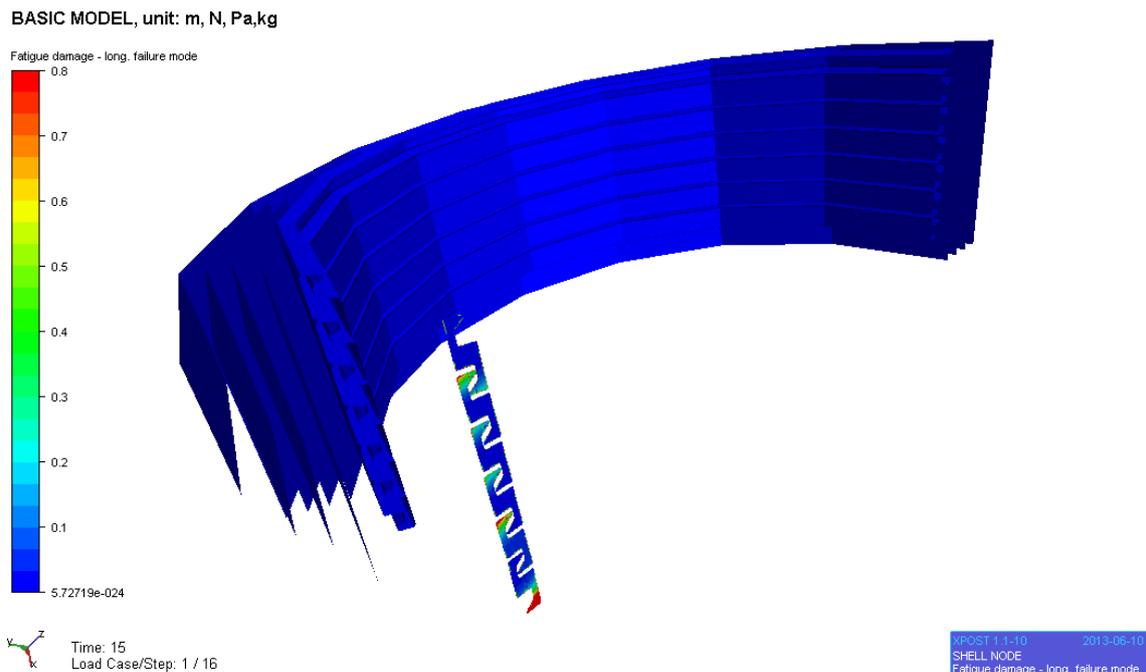
Figure 5-4 Fatigue damage for the part of flexible riser

the zeta layer's cross section has the large damage than the other place. So the critical point is selected along the edge. The reason for selecting point 10197 and point 6272 is because that these two points are at the inner position of the zeta layers. So the damage cause is totally because of the zeta layer itself. Most of the reason is friction and normal stress. For the other part except for the point 10197 and point 6272, the fatigue damage is also very important but mostly the damage is caused by other layer. What's more, the finite element size is different for different position along the edge of the zeta layer's cross section. The blue color in the Figure 5-5 the selected critical point in zeta layer is showing the lowest fatigue damage with the value of 5.72E-24. But the mainly interesting point in this report is to discuss the mean stress correction's influence on the fatigue damage. So the point location and dividing finite element are not that significant. It is also should be

noticed that this zeta section is in the middle of the flexible riser's part. This is to neglect the boundary condition's influence.
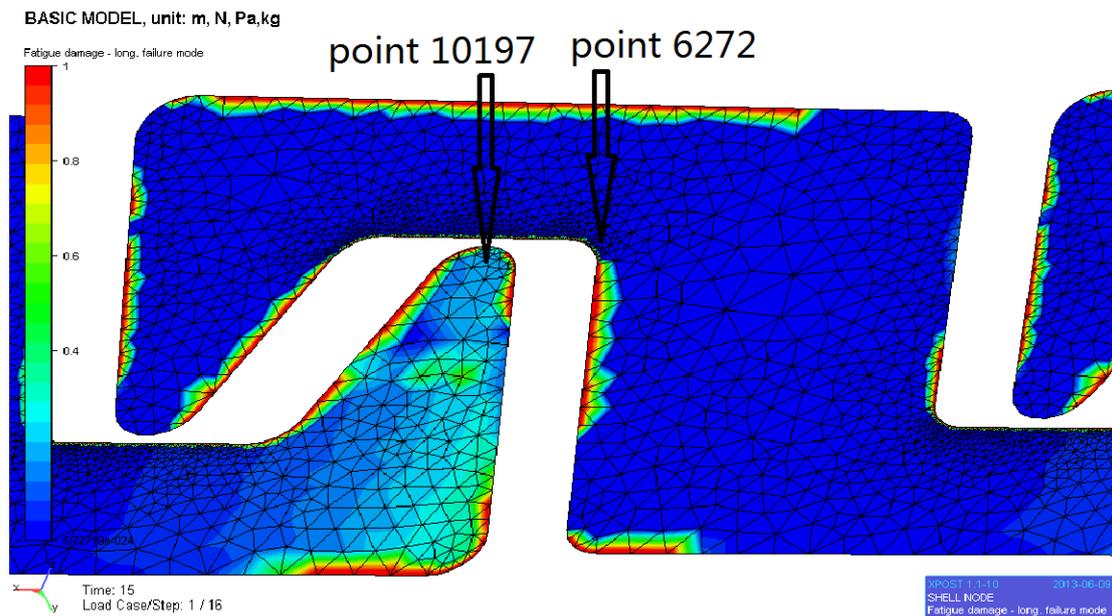
Figure 5-5 the selected critical point in zeta layer

The mean stress correction code 22,21 8,7,6,5,4,3,2,1,0 are the different way to consider the mean stress correcting, which will be used in the fatigue analysis. The meaning of each code could be found in the chapter 1. The fatigue damage for different mean stress correction with linear and nonlinear material are showing in the Appendix 1

Add the fatigue damage for each of the mean stress correcting method, the accumulate fatigue damage with linear and nonlinear material is showing in the **Figure 5-6 Accumulative damage comparison with linear and nonlinear material for point 10197 in zeta spiral** .
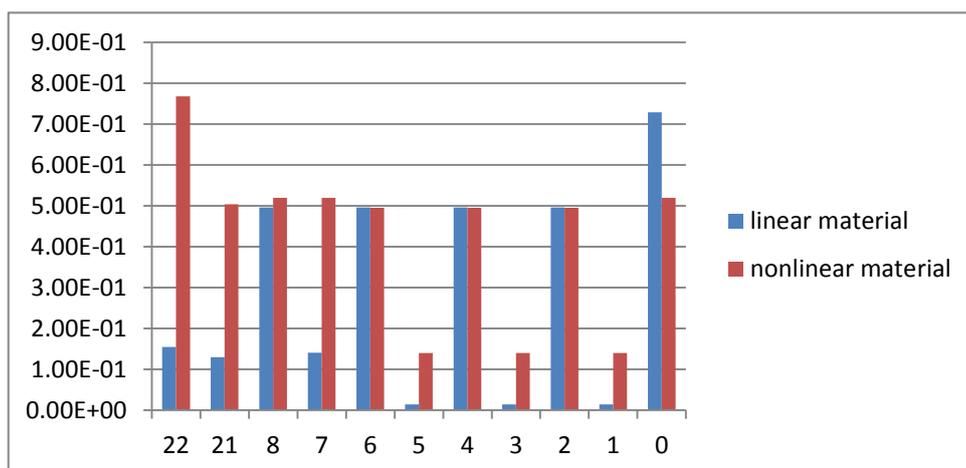
Figure 5-6 Accumulative damage comparison with linear and nonlinear material for point 10197 in zeta spiral

mean stress correction code	22	21	8	7	6	5	4	3	2	1	0
linear material	3.32E-05	6.23E-06	1.61E-04	1.88E-04	1.61E-04	1.88E-04	1.61E-04	1.88E-04	1.61E-04	1.88E-04	2.24E-03
nonlinear material	0.000159	0.000235	0.000173	0.001085	0.000156	0.000182	0.000156	0.000182	0.000156	0.000182	0.001731

Table 5-4 Accumulative damage comparison with linear and nonlinear material for point 10197 in zeta spiral

It could read from the **Table 5-4 Accumulative damage comparison with linear and nonlinear material for point 10197 in zeta spiral** that the linear material has the smaller fatigue damage comparing with the nonlinear material except for code 7, code 8, code 21 and code 22. The code zero has the largest fatigue damage without the mean stress correction. This is due to the material chosen and the different analysis process. The same situation will be found in the point 6272 in the Appendix 1. The mean stress is becoming much larger without correcting if the stress itself is very large. This is the reason that large mean stress may cause large damage.
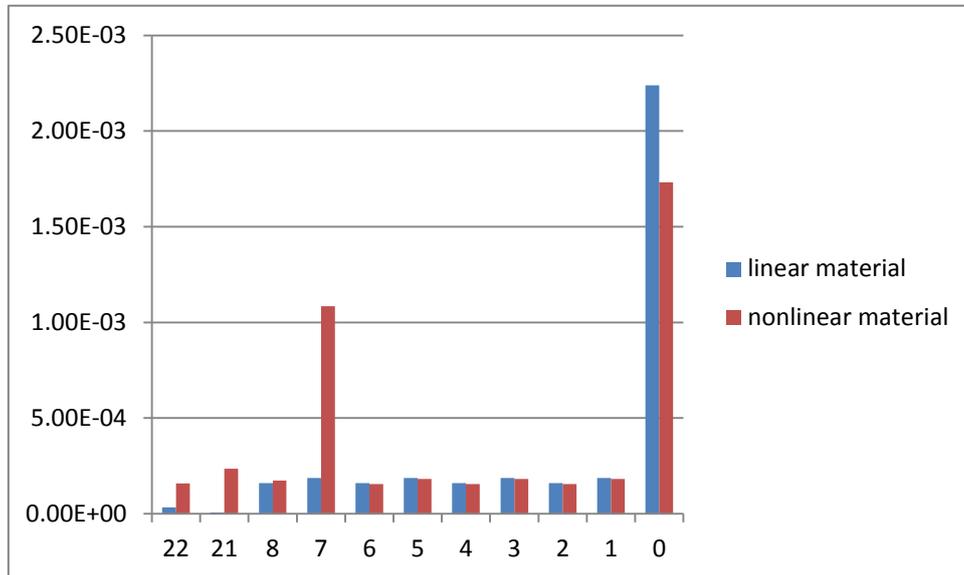
Figure 5-7 Accumulative damage comparison with linear and nonlinear material for point 6272 in zeta spiral

mean stress correction code	22	21	8	7	6	5	4	3	2	1	0
linear material	3.32E-05	6.23E-06	1.61E-04	1.88E-04	1.61E-04	1.88E-04	1.61E-04	1.88E-04	1.61E-04	1.88E-04	2.24E-03
nonlinear material	1.59E-04	2.35E-04	1.73E-04	1.09E-03	1.56E-04	1.82E-04	1.56E-04	1.82E-04	1.56E-04	1.82E-04	1.73E-03

Table 5-5 Accumulative damage comparison with linear and nonlinear material for point 6272 in zeta spiral

The result from point 6272 is showing in the **Table 5-5**. By comparing the point between number 6272 and number 10197, it seems like the point 10197 has a little bit larger fatigue damage in average.

6 Conclusions

This master thesis aims to find out the critical part of the flexible riser then to do the fatigue analysis. The conclusions should be illustrated by the following sections
- Static analysis
- Dynamic analysis
- Rain flow counting
- Fatigue analysis
- Future work

The process of ensuring the configuration of the riser and finding the critical dangerous point are also included inside.

6.1 Static analysis

The result showing in the Chapter 4 is from the static analysis the riser. Before modeling the whole riser in the RFLEX, the bottom side of the riser should be decided in the seabed correctly to avoid the large bending moment. This is because this thesis aims to do the fatigue analysis. So the displacement changing of the flexible riser should be as small as possible in order to simulate the real situation, which is the flexible riser's daily service process. First of all, stress free configuration should be found. This is not only requirement from the input file for the RFLEX but also the farthest position of the riser's bottom could reach. The aiming of considering the dangerous situation with the current and wave direction from the same direction is to consider the fatigue analysis much more conservative. The distribution of the axial force is almost the same along the flexible riser's length for the bending stiffener with a very large value, say 866 KN. The mainly section which should be focused in along the flexible rise is the bending stiffener. Since normalized bending stiffness is already given, the only difficult part is to find the bending moment for the top of the riser. For one certain angle, the bending moment will change the direction at one certain point in the riser. By calculating the 10 situations with the bottom situation from 250 m to 380 m, the minimum bending moment line could be found finally. This could be found in the Figure 4-2 flexible riser's bottom position in sea bed of x axial. What's more, the bending moment from the dynamic analysis should also be found in principle. The reason for selecting the position 250 m is that the direction will change from negative to positive with the increasing of the current and wave velocity. So the one has the largest negative bending moment at the top of the bending stiffener is selected. Which means, the position is less than 250 m is reasonable. However, another reason is also to be considered by neglecting choosing the position less than 250 m. It is that the bending moment at the end of the bending stiffener is relative small with the value from -40 to 14 KNm according to Table 4-2 axial force along the bending stiffener. Since the normalized bending stiffness in the bottom of the bending stiffener, the large bending moment will happen in this place and it will become sensitive. So it is better to have this number 32 point with the value as small as possible. It should be noticed that from the Figure 4-2 the top side of the bending stiffener is much more sensitive than the bottom side to the flexible riser's bottom position in the sea bed. The distribution of the flexible riser is very important during the operating service process. It could also be deduced that the top angle of the bending stiffener may be sensitive, too. Both the top angle and bottom position should be set at the right position together. Sometimes it is very difficult to see from the shape of the connection between the flexible riser and bending stiffener because very little change angle in the connecting position may cause a very large bending moment as the very large axial force there.

6.2 Dynamic analysis

Dynamic analysis has two functions here. One of them is to find the critical point along the bending stiffener. By considering the larger curvature giving the larger damage, the largest curvature should be found in the bending stiffener. With adding the static curvature, dynamic mean curvature and standard deviation in total, the total damage is found for each of the point along the bending stiffener. Before making the decision, the sea state probability should also be taken into considered. The critical point is node number 8 according to the Table 4-5 total estimate damage for bending stiffener with the value 9.8988E-04 (1/m). For the other point, like point 7 or point 18, it is also considerable large value. But this estimate damage is just used to compare the damage. Much more investigation should be done in the following.

6.3 Rain flow counting

This analysis process has the function to transfer the curvature time series to the blocking range with the combination of both curvature range and mean curvature. There are 38 cases is got from the blocking of the rain flow counting method. In principle, the more cases has been divided, which means to divide the range of the mean curvature and curvature range in more sections, the more accurate result should be found. However, this will increase the analytical time during the fatigue analysis. So the 38 cases, which has the distribution like small values with large cycle number is reasonable. It fits the situation in real.

6.4 Fatigue analysis

Before doing the fatigue analysis, the critical point in the special place should be found in the certain layer. It could be sea from the Figure 5-4 Fatigue damage for the part of flexible riser that only the zeta layer has the large fatigue damage. From the Figure 5-5 the selected critical point in zeta layer, there are many points has the large fatigue damage. By considering the damage from the same material, only the point 10197 and point 6272 are selected to do the fatigue life estimated.
The result is difficult to say because there are 11 methods for two types of the material in two critical points. The conclusion will be found in the by comparing the damage with these two point, the point 10197 has a little bit larger damage value. And the code number 2,4,6,8 have almost the same result. This is because they have the same kind of interpolation of the mean stress correction. However, the point 10197 is locating on the side element, which is much approaching the boundary condition. This is another reason which could cause the large fatigue damage. The point in which element is smaller for the point 10197 than for the point 6272 locates on the critical position. When focus on the same mean stress correction code, the result should be the same. But there is numerical unsteadily happening in some case. For example, the nonlinear material is used in for point 6272 with code 7 and 8.
The result with the Goodman correlation has almost the same fatigue damage with the odd code number like 2,4,6,8. The Gerber has also the same result. The code 21 and 22 has the large difference even for the same kind of material. So it is good to do the mean stress correction with the nonlinear material. If the linear material is used, only the small range of cycle should be used in order to get the reasonable result. As the result showing in the Table 5-4, the Goodman interpolation has the large fatigue damage when calculating the mean stress. If adding the mean stress by three directions simply, namely $\sigma_{xx} + \sigma_{yy} + \sigma_{zz}$, the difference will be much larger, which means this method just considers the value of three direction but don't consider the directions for the stress.
If just taken the point 6272 into consideration, The reason for code=5 is largest is due to the formulation of calculating the mean stress as. $\bar{\sigma} = \frac{1}{2}\left(\sigma_j^{max} + \sigma_j^{min}\right), j = 1,2$. It just considers two

direction of the mean stress. This may collect much more energy to these two directions instead of considering three directions in total. It is just the average value of the max and min stress with the formulation showing. Accordingly, the second largest result's methods are code=7 and code=8, which the mean stress is$\bar{\sigma} = \sqrt{\sigma_{xx}^2 + \sigma_{yy}^2 + \sigma_{zz}^2 - \sigma_{xx}\sigma_{yy} - \sigma_{yy}\sigma_{zz} - \sigma_{zz}\sigma_{xx} + 3\sigma_{xy}^2 + 3\sigma_{yz}^2 + 3\sigma_{xz}^2}$.

If we change this method into the two directions, the formulation should be

$\bar{\sigma} = \sqrt{\sigma_{xx}^2 + \sigma_{yy}^2 - \sigma_{xx}\sigma_{yy} + 3\sigma_{xy}^2}$ based on the Von Mises Stress calculation. The result should be much less than the current one. In addition the damage will decrease in a small scale. What's more, the Goodman interpolation method $\bar{\sigma} = \sigma_{xx} + \sigma_{yy} + \sigma_{zz}$ has the third largest value. But this doesn't take the max or the min value of the stress into consideration. So the small result might be that the most of the values are no more than 50% of the largest one.

For the nonlinear material, it almost the same as the linear material except the code=21 and code= 22. The value is larger than the linear material. This is assumed the fatigue curve given at constant mean stress. If the mean stress is constant, the nonlinear material will have the larger strain with small young's model. So the damage may larger as the result showing.

The code=5,6,7,8 should be almost the same since it considered the pressure armor only. The way of correcting the mean stress should also lead to the same result.

In all, it could be concluded

- The linear material has the larger fatigue damage with the code 0, 1, 2, 3, 4, 5, 6 and nonlinear material has the larger fatigue damage with the code 7,8, 21, 22.
- Different position in the riser may give the different fatigue damage. zeta layer has the large fatigue damage comparing with out layers
- Mean stress correction need to be considered during the fatigue analysis when the nonlinear material is used.

6.5 Future work

If much more investigation should be done in the future, the suggestion is given as the following

- The range and curvature of the tension should be included
- More blocking sea state and rain flow counting result should be investigated
- Much more location along the riser could be found as the critical points
- Different kind of material could be used in the input data, both for linear and nonlinear material
- For the riser's structure, the flat spiral could be included into the riser
- Wind influence on the support vessel should be considered
- Different combination of the direction for wave and current should be input
- Different SN cures could be considered

Most of the work should be done to get a more accurate result and fatigue life.

7 Reference

1 Langhelle, Nina Kristin, Berge Stig, Flexible Risers - Corrosion Fatigue. Floating Production Systems and Flexible Risers,2009, page7-8

2 P. C. Paris, M. P. Gomez and W. E. Anderson. A rational analytic theory of fatigue. The Trend in Engineering (1961). 13, 9-14.

3 SANG TAE KIM, DAMIR TADJIEV AND HYUN TAE YANG, Fatigue Life Prediction under Random Loading Conditions in 7475–T7351 Aluminum Alloy using the RMS Model, Department of Mechanical Engineering Youngman University 214-1 Dae-dong, Gyeongsan, 712-749 South Korea,2005, page9-10.

4 Torgeir Moan, TMR4190 Finite element modeling and analysis of marine structures,2003, page 12.14-12.17

5 DET N ORSKE V ERITAS, FATIGUE DESIGN OF OFFSHORE STEEL STRUCTURES, 2010, page17-18

6 Svein Sævik, BFLEX 2010 Version 3.0.5 User Manual, MARINTEK, page 10-11.

7 Svein Sævik, BFLEX 2010 Version 3.0.5 User Manual, MARINTEK, page 14.

8 Svein Sævik, RFLEX Version 4.0 User Manual, MARINTEK

9 Svein Sævik, RFLEX Version 4.0 Theory Manual, MARINTEK

10 O.M.Faltinsen, sea loads on ships and offshore structures,1990,page 30

11. Svein Sævik, pipedata ,MARINTEK

Appendix

1. Fatigue damage

case number	mean stress correction code										
	22	21	8	7	6	5	4	3	2	1	0
1	1.98 E-02	2.96 E-02	9.25 E-02	5.41 E-02	9.25 E-02	5.41 E-03	9.25 E-02	5.41 E-03	9.25 E-02	5.41 E-03	6.92 E-02
2	1.44 E-02	1.98 E-02	6.49 E-02	2.88 E-02	6.49 E-02	2.88 E-03	6.49 E-02	2.88 E-03	6.49 E-02	2.88 E-03	4.86 E-02
3	8.69 E-03	1.20 E-02	3.91 E-02	1.74 E-02	3.91 E-02	1.74 E-03	3.91 E-02	1.74 E-03	3.91 E-02	1.74 E-03	2.88 E-02
4	2.77 E-25	2.77 E-25	2.77 E-25	2.77 E-26	2.77 E-25	2.77 E-27	2.77 E-25	2.77 E-27	2.77 E-25	2.77 E-27	2.77 E-25
5	4.15 E-03	5.82 E-03	1.88 E-02	8.75 E-03	1.88 E-02	8.75 E-04	1.88 E-02	8.75 E-04	1.88 E-02	8.75 E-04	1.38 E-02
6	1.15 E-25	1.15 E-25	1.15 E-25	4.60 E-10	1.15 E-25	4.60 E-11	1.15 E-25	4.60 E-11	1.15 E-25	4.60 E-11	1.15 E-25
7	1.48 E-03	2.05 E-03	6.66 E-03	2.96 E-03	6.66 E-03	2.96 E-04	6.66 E-03	2.96 E-04	6.66 E-03	2.96 E-04	4.88 E-03
8	7.19 E-09	7.93 E-09	3.53 E-08	2.80 E-08	3.53 E-08	2.80 E-09	3.53 E-08	2.80 E-09	3.53 E-08	2.80 E-09	3.77 E-07
9	1.06 E-01	5.93 E-02	2.71 E-01	2.71 E-02	2.71 E-01	2.71 E-03	2.71 E-01	2.71 E-03	2.71 E-01	2.71 E-03	5.61 E-01
10	2.15 E-26	2.15 E-26	2.15 E-26	2.15 E-27	2.15 E-26	2.15 E-28	2.15 E-26	2.15 E-28	2.15 E-26	2.15 E-28	2.15 E-26
11	5.09 E-10	5.50 E-10	2.50 E-09	2.01 E-09	2.50 E-09	2.01 E-10	2.50 E-09	2.01 E-10	2.50 E-09	2.01 E-10	4.21 E-08
12	3.46 E-04	4.78 E-04	1.56 E-03	6.97 E-04	1.56 E-03	6.97 E-05	1.56 E-03	6.97 E-05	1.56 E-03	6.97 E-05	1.15 E-03
13	1.25 E-26	1.25 E-26	1.25 E-26	1.25 E-27	1.25 E-26	1.25 E-28	1.25 E-26	1.25 E-28	1.25 E-26	1.25 E-28	1.25 E-26
14	1.68 E-04	2.33 E-04	7.57 E-04	3.41 E-04	7.57 E-04	3.41 E-05	7.57 E-04	3.41 E-05	7.57 E-04	3.41 E-05	5.56 E-04
15	6.87 E-27	6.87 E-27	6.87 E-27	3.80 E-11	6.87 E-27	3.80 E-12	6.87 E-27	3.80 E-12	6.87 E-27	3.80 E-12	6.87 E-27
16	5.61 E-27	5.61 E-27	5.61 E-27	5.61 E-28	5.61 E-27	5.61 E-29	5.61 E-27	5.61 E-29	5.61 E-27	5.61 E-29	5.61 E-27
17	1.05 E-04	1.45 E-04	4.72 E-04	2.10 E-04	4.72 E-04	2.10 E-05	4.72 E-04	2.10 E-05	4.72 E-04	2.10 E-05	3.45 E-04
18	3.01 E-27	3.01 E-27	3.01 E-27	3.01 E-28	3.01 E-27	3.01 E-29	3.01 E-27	3.01 E-29	3.01 E-27	3.01 E-29	3.01 E-27
19	2.09 E-27	2.09 E-27	2.09 E-27	2.09 E-28	2.09 E-27	2.09 E-29	2.09 E-27	2.09 E-29	2.09 E-27	2.09 E-29	2.09 E-27
20	1.98 E-27	1.98 E-27	1.98 E-27	1.98 E-28	1.98 E-27	1.98 E-29	1.98 E-27	1.98 E-29	1.98 E-27	1.98 E-29	1.98 E-27
21	1.95 E-27	1.95 E-27	1.95 E-27	1.95 E-28	1.95 E-27	1.95 E-29	1.95 E-27	1.95 E-29	1.95 E-27	1.95 E-29	1.95 E-27

Fatigue damage for different mean stress correction code with linear material for point 10197

22	4.52 E-11	4.95 E-11	2.22 E-10	1.81 E-10	2.22 E-10	1.81 E-11	2.22 E-10	1.81 E-11	2.22 E-10	1.81 E-11	3.60 E-09
23	3.77 E-05	5.15 E-05	1.68 E-04	7.15 E-05	1.68 E-04	7.15 E-06	1.68 E-04	7.15 E-06	1.68 E-04	7.15 E-06	1.23 E-04
24	2.52 E-05	3.49 E-05	1.13 E-04	5.05 E-05	1.13 E-04	5.05 E-06	1.13 E-04	5.05 E-06	1.13 E-04	5.05 E-06	8.30 E-05
25	7.53 E-28	7.53 E-28	7.53 E-28	7.53 E-29	7.53 E-28	7.53 E-30	7.53 E-28	7.53 E-30	7.53 E-28	7.53 E-30	7.53 E-28
26	5.33 E-28	5.33 E-28	5.33 E-28	5.33 E-29	5.33 E-28	5.33 E-30	5.33 E-28	5.33 E-30	5.33 E-28	5.33 E-30	5.33 E-28
27	4.21 E-28	4.21 E-28	4.21 E-28	4.21 E-29	4.21 E-28	4.21 E-30	4.21 E-28	4.21 E-30	4.21 E-28	4.21 E-30	4.21 E-28
28	1.12 E-11	1.22 E-11	5.50 E-11	4.46 E-11	5.50 E-11	4.46 E-12	5.50 E-11	4.46 E-12	5.50 E-11	4.46 E-12	8.86 E-10
29	9.53 E-06	1.31 E-05	4.27 E-05	1.88 E-05	4.27 E-05	1.88 E-06	4.27 E-05	1.88 E-06	4.27 E-05	1.88 E-06	3.20 E-05
30	3.79 E-28	3.79 E-28	3.79 E-28	3.79 E-29	3.79 E-28	3.79 E-30	3.79 E-28	3.79 E-30	3.79 E-28	3.79 E-30	3.79 E-28
31	8.25 E-06	1.14 E-05	3.71 E-05	1.67 E-05	3.71 E-05	1.67 E-06	3.71 E-05	1.67 E-06	3.71 E-05	1.67 E-06	2.77 E-05
32	3.35 E-28	3.35 E-28	3.35 E-28	3.35 E-29	3.35 E-28	3.35 E-30	3.35 E-28	3.35 E-30	3.35 E-28	3.35 E-30	3.35 E-28
33	2.02 E-28	2.02 E-28	2.02 E-28	2.02 E-29	2.02 E-28	2.02 E-30	2.02 E-28	2.02 E-30	2.02 E-28	2.02 E-30	2.02 E-28
34	1.88 E-28	1.88 E-28	1.88 E-28	6.37 E-13	1.88 E-28	6.37 E-14	1.88 E-28	6.37 E-14	1.88 E-28	6.37 E-14	1.88 E-28
35	1.88 E-28	1.88 E-28	1.88 E-28	1.88 E-29	1.88 E-28	1.88 E-30	1.88 E-28	1.88 E-30	1.88 E-28	1.88 E-30	1.88 E-28
36	2.11 E-11	2.32 E-11	1.04 E-10	8.26 E-11	1.04 E-10	8.26 E-12	1.04 E-10	8.26 E-12	1.04 E-10	8.26 E-12	1.24 E-09
37	1.68 E-28	1.68 E-28	1.68 E-28	1.68 E-29	1.68 E-28	1.68 E-30	1.68 E-28	1.68 E-30	1.68 E-28	1.68 E-30	1.68 E-28
38	1.68 E-28	1.68 E-28	1.68 E-28	1.68 E-29	1.68 E-28	1.68 E-30	1.68 E-28	1.68 E-30	1.68 E-28	1.68 E-30	1.68 E-28
sum	1.55 E-01	1.30 E-01	4.96 E-01	1.41 E-01	4.96 E-01	1.41 E-02	4.96 E-01	1.41 E-02	4.96 E-01	1.41 E-02	7.29 E-01

Table 1-1Linear material damage for point 10197 in zeta spiral

Fatigue damage for different mean stress correction code with nonlinear material for point 10197											
case number	mean stress correction code										
	22	21	8	7	6	5	4	3	2	1	0
1	9.62 E-02	1.14 E-01	3.87 E-01	3.87 E-01	9.16 E-02	5.39 E-02	9.16 E-02	5.39 E-02	9.16 E-02	5.39 E-02	3.87 E-01
2	7.06 E-02	7.71 E-02	6.29 E-02	6.29 E-02	6.46 E-02	2.89 E-02	6.46 E-02	2.89 E-02	6.46 E-02	2.89 E-02	6.29 E-02
3	4.25 E-02	4.67 E-02	3.79 E-02	3.79 E-02	3.89 E-02	1.75 E-02	3.89 E-02	1.75 E-02	3.89 E-02	1.75 E-02	3.79 E-02
4	2.77 E-25	2.77 E-26	3.05 E-10	4.18 E-09	2.77 E-25	2.77 E-26	2.77 E-25	2.77 E-26	2.77 E-25	2.77 E-26	3.05 E-10
5	2.02 E-02	2.25 E-02	2.24 E-02	2.24 E-02	1.86 E-02	8.73 E-03	1.86 E-02	8.73 E-03	1.86 E-02	8.73 E-03	2.24 E-02
6	1.15	4.80	3.60	4.24	1.15	4.65	1.15	4.65	1.15	4.65	3.60

	E-25	E-10	E-10	E-09	E-25	E-10	E-25	E-10	E-25	E-10	E-10
7	7.24 E-03	7.96 E-03	6.28 E-03	6.28 E-03	6.62 E-03	2.96 E-03	6.62 E-03	2.96 E-03	6.62 E-03	2.96 E-03	6.28 E-03
8	3.59 E-08	3.15 E-08	7.24 E-08	1.87 E-07	3.59 E-08	2.86 E-08	3.59 E-08	2.86 E-08	3.59 E-08	2.86 E-08	7.24 E-08
9	5.30 E-01	2.34 E-01	4.87 E-07	5.80 E-07	2.74 E-01	2.74 E-02	2.74 E-01	2.74 E-02	2.74 E-01	2.74 E-02	4.87 E-07
10	2.15 E-26	2.15 E-27	4.08 E-15	1.01 E-13	2.15 E-26	2.15 E-27	2.15 E-26	2.15 E-27	2.15 E-26	2.15 E-27	4.08 E-15
11	2.56 E-09	2.21 E-09	1.01 E-09	7.04 E-09	2.56 E-09	2.07 E-09	2.56 E-09	2.07 E-09	2.56 E-09	2.07 E-09	1.01 E-09
12	2.19 E-07	1.96 E-07	1.54 E-03	1.54 E-03	2.19 E-07	1.67 E-07	2.19 E-07	1.67 E-07	2.19 E-07	1.67 E-07	1.54 E-03
13	1.25 E-26	1.25 E-27	6.07 E-12	9.14 E-11	1.25 E-26	1.25 E-27	1.25 E-26	1.25 E-27	1.25 E-26	1.25 E-27	6.07 E-12
14	8.21 E-04	9.05 E-04	7.64 E-04	7.64 E-04	7.53 E-04	3.41 E-04	7.53 E-04	3.41 E-04	7.53 E-04	3.41 E-04	7.64 E-04
15	6.87 E-27	4.05 E-11	1.19 E-11	1.52 E-10	6.87 E-27	3.91 E-11	6.87 E-27	3.91 E-11	6.87 E-27	3.91 E-11	1.19 E-11
16	5.61 E-27	5.61 E-28	2.22 E-15	5.35 E-14	5.61 E-27	5.61 E-28	5.61 E-27	5.61 E-28	5.61 E-27	5.61 E-28	2.22 E-15
17	4.50 E-27	4.50 E-28	4.50 E-04	4.50 E-04	4.50 E-27	4.50 E-28	4.50 E-27	4.50 E-28	4.50 E-27	4.50 E-28	4.50 E-04
18	3.01 E-27	3.01 E-28	1.68 E-12	2.49 E-11	3.01 E-27	3.01 E-28	3.01 E-27	3.01 E-28	3.01 E-27	3.01 E-28	1.68 E-12
19	2.09 E-27	2.09 E-28	5.56 E-14	1.10 E-12	2.09 E-27	2.09 E-28	2.09 E-27	2.09 E-28	2.09 E-27	2.09 E-28	5.56 E-14
20	1.98 E-27	1.98 E-28	6.33 E-15	1.41 E-13	1.98 E-27	1.98 E-28	1.98 E-27	1.98 E-28	1.98 E-27	1.98 E-28	6.33 E-15
21	1.95 E-27	1.95 E-28	2.77 E-13	4.78 E-12	1.95 E-27	1.95 E-28	1.95 E-27	1.95 E-28	1.95 E-27	1.95 E-28	2.77 E-13
22	2.29 E-10	1.99 E-10	3.53 E-10	1.76 E-09	2.28 E-10	1.87 E-10	2.28 E-10	1.87 E-10	2.28 E-10	1.87 E-10	3.53 E-10
23	1.85 E-04	2.00 E-04	1.28 E-04	1.28 E-04	1.67 E-04	7.16 E-05	1.67 E-04	7.16 E-05	1.67 E-04	7.16 E-05	1.28 E-04
24	1.23 E-04	1.36 E-04	1.08 E-04	1.08 E-04	1.13 E-04	5.05 E-05	1.13 E-04	5.05 E-05	1.13 E-04	5.05 E-05	1.08 E-04
25	7.53 E-28	7.53 E-29	3.07 E-15	6.76 E-14	7.53 E-28	7.53 E-29	7.53 E-28	7.53 E-29	7.53 E-28	7.53 E-29	3.07 E-15
26	5.33 E-28	5.33 E-29	7.07 E-14	1.22 E-12	5.33 E-28	5.33 E-29	5.33 E-28	5.33 E-29	5.33 E-28	5.33 E-29	7.07 E-14
27	4.21 E-28	4.21 E-29	8.35 E-15	1.68 E-13	4.21 E-28	4.21 E-29	4.21 E-28	4.21 E-29	4.21 E-28	4.21 E-29	8.35 E-15
28	5.64 E-11	4.90 E-11	5.80 E-11	3.13 E-10	5.63 E-11	4.60 E-11	5.63 E-11	4.60 E-11	5.63 E-11	4.60 E-11	5.80 E-11
29	4.67 E-05	5.08 E-05	3.89 E-05	3.89 E-05	4.26 E-05	1.88 E-05	4.26 E-05	1.88 E-05	4.26 E-05	1.88 E-05	3.89 E-05
30	3.79 E-28	3.79 E-29	4.48 E-15	9.32 E-14	3.79 E-28	3.79 E-29	3.79 E-28	3.79 E-29	3.79 E-28	3.79 E-29	4.48 E-15
31	3.96 E-05	4.34 E-05	3.76 E-05	3.76 E-05	3.63 E-05	1.64 E-05	3.63 E-05	1.64 E-05	3.63 E-05	1.64 E-05	3.76 E-05
32	3.35 E-28	3.35 E-29	1.01 E-16	2.47 E-15	3.35 E-28	3.35 E-29	3.35 E-28	3.35 E-29	3.35 E-28	3.35 E-29	1.01 E-16
33	2.02 E-28	2.02 E-29	8.78 E-16	1.92 E-14	2.02 E-28	2.02 E-29	2.02 E-28	2.02 E-29	2.02 E-28	2.02 E-29	8.78 E-16

34	1.88 E-28	7.05 E-13	2.01 E-13	2.74 E-12	1.88 E-28	6.84 E-13	1.88 E-28	6.84 E-13	1.88 E-28	6.84 E-13	2.01 E-13
35	1.88 E-28	1.88 E-29	8.37 E-14	1.28 E-12	1.88 E-28	1.88 E-29	1.88 E-28	1.88 E-29	1.88 E-28	1.88 E-29	8.37 E-14
36	1.07 E-10	9.37 E-11	1.31 E-10	4.52 E-10	1.07 E-10	8.59 E-11	1.07 E-10	8.59 E-11	1.07 E-10	8.59 E-11	1.31 E-10
37	1.68 E-28	1.68 E-29	1.87 E-15	3.89 E-14	1.68 E-28	1.68 E-29	1.68 E-28	1.68 E-29	1.68 E-28	1.68 E-29	1.87 E-15
38	1.68 E-28	1.68 E-29	1.66 E-15	3.49 E-14	1.68 E-28	1.68 E-29	1.68 E-28	1.68 E-29	1.68 E-28	1.68 E-29	1.66 E-15
sum	7.68 E-01	5.04 E-01	5.20 E-01	5.20 E-01	4.95 E-01	1.40 E-01	4.95 E-01	1.40 E-01	4.95 E-01	1.40 E-01	5.20 E-01

Table 2-2 Nonlinear material damage for point 10197 in zeta spiral

Fatigue damage for different mean stress correction code with linear material for point 6272										
case number	mean stress correction code									
	22	21	8	7	6	5	4	3	2	1	0
1	3.87 E-24	3.87 E-24	1.21 E-07	2.13 E-07	1.21 E-07	2.13 E-07	1.21 E-07	2.13 E-07	1.21 E-07	2.13 E-07	1.04 E-05
2	1.51 E-05	3.08 E-06	7.38 E-05	1.00 E-04	7.38 E-05	1.00 E-04	7.38 E-05	1.00 E-04	7.38 E-05	1.00 E-04	1.34 E-03
3	3.71 E-08	3.79 E-25	1.82 E-07	2.36 E-07	1.82 E-07	2.36 E-07	1.82 E-07	2.36 E-07	1.82 E-07	2.36 E-07	9.72 E-06
4	2.77 E-25	2.77 E-25	2.77 E-25	2.77 E-25	2.77 E-25	2.77 E-25	2.77 E-25	2.77 E-25	2.77 E-25	2.77 E-25	2.77 E-25
5	1.93 E-07	3.46 E-08	9.48 E-07	1.23 E-06	9.48 E-07	1.23 E-06	9.48 E-07	1.23 E-06	9.48 E-07	1.23 E-06	3.32 E-05
6	1.15 E-25	1.15 E-25	1.15 E-25	1.15 E-25	1.15 E-25	1.15 E-25	1.15 E-25	1.15 E-25	1.15 E-25	1.15 E-25	1.15 E-25
7	6.14 E-09	6.28 E-26	3.01 E-08	3.92 E-08	3.01 E-08	3.92 E-08	3.01 E-08	3.92 E-08	3.01 E-08	3.92 E-08	1.61 E-06
8	3.35 E-26	3.35 E-26	3.35 E-26	3.35 E-26	3.35 E-26	3.35 E-26	3.35 E-26	3.35 E-26	3.35 E-26	3.35 E-26	3.35 E-26
9	1.77 E-05	3.09 E-06	8.51 E-05	8.52 E-05	8.51 E-05	8.52 E-05	8.51 E-05	8.52 E-05	8.51 E-05	8.52 E-05	8.30 E-04
10	2.15 E-26	2.15 E-26	2.15 E-26	2.15 E-26	2.15 E-26	2.15 E-26	2.15 E-26	2.15 E-26	2.15 E-26	2.15 E-26	2.15 E-26
11	2.03 E-26	2.03 E-26	2.03 E-26	2.03 E-26	2.03 E-26	2.03 E-26	2.03 E-26	2.03 E-26	2.03 E-26	2.03 E-26	2.03 E-26
12	2.06 E-09	3.57 E-10	1.01 E-08	1.31 E-08	1.01 E-08	1.31 E-08	1.01 E-08	1.31 E-08	1.01 E-08	1.31 E-08	5.08 E-07
13	1.25 E-26	1.25 E-26	1.25 E-26	1.25 E-26	1.25 E-26	1.25 E-26	1.25 E-26	1.25 E-26	1.25 E-26	1.25 E-26	1.25 E-26
14	7.29 E-10	7.65 E-27	3.58 E-09	4.67 E-09	3.58 E-09	4.67 E-09	3.58 E-09	4.67 E-09	3.58 E-09	4.67 E-09	1.92 E-07
15	6.87 E-27	6.87 E-27	6.87 E-27	6.87 E-27	6.87 E-27	6.87 E-27	6.87 E-27	6.87 E-27	6.87 E-27	6.87 E-27	6.87 E-27
16	5.61 E-27	5.61 E-27	5.61 E-27	5.61 E-27	5.61 E-27	5.61 E-27	5.61 E-27	5.61 E-27	5.61 E-27	5.61 E-27	5.61 E-27
17	8.36	1.44	4.10	5.24	4.10	5.24	4.10	5.24	4.10	5.24	1.94

	E-10	E-10	E-09	E-09	E-09	E-09	E-09	E-09	E-09	E-09	E-07
18	3.01 E-27	3.01 E-27	3.01 E-27	3.01 E-27	3.01 E-27	3.01 E-27	3.01 E-27	3.01 E-27	3.01 E-27	3.01 E-27	3.01 E-27
19	2.09 E-27	2.09 E-27	2.09 E-27	2.09 E-27	2.09 E-27	2.09 E-27	2.09 E-27	2.09 E-27	2.09 E-27	2.09 E-27	2.09 E-27
20	1.98 E-27	1.98 E-27	1.98 E-27	1.98 E-27	1.98 E-27	1.98 E-27	1.98 E-27	1.98 E-27	1.98 E-27	1.98 E-27	1.98 E-27
21	1.95 E-27	1.95 E-27	1.95 E-27	1.95 E-27	1.95 E-27	1.95 E-27	1.95 E-27	1.95 E-27	1.95 E-27	1.95 E-27	1.95 E-27
22	1.74 E-27	1.74 E-27	1.74 E-27	1.74 E-27	1.74 E-27	1.74 E-27	1.74 E-27	1.74 E-27	1.74 E-27	1.74 E-27	1.74 E-27
23	1.90 E-07	2.76 E-08	9.22 E-07	8.43 E-07	9.22 E-07	8.43 E-07	9.22 E-07	8.43 E-07	9.22 E-07	8.43 E-07	1.24 E-05
24	1.50 E-10	2.58 E-11	7.34 E-10	9.43 E-10	7.34 E-10	9.43 E-10	7.34 E-10	9.43 E-10	7.34 E-10	9.43 E-10	3.67 E-08
25	7.53 E-28	7.53 E-28	7.53 E-28	7.53 E-28	7.53 E-28	7.53 E-28	7.53 E-28	7.53 E-28	7.53 E-28	7.53 E-28	7.53 E-28
26	5.33 E-28	5.33 E-28	5.33 E-28	5.33 E-28	5.33 E-28	5.33 E-28	5.33 E-28	5.33 E-28	5.33 E-28	5.33 E-28	5.33 E-28
27	4.21 E-28	4.21 E-28	4.21 E-28	4.21 E-28	4.21 E-28	4.21 E-28	4.21 E-28	4.21 E-28	4.21 E-28	4.21 E-28	4.21 E-28
28	3.97 E-28	3.97 E-28	3.97 E-28	3.97 E-28	3.97 E-28	3.97 E-28	3.97 E-28	3.97 E-28	3.97 E-28	3.97 E-28	3.97 E-28
29	5.62 E-09	1.16 E-09	2.75 E-08	3.85 E-08	2.75 E-08	3.85 E-08	2.75 E-08	3.85 E-08	2.75 E-08	3.85 E-08	5.49 E-07
30	3.79 E-28	3.79 E-28	3.79 E-28	3.79 E-28	3.79 E-28	3.79 E-28	3.79 E-28	3.79 E-28	3.79 E-28	3.79 E-28	3.79 E-28
31	4.90 E-10	8.21 E-11	2.40 E-09	2.90 E-09	2.40 E-09	2.90 E-09	2.40 E-09	2.90 E-09	2.40 E-09	2.90 E-09	7.85 E-08
32	3.35 E-28	3.35 E-28	3.35 E-28	3.35 E-28	3.35 E-28	3.35 E-28	3.35 E-28	3.35 E-28	3.35 E-28	3.35 E-28	3.35 E-28
33	2.02 E-28	2.02 E-28	2.02 E-28	2.02 E-28	2.02 E-28	2.02 E-28	2.02 E-28	2.02 E-28	2.02 E-28	2.02 E-28	2.02 E-28
34	1.88 E-28	1.88 E-28	1.88 E-28	1.88 E-28	1.88 E-28	1.88 E-28	1.88 E-28	1.88 E-28	1.88 E-28	1.88 E-28	1.88 E-28
35	1.88 E-28	1.88 E-28	1.88 E-28	1.88 E-28	1.88 E-28	1.88 E-28	1.88 E-28	1.88 E-28	1.88 E-28	1.88 E-28	1.88 E-28
36	1.68 E-28	1.68 E-28	1.68 E-28	1.68 E-28	1.68 E-28	1.68 E-28	1.68 E-28	1.68 E-28	1.68 E-28	1.68 E-28	1.68 E-28
37	1.68 E-28	1.68 E-28	1.68 E-28	1.68 E-28	1.68 E-28	1.68 E-28	1.68 E-28	1.68 E-28	1.68 E-28	1.68 E-28	1.68 E-28
38	1.68 E-28	1.68 E-28	1.68 E-28	1.68 E-28	1.68 E-28	1.68 E-28	1.68 E-28	1.68 E-28	1.68 E-28	1.68 E-28	1.68 E-28
sum	3.32 E-05	6.23 E-06	1.61 E-04	1.88 E-04	1.61 E-04	1.88 E-04	1.61 E-04	1.88 E-04	1.61 E-04	1.88 E-04	2.24 E-03

Table 错误!文档中没有指定样式的文字。-3 Linear material damage for point 6272 in zeta spiral

Fatigue damage for different mean stress correction code with nonlinear material for point 6272											
cas e nu mbe	mean stress correction code										
	22	21	8	7	6	5	4	3	2	1	0

r											
1	9.99 E-08	1.81 E-07	1.45 E-07	1.57 E-06	9.99 E-08	1.75 E-07	9.99 E-08	1.75 E-07	9.99 E-08	1.75 E-07	1.45 E-06
2	7.20 E-05	1.16 E-04	8.82 E-05	6.53 E-04	7.16 E-05	9.71 E-05	7.16 E-05	9.71 E-05	7.16 E-05	9.71 E-05	8.82 E-04
3	1.69 E-07	2.32 E-07	1.75 E-07	1.60 E-06	1.69 E-07	2.20 E-07	1.69 E-07	2.20 E-07	1.69 E-07	2.20 E-07	1.75 E-06
4	2.77 E-25	2.77 E-25	2.77 E-26	2.77 E-26	2.77 E-25	2.77 E-25	2.77 E-25	2.77 E-25	2.77 E-25	2.77 E-25	2.77 E-25
5	9.00 E-07	1.27 E-06	9.60 E-07	8.28 E-06	8.99 E-07	1.17 E-06	8.99 E-07	1.17 E-06	8.99 E-07	1.17 E-06	9.60 E-06
6	1.15 E-25	1.15 E-25	1.15 E-26	1.15 E-26	1.15 E-25	1.15 E-25	1.15 E-25	1.15 E-25	1.15 E-25	1.15 E-25	1.15 E-25
7	2.78 E-08	3.82 E-08	2.87 E-08	2.64 E-07	2.78 E-08	3.61 E-08	2.78 E-08	3.61 E-08	2.78 E-08	3.61 E-08	2.87 E-07
8	3.35 E-26	3.35 E-26	3.35 E-27	5.45 E-10	3.35 E-26	3.35 E-26	3.35 E-26	3.35 E-26	3.35 E-26	3.35 E-26	3.35 E-26
9	8.45 E-05	1.16 E-04	8.28 E-05	4.16 E-04	8.26 E-05	8.28 E-05	8.26 E-05	8.28 E-05	8.26 E-05	8.28 E-05	8.28 E-04
10	2.15 E-26	2.15 E-26	2.15 E-27	2.15 E-27	2.15 E-26	2.15 E-26	2.15 E-26	2.15 E-26	2.15 E-26	2.15 E-26	2.15 E-26
11	2.03 E-26	2.03 E-26	2.03 E-27	5.18 E-11	2.03 E-26	2.03 E-26	2.03 E-26	2.03 E-26	2.03 E-26	2.03 E-26	2.03 E-26
12	1.54 E-26	1.54 E-26	2.12 E-10	2.12 E-09	1.54 E-26	1.54 E-26	1.54 E-26	1.54 E-26	1.54 E-26	1.54 E-26	2.12 E-09
13	1.25 E-26	1.25 E-26	1.25 E-27	1.25 E-27	1.25 E-26	1.25 E-26	1.25 E-26	1.25 E-26	1.25 E-26	1.25 E-26	1.25 E-26
14	3.31 E-09	4.56 E-09	3.43 E-09	3.16 E-08	3.31 E-09	4.32 E-09	3.31 E-09	4.32 E-09	3.31 E-09	4.32 E-09	3.43 E-08
15	6.87 E-27	6.87 E-27	6.87 E-28	6.87 E-28	6.87 E-27	6.87 E-27	6.87 E-27	6.87 E-27	6.87 E-27	6.87 E-27	6.87 E-27
16	5.61 E-27	5.61 E-27	5.61 E-28	5.61 E-28	5.61 E-27	5.61 E-27	5.61 E-27	5.61 E-27	5.61 E-27	5.61 E-27	5.61 E-27
17	4.50 E-27	4.50 E-27	4.50 E-28	4.50 E-28	4.50 E-27	4.50 E-27	4.50 E-27	4.50 E-27	4.50 E-27	4.50 E-27	4.50 E-27
18	3.01 E-27	3.01 E-27	3.01 E-28	3.01 E-28	3.01 E-27	3.01 E-27	3.01 E-27	3.01 E-27	3.01 E-27	3.01 E-27	3.01 E-27
19	2.09 E-27	2.09 E-27	2.09 E-28	2.09 E-28	2.09 E-27	2.09 E-27	2.09 E-27	2.09 E-27	2.09 E-27	2.09 E-27	2.09 E-27
20	1.98 E-27	1.98 E-27	1.98 E-28	1.98 E-28	1.98 E-27	1.98 E-27	1.98 E-27	1.98 E-27	1.98 E-27	1.98 E-27	1.98 E-27
21	1.95 E-27	1.95 E-27	1.95 E-28	1.95 E-28	1.95 E-27	1.95 E-27	1.95 E-27	1.95 E-27	1.95 E-27	1.95 E-27	1.95 E-27
22	1.74 E-27	1.74 E-27	1.74 E-28	1.74 E-28	1.74 E-27	1.74 E-27	1.74 E-27	1.74 E-27	1.74 E-27	1.74 E-27	1.74 E-27
23	9.16 E-07	1.05 E-06	7.65 E-07	4.44 E-06	9.05 E-07	8.27 E-07	9.05 E-07	8.27 E-07	9.05 E-07	8.27 E-07	7.65 E-06
24	6.85 E-10	9.32 E-10	7.00 E-10	6.35 E-09	6.84 E-10	8.78 E-10	6.84 E-10	8.78 E-10	6.84 E-10	8.78 E-10	7.00 E-09
25	7.53 E-28	7.53 E-28	7.53 E-29	7.53 E-29	7.53 E-28	7.53 E-28	7.53 E-28	7.53 E-28	7.53 E-28	7.53 E-28	7.53 E-28
26	5.33 E-28	5.33 E-28	5.33 E-29	5.33 E-29	5.33 E-28	5.33 E-28	5.33 E-28	5.33 E-28	5.33 E-28	5.33 E-28	5.33 E-28
27	4.21 E-28	4.21 E-28	4.21 E-29	4.21 E-29	4.21 E-28	4.21 E-28	4.21 E-28	4.21 E-28	4.21 E-28	4.21 E-28	4.21 E-28

28	3.97 E-28	3.97 E-28	3.97 E-29	9.65 E-13	3.97 E-28	3.97 E-28	3.97 E-28	3.97 E-28	3.97 E-28	3.97 E-28	3.97 E-28
29	2.68 E-08	4.38 E-08	3.36 E-08	2.59 E-07	2.67 E-08	3.74 E-08	2.67 E-08	3.74 E-08	2.67 E-08	3.74 E-08	3.36 E-07
30	3.79 E-28	3.79 E-28	3.79 E-29	3.79 E-29	3.79 E-28	3.79 E-28	3.79 E-28	3.79 E-28	3.79 E-28	3.79 E-28	3.79 E-28
31	2.27 E-09	3.01 E-09	2.25 E-09	1.87 E-08	2.27 E-09	2.74 E-09	2.27 E-09	2.74 E-09	2.27 E-09	2.74 E-09	2.25 E-08
32	3.35 E-28	3.35 E-28	3.35 E-29	3.35 E-29	3.35 E-28	3.35 E-28	3.35 E-28	3.35 E-28	3.35 E-28	3.35 E-28	3.35 E-28
33	2.02 E-28	2.02 E-28	2.02 E-29	2.02 E-29	2.02 E-28	2.02 E-28	2.02 E-28	2.02 E-28	2.02 E-28	2.02 E-28	2.02 E-28
34	1.88 E-28	1.88 E-28	1.88 E-29	1.88 E-29	1.88 E-28	1.88 E-28	1.88 E-28	1.88 E-28	1.88 E-28	1.88 E-28	1.88 E-28
35	1.88 E-28	1.88 E-28	1.88 E-29	1.88 E-29	1.88 E-28	1.88 E-28	1.88 E-28	1.88 E-28	1.88 E-28	1.88 E-28	1.88 E-28
36	1.68 E-28	1.68 E-28	1.68 E-29	1.24 E-12	1.68 E-28	1.68 E-28	1.68 E-28	1.68 E-28	1.68 E-28	1.68 E-28	1.68 E-28
37	1.68 E-28	1.68 E-28	1.68 E-29	1.68 E-29	1.68 E-28	1.68 E-28	1.68 E-28	1.68 E-28	1.68 E-28	1.68 E-28	1.68 E-28
38	1.68 E-28	1.68 E-28	1.68 E-29	1.68 E-29	1.68 E-28	1.68 E-28	1.68 E-28	1.68 E-28	1.68 E-28	1.68 E-28	1.68 E-28
sum	1.59 E-04	2.35 E-04	1.73 E-04	1.09 E-03	1.56 E-04	1.82 E-04	1.56 E-04	1.82 E-04	1.56 E-04	1.82 E-04	1.73 E-03

Table 4-4 Nonlinear material damage for point 6272 in zeta spiral

RFLEX code

1) Inpmod.inp

```
INPMOD IDENTIFICATION TEXT  3.6
'------------------------------------------------------------------
File generated by :DeepC V4.5-05
   Exported from analysis : Analysis1
   DATE : April 18, 2013 - 17:00:55
'------------------------------------------------------------------
        UNIT NAME SPECIFICATION
'------------------------------------------------------------------
'   ut ul um uf grav    gcons
    s  m  Kg N  9.80665 1
'=======================================================================
'      DATA SECTION C
'=======================================================================
'------------------------------------------------------------------
        NEW SINGLE RISER
'------------------------------------------------------------------
    AR   SLEND1
'SINGLE RISER SC
'  21.5 9.5
'SLEND1 SLEND1
'1 zby 51.0 -1.15 21.5 0.0
'------------------------------------------------------------------
        ARBITRARY SYSTEM AR
'------------------------------------------------------------------
'   nsnod nlin nsnfix nves nricon nspr nakc
    2    1    2      1    0     0    0
'~~~~~~~~~~~~~~~~~~~~~~~~~~~~~~~~~~~~~~~~~~~~~~~~~~~~~~~~~~~~~~~~~~~~~~~~~~
'   ibtang zbot ibot3d
    0     -365   0
'~~~~~~~~~~~~~~~~~~~~~~~~~~~~~~~~~~~~~~~~~~~~~~~~~~~~~~~~~~~~~~~~~~~~~~~~~~
'   Line types
'Line1
'   ilinty isnod1 isnod2
    1    1     2
'~~~~~~~~~~~~~~~~~~~~~~~~~~~~~~~~~~~~~~~~~~~~~~~~~~~~~~~~~~~~~~~~~~~~~~~~~~
'   Boundary conditions fixed nodes
'~~~~~~~~~~~~~~~~~~~~~~~~~~~~~~~~~~~~~~~~~~~~~~~~~~~~~~~~~~~~~~~~~~~~~~~~~~
'   isnod vessel_no ix   iy   iz   irx  iry  irz  chcoo    chupro
    1    1      1    1    1    1    1    1    VESSEL    NO
'   x0      y0      z0      x1      y1      z1      rot    dir
    -315.0    0     -365.0    51.0    0    21.5      86.60      0.0
'   isnod vessel_no ix   iy   iz   irx  iry  irz  chcoo    chupro
    2    0      1    1    1    0    0    0    GLOBAL    NO
'   x0      y0      z0      x1      y1       z1      rot    dir
    250      0     -3.65e+002    250    0   -3.65e+002   0      0
'4.312771731e+002 0      -365
'vessel number   idwftr xg yg zg dirx
1 zby 0 0 0 0
'~~~~~~~~~~~~~~~~~~~~~~~~~~~~~~~~~~~~~~~~~~~~~~~~~~~~~~~~~~~~~~~~~~~~~~~~~~
'   Boundary conditions free nodes
'~~~~~~~~~~~~~~~~~~~~~~~~~~~~~~~~~~~~~~~~~~~~~~~~~~~~~~~~~~~~~~~~~~~~~~~~~~
'~~~~~~~~~~~~~~~~~~~~~~~~~~~~~~~~~~~~~~~~~~~~~~~~~~~~~~~~~~~~~~~~~~~~~~~~~~
```

```
'    Linear springs to global fixed system
'~~~~~~~~~~~~~~~~~~~~~~~~~~~~~~~~~~~~~~~~~~~~~~~~~~~~~~~~~~~~~~~~~~~~~~~~~
'-----------------------------------------------------------------
'   Pipe in pipe specification
'-----------------------------------------------------------------
'   Line and segment specification
'-----------------------------------------------------------------
      NEW LINE DATA
'-----------------------------------------------------------------
'   ilinty nseg icnlty ifluty
    1    37   0    37
'   icmpty icn1ty iexwty nelseg slgth     nstrps    nstrpd    slgth0
    32    0    0    1    0.25    3    1    0.25
    33    0    0    1    0.25    3    1    0.25
    34    0    0    1    0.25    3    1    0.25
    35    0    0    1    0.25    3    1    0.25
    36    0    0    1    0.25    3    1    0.25
    2     0    0    1    0.25    3    1    0.25
    3     0    0    1    0.25    3    1    0.25
    4     0    0    1    0.25    3    1    0.25
    5     0    0    1    0.25    3    1    0.25
    6     0    0    1    0.25    3    1    0.25
    7     0    0    1    0.25    3    1    0.25
    8     0    0    1    0.25    3    1    0.25
    9     0    0    1    0.25    3    1    0.25
    10    0    0    1    0.25    3    1    0.25
    11    0    0    1    0.25    3    1    0.25
    13    0    0    1    0.25    3    1    0.25
    14    0    0    1    0.25    3    1    0.25
    15    0    0    1    0.25    3    1    0.25
    16    0    0    1    0.25    3    1    0.25
    17    0    0    1    0.25    3    1    0.25
    18    0    0    1    0.25    3    1    0.25
    19    0    0    1    0.25    3    1    0.25
    20    0    0    1    0.25    3    1    0.25
    21    0    0    1    0.25    3    1    0.25
    22    0    0    1    0.25    3    1    0.25
    24    0    0    1    0.25    3    1    0.25
    25    0    0    1    0.25    3    1    0.25
    26    0    0    1    0.25    3    1    0.25
    27    0    0    1    0.25    3    1    0.25
    28    0    0    1    0.25    3    1    0.25
    29    0    0    1    0.25    3    1    0.25
    30    0    0    1    0.25    3    1    0.25
    1     0    0    44   11      3    1    11
    12    0    0    41   41      3    1    41
    23    0    0    330  330     3    1    330
    31    0    0    150  150     3    1    150
    23    0    0    25   25      3    1    25
'=========================================================================
'     DATA SECTION D
'=========================================================================
'-----------------------------------------------------------------
      NEW COMPONENT CRS1
'-----------------------------------------------------------------
'   Section:  SectAxiSym1
'-----------------------------------------------------------------
'   icmpty temp
```

```
     1    20
'------------------------------------------------------------
'   ams   ae         ai          rgyr  ast wst dst thst r-extcnt r-intcnt
    376.9 1.84745283e-001 4.082813813e-002 0.121 /  /  /  /   0.2425   0.114
'   iea iej igt ipress imf
    1   1   1   0     0
'   ea
    1.37e+009
'   ejy
    596700
'   gt+   gt-
    420100
'------------------------------------------------------------
'    Hydrodynamic force coefficients
'   cqx cqy cax cay clx cly icode d_hydro
    5.e-002 1   1   1   0   0   2
'------------------------------------------------------------
'    Capacity parameters (dummy)
'   tb ycurmx
0
        NEW COMPONENT FLUID
'------------------------------------------------------------
'    Internal fluid:  InternalFluid1
'~~~~~~~~~~~~~~~~~~~~~~~~~~~~~~~~~~~~~~~~~~~~~~~~~~~~~~~~~~~~~~~~~~~~~
'   icmpty
    37
'   rhoi vveli pressi dpress idir
    800  0    0    0    1
'==================================================================
'      DATA SECTION E
'==================================================================
'------------------------------------------------------------------
        ENVIRONMENT IDENTIFICATION
'------------------------------------------------------------------
Environment Condition: RegularCondition1
'------------------------------------------------------------------
'   idenv
    RKFHRT
'------------------------------------------------------------------
        WATERDEPTH AND WAVETYPE
'------------------------------------------------------------------
'   wdepth noirw norw ncusta
    365    1    0    1
'------------------------------------------------------------------
        ENVIRONMENT CONSTANTS
'------------------------------------------------------------------
'   airden watden wakivi
    1.226  1025   1.19e-006
NEW IRREGULAR SEASTATE
1 9 0 0 0
WAVE SPECTRUM WIND
'HS(small)  TP(large)
1.0    6.0
'HSSS
DIRECTION PARAMETERS
0
'------------------------------------------------------------------
'      REGULAR WAVE DATA
```

```
'---------------------------------------------------------------
'   nrwc amplit period wavedir
'   1    5    15    90
'---------------------------------------------------------------
        NEW CURRENT STATE
'---------------------------------------------------------------
'   Current name: CurrentProfile1
'   icusta nculev
    1      6
'   curlev    curdir    curvel
    0         0         0.54
   -4         0         0.43
   -100       0         0.32
   -225       0         0.18
   -265       0         0.11
   -365       0         0
'---------------------------------------------------------------
'===============================================================================
'     DATA SECTION F
'===============================================================================
SUPPORT VESSEL IDENTIFICATION
' Reference data used scaling RAO in roll, pitch and yaw:
' DEPTH= 1000.    GRAV = 9.810
'txmo1, 1 line

'idhftr
zby
'---------------------------------------------------------
 HFTRAN REFERENCE POSITION
'---------------------------------------------------------
' zg
  0.
'---------------------------------------------------------
 HFTRANSFER CONTROL DATA
'---------------------------------------------------------
'ndhftr  nwhftr  isymhf  itypin
    16      58      0       2
'---------------------------------------------------------
 WAVE DIRECTIONS
```

2) Dynmod.inp

```
'===============================================================================
'      DATA SECTION A control information
'===============================================================================
'---------------------------------------------------------------------
        DYNMOD CONTROL INFORMATION  3.6
'---------------------------------------------------------------------
File generated by :DeepC V4.5-05
   Export from: Analysis1, DATE : April 18, 2013 - 17:01:16
 dynamic analysis
'---------------------------------------------------------------------
'   irunco  ianal  idris  idenv  idstat idirr idres
   ANAL   IRREGU   SLEND1   RKFHRT   STA1   IRR1   DYN1
'===============================================================================
'     DATA SECTION D
'===============================================================================
'---------------------------------------------------------------------
```

```
IRREGULAR TIMESERIES PARAMETERS
1 10800.0 0.2
IRREGULAR RESPONSE ANALYSIS
1 10800.0 0.2 NEW NONE NONE 0.0
IRREGULAR WAVE PROCEDURE
1 1 0 NODE 1
'================================================================
'     DATA SECTION F
'================================================================
'----------------------------------------------------------------
      TIME DOMAIN PROCEDURE
'----------------------------------------------------------------
'   itdmet inewil idisst iforst icurst istrst
    2    1    1    1    1    0
'   betin gamma theta a1 a2    a1t a1to a1b a2t a2to a2b
    4    0.5  1.5  0 1.e-003 0   0    0   0   0    0
'   indint indhyd maxhit epshyd  tramp indrel iconre istepr ldamp
    1    1    5    1.e-002 10   0    0    0    0
'----------------------------------------------------------------
       NONLINEAR INTEGRATION PROCEDURE
'----------------------------------------------------------------
'   itfreq isolit maxit daccu   icocod ivarst istat
    1    1    10   1.e-006 1    2    1
       ENVELOPE CURVE SPECIFICATION
'----------------------------------------------------------------
'   ienvd ienvf ienvc tenvs tenve nprend nprenv nprenc ifilmp ifilas
    1    1    1    0    3    1    1    1    3    0
'
'TIME DOMAIN LOADING
'SEGV 1 NOFILE
'1 1 0 5 1
DISPLACEMENT RESPONSE STORAGE
1 6 0
1                1                1
1                16               1
1                32               1
1                33               1
1                34               1
1                35               1
FORCE RESPONSE STORAGE
1 6 0
1                1                1
1                16               1
1                32               1
1                33               1
1                34               1
1                35               1
CURVATURE RESPONSE STORAGE
1 8 0
1                1                1

1                15               ALL
1                16               1

'1               23               ALL
1                24               ALL
'1               25               ALL
1                32               1
```

```
1                  33                  1
1                  34                  1
1                  35                  1
ENVELOPE CURVE SPECIFICATION
1 1 1 0 10800 1 1 1 2
'================================================================
END
'================================================================
```

Stamod.inp

```
'================================================================
'      DATA SECTION A
'================================================================
'----------------------------------------------------------------
         STAMOD CONTROL INFORMATION  3.6
'----------------------------------------------------------------
File generated by :DeepC V4.5-05
    Export from: Analysis1, DATE : April 18, 2013 - 17:00:56
Analysis1 static analysis
'----------------------------------------------------------------
'  irunco idris  ianal iprdat iprcat iprfem ipform iprnor ifilm
      1    SLEND1 1    5     1     1     2     1     2
'----------------------------------------------------------------
         RUN IDENTIFICATION
'----------------------------------------------------------------
    STA1
'----------------------------------------------------------------
         ENVIRONMENT REFERENCE IDENTIFIER
'----------------------------------------------------------------
'  idenv
    RKFHRT
'================================================================
'      DATA SECTION B
'================================================================
'----------------------------------------------------------------
         STATIC CONDITION INPUT
'----------------------------------------------------------------
'  nlcomp icurin curfac lcons isolvr
    0     1     1     1     2
'----------------------------------------------------------------
         COMPUTATIONAL PROCEDURE
'----------------------------------------------------------------
'   ameth
    FEM
'----------------------------------------------------------------
         FEM ANALYSIS PARAMETERS
'----------------------------------------------------------------
'----------------------------------------------------------------
         LOAD GROUP DATA
'----------------------------------------------------------------
'  nstep maxit racu
    20   500  1.e-006
'  lotype
VOLU
SFOR
'----------------------------------------------------------------
         LOAD GROUP DATA
```

```
'-------------------------------------------------------------
'   nstep maxit racu
    200   500   1.e-006
'   lotype
DISP
'-------------------------------------------------------------
        LOAD GROUP DATA
'-------------------------------------------------------------
'   nstep maxit racu
    20   500   1.e-006
'   lotype
FLOA
'-------------------------------------------------------------
        LOAD GROUP DATA
'-------------------------------------------------------------
'   nstep maxit racu
    20   500   1.e-006
'   lotype
CURR
FRIC
'=========================================================================
END
'=========================================================================
```

Outmode.inp

```
'DATA GROUP A
'-------------------------------------------------------------------
        OUTMOD IDENTIFICATION TEXT 3.2
'------------------------------------------------------------------ A1 -
***   FUNCTIONAL TEST  ; TENSIONER     ***
***       dead band 500-1500 N         ***
***   Regular motion Xa = 0.6m T=10 s   ***
'-------------------------------------------------------------------
PRINT
'NEW PLOT FILE
'TIME DOMAIN PARAMETERS
'1 1 1
'PRINT
'DYNCURV TIME SERIES
'1 1 1 10800 2
'1 24 1
'1 15 1
'PRINT
IFNIRR CONTROL INFORMATION
CURVATURE ENVELOPE CURVES
1 1
PLOT
END
```

Run.bat(the batch file for running the program)

```
@echo off
cd /d %~dp0
echo Analysis_inpmod.inp > a.inp
echo Analysis_inpmod.res >> a.inp
echo Analysis_ifninp.sam >> a.inp
inpmod.exe < a.inp
```

```
echo Analysis_stamod.inp > b.inp
echo Analysis_stamod.res >> b.inp
echo Analysis_ifninp.sam >> b.inp
echo Analysis_ifnsys.sam >> b.inp
echo Analysis_ifndmp.sam >> b.inp
echo Analysis_ifnsta.ffi >> b.inp
echo ini-Analysis.sam >> b.inp
stamod.exe < b.inp
echo Analysis_dynmod.inp > c.inp
echo Analysis_dynmod.res >> c.inp
echo Analysis_ifninp.sam >> c.inp
echo Analysis_ifnsys.sam >> c.inp
echo Analysis_ifndmp.sam >> c.inp
echo Analysis_ifnirr.ffi >> c.inp
echo Analysis_ifndyn.ffi >> c.inp
echo Analysis_ifrdyn.raf >> c.inp
echo ini-Analysis.sam >> c.inp
echo pre-Analysis.sam >> c.inp
echo tsf-Analysis.ffi >> c.inp
dynmod.exe < c.inp
echo Analysis_outmod.inp > d.inp
echo Analysis_outmod.res >> d.inp
echo Analysis_ifnsta.ffi >> d.inp
echo Analysis_ifnirr.ffi >> d.inp
echo Analysis_ifndyn.ffi >> d.inp
echo Analysis_ifnfre.ffi >> d.inp
echo Analysis_ifnplo.ffi >> d.inp
outmod.exe < d.inp
```

BFLEX2010

```
HEAD BASIC MODEL, unit: m, N, Pa,kg
HEAD version 3.0.7
#      MAXIT NDIM ISOLVR NPOINT IPRINT CONR    GAC  ISTRES
CONTROL 100  3    2     16     11   1.00E-05 9.81 STRESSFREE
#DYNCONT  1    0.0   0.09  -0.05
#     MODE       FACTOR  RESULT LIST
VISRES  INTEGRATION 1      SIGMA-XX-AX SIGMA-XX
#
#      Time    DT(time step) DTVI DT0   Type   STEPTYPE ITERCO ITCRIT MAXIT MAXDIV CONR
TIMECO   25.0   0.5        1.0 201.0 STATIC  AUTO    NONE   ALL   50   5      1.00E-5
#
#     TYPE      NODE X-COORD Y-COORD Z-COORD
NOCOOR COORDINATES 1   0.00    0.00     0.00
            11   0.10    0.00     0.00
# Element property input:
#   name   type   rad     th   CDr Cdt CMr CMt wd     ws      ODp     ODw     rks
#ELPROP core    pipe    3.28E+00 0.05513  0.8     0.1    1      0.1     1.80E+02 7.08E+01
         3.99E-01 3.99E-01 0.5
#ELPROP GROUP2 pipe    1.63E-01 0.00599  0.8     0.1    1      0.1     4.30E+01 6.28E+00
         3.26E-01 3.26E-01 0.5
#ELPROP GROUP3 pipe    1.71E-01 0.00599  0.8     0.1    1      0.1     4.54E+01 6.58E+00
         3.42E-01 3.42E-01 0.5
#ELPROP GROUP4 pipe    1.79E-01 0.00599  0.8     0.1    1      0.1     4.70E+01 6.89E+00
         3.57E-01 3.57E-01 0.5
```

```
#ELPROP GROUP5  pipe      1.87E-01 0.00599 0.8      0.1       1       0.1       4.93E+01 7.20E+00
          3.73E-01 3.73E-01 0.5
#
#       TYPE      ElementID X    Y     Z
ELORIENT COORDINATES 1        0.00 1.00 0.00
          10       0.00 1.00 0.00
#       TYPE      ElementID X    Y     Z
ELORIENT COORDINATES 101       0.00 1.00 0.00
          110      0.00 1.00 0.00
#       TYPE      Element ID X    Y     Z
ELORIENT COORDINATES 201       0.00 1.00 0.00
          210      0.00 1.00 0.00
#       TYPE      Element ID X    Y     Z
ELORIENT COORDINATES 301       0.00 1.00 0.00
          310      0.00 1.00 0.00
#       TYPE      Element ID X    Y     Z
ELORIENT COORDINATES 401       0.00 1.00 0.00
          410      0.00 1.00 0.00
#
#       Type    NODID DOF
BONCON GLOBAL  1    1
BONCON GLOBAL  1    2
BONCON GLOBAL  1    3
BONCON GLOBAL  1    4
BONCON GLOBAL  1    6
#
BONCON GLOBAL  11   2
BONCON GLOBAL  11   3
BONCON GLOBAL  11   4
BONCON GLOBAL  11   6
#
#  ELGR      ELTY    MATNAME    ELID NOD1 NOD2 NOD3 NOD4
ELCON core     PIPE52 NYEMAT   1   1    2
                     10  10   11
#  ELGR      ELTY    MATNAME    ELID NOD1 NOD2 NOD3 NOD4
ELCON GROUP2    PIPE52 NYEMAT   101  1    2
                     110 10   11
#  ELGR      ELTY    MATNAME    ELID NOD1 NOD2 NOD3 NOD4
ELCON GROUP3    PIPE52 NYEMAT   201  1    2
                     210 10   11
#  ELGR      ELTY    MATNAME    ELID NOD1 NOD2 NOD3 NOD4
ELCON GROUP4    PIPE52 NYEMAT   301  1    2
                     310 10   11
#  ELGR      ELTY    MATNAME    ELID NOD1 NOD2 NOD3 NOD4
ELCON GROUP5    PIPE52 NYEMAT   401  1    2
                     410 10   11
#        NAME     TYPE     IFRIC DISFAC FORFAC GEOFAC ENDFAC ID    TIMEINI ITCODE ELIDNUMBER IELBFL
FIMOD CONTDEN NELGR EL1GRP  EL2GRP   EL3GRP
CROSSECTION NYEMAT FLEXCROSS 1   1000.0  2.0 0.0   0.0   0.2286  1.0   31    19      1     0.0
364.656 5  core  GROUP2  GROUP3  GROUP4  GROUP5
# CTYPE THK     MATNAME    FRIC LAY-ANG  RNUM TEMP MATNAME_NL CCODE    CFATFL AREA     IT INY
IRKS WIDTH
#7.70E-05
CARC   7.00E-03 CARCMAT 0.25      88.868   1       0        none      CARCASS10mm      fdatazeta 0
          0        0        0        0
THER   3.99E-03 THERMAT 0.15      0        0       0        none      NONE    none    0       0
          0        0        0
```

```
THER     1.20E-02 THERMAT 0.15      0         0         0         none       NONE      none      0         0
         0         0         0
THER     1.02E-03 THERMAT 0.15      0         0         0         none       NONE      none      0         0
         0         0         0
ZETA     1.20E-02 ZETAMAT 0.25      89.150    1         0         none       zeta10mm fdatazeta 3.22E-04  0
         0         0         0
#SPIR    5.99E-03 ZETAMAT 0.25   88.868 1 0 none  spiral10mm fdata  9.60E-05  0  0  0  0
THER     1.52E-03 THERMAT 0.15      0         0         0         none       NONE      none      0         0
         0         0         0
TENS     5.99E-03 TENSMAT 0.25      44        54        0         none       TENSILE10mm         fdata
         6.57E-05 0         0         0         0
THER     4.10E-04 THERMAT 0.15      0         0         0         none       NONE      none      0         0
         0         0         0
THER     1.52E-03 THERMAT 0.15      0         0         0         none       NONE      none      0         0
         0         0         0
TENS     5.99E-03 TENSMAT 0.25      -44       57        0         none       TENSILE10mm         fdata
         6.61E-05 0         0         0         0
THER     4.10E-04 THERMAT 0.15      0         0         0         none       NONE      none      0         0
         0         0         0
THER     1.52E-03 THERMAT 0.15      0         0         0         none       NONE      none      0         0
         0         0         0
TENS     5.99E-03 TENSMAT 0.25      42        61        0         none       TENSILE10mm         fdata
         6.53E-05 0         0         0         0
THER     4.10E-04 THERMAT 0.15      0         0         0         none       NONE      none      0         0
         0         0         0
THER     1.52E-03 THERMAT 0.15      0         0         0         none       NONE      none      0         0
         0         0         0
TENS     5.99E-03 TENSMAT 0.25      -42       64        0         none       TENSILE10mm         fdata
         6.55E-05 0         0         0         0
THER     4.10E-04 THERMAT 0.15      0         0         0         none       NONE      none      0         0
         0         0         0
THER     4.10E-04 THERMAT 0.15      0         0         0         none       NONE      none      0         0
         0         0         0
THER     1.20E-02 THERMAT 0.15      0         0         0         none       NONE      none      0         0
         0         0         0
#
#       NAME        Type  Y0 Z0 CCURV P1        P2      P3     P4 NINTER ICODE
CROSSGEOM TENS-TENSILE10mm   BFLEX 0  0  S    5.9900E-3   0.0000  0.0000  0.0000    10      0
                              S   12.0000E-3  90.0000  0.0000  0.0000    10      1
                              S    5.9900E-3 180.0000  0.0000  0.0000    10      0
                              S   12.0000E-3 270.0000  0.0000  0.0000    10      1
#
CROSSGEOM SPIR-spiral10mm   BFLEX  0  0
                              S     5.9900E-3  90.0000  0.0000  0.0000    10      0
                              S    15.0000E-3 180.0000  0.0000  0.0000    10      2
                              S     5.9900E-3 270.0000  0.0000  0.0000    10      0
                              S    15.0000E-3   0.0000  0.0000  0.0000    10      1
CROSSGEOM ZETA-zeta10mm BFLEX 0  0  CI    90.0000    197.0000 0.6213E-3  0.0000    7       0
                              S    5.1316E-3 107.0000  0.0000    0.0000   18      0
                             CI    197.0000    343.0000 0.6213E-3  0.0000   15      2
                              S    2.9400E-3 253.0000  0.0000    0.0000    8      0
                             CO    163.0000     90.0000 0.6213E-3  0.0000    4      0
                              S    2.6717E-3 180.0000  0.0000    0.0000   45      3
                             CO     90.0000     17.0000 0.6213E-3  0.0000   15      0
                              S    5.2118E-3 107.0000  0.0000    0.0000   24      0
                             CI    197.0000    270.0000 0.6213E-3  0.0000    4      0
                              S   10.7874E-3 180.0000  0.0000    0.0000   30      1
                             CI    270.0000     17.0000 0.6213E-3  0.0000    7      0
```

```
                            S     5.1316E-3  287.0000  0.0000     0.0000   23    0
                            CI   17.0000    163.0000  0.6213E-3  0.0000    7    2
                            S     2.9400E-3   73.0000  0.0000     0.0000    8    0
                            CO  343.0000    270.0000  0.6213E-3  0.0000   15    0
                            S     2.6717E-3    0.0000  0.0000     0.0000   45    3
                            CO  270.0000    197.0000  0.6213E-3  0.0000   15    0
                            S     5.2118E-3  287.0000  0.0000     0.0000   15    0
                            CI   17.0000     90.0000  0.6213E-3  0.0000    4    0
                            S    10.7874E-3    0.0000  0.0000     0.0000   20    1
                          # CI   90.0000    197.0000  0.6213E-3  0.0000    7    0
                          # S     5.1956E-3  107.0000  0.0000     0.0000   23    0
                          #CI   197.0000    343.0000  0.6213E-3  0.0000    7    2
                          # S     1.8940E-3  253.0000  0.0000     0.0000    8    0
                          #CO  163.0000     90.0000  0.6213E-3  0.0000    4    0
                          # S     4.1717E-3  180.0000  0.0000     0.0000   12    3
                          #CO   90.0000     17.0000  0.6213E-3  0.0000    4    0
                          # S     6.6218E-3  107.0000  0.0000     0.0000   24    0
                          #CI   197.0000    270.0000  0.6213E-3  0.0000    4    0
                          # S    12.2874E-3  180.0000  0.0000     0.0000   49    1
                          #CI   270.0000     17.0000  0.6213E-3  0.0000    7    0
                          # S     5.1956E-3  287.0000  0.0000     0.0000   23    0
                          #CI   17.0000    163.0000  0.6213E-3  0.0000    7    2
                          # S     1.8940E-3   73.0000  0.0000     0.0000    8    0
                          #CO  343.0000    270.0000  0.6213E-3  0.0000    4    0
                          # S     4.1717E-3    0.0000  0.0000     0.0000   14    3
                          #CO  270.0000    197.0000  0.6213E-3  0.0000    4    0
                          # S     6.6218E-3  287.0000  0.0000     0.0000   24    0
                          #CI   17.0000     90.0000  0.6213E-3  0.0000    4    0
                          # S    12.2874E-3    0.0000  0.0000     0.0000   49    1
CROSSGEOM  CARC-CARCASS10mm  BFLEX  0  0  S   10.0000E-3    0.0000  0.0000  1.4000E-3   10    2
                            S     5.0000E-3   90.0000  0.0000  1.4000E-3   10    0
                            S    27.5000E-3  180.0000  0.0000  1.4000E-3   10    0
                            S     7.0000E-3  270.0000  0.0000  1.4000E-3   10    0
                            S    27.5000E-3  180.0000  0.0000  1.4000E-3   10    0
                            S     5.0000E-3   90.0000  0.0000  1.4000E-3   10    0
                            S    10.0000E-3    0.0000  0.0000  1.4000E-3   10    2
#
#exper pressure 0 AND dry mass
PELOAD 100    200
#inner pressure 7000pi 48.2633011MPA
#     HIST ELNR1  P1    ELNR2 P2
PILOAD 300  1    12.6E+06  10   12.6E+06
#
#Mean Tensile loads 1MN
# TYPE HIST NO.  DIR NODE  VALUE [N]
CLOAD 400    1   11   859.3E+03
#cyclling stress range for 12 loads simultaneously
#CLOAD  100    1   11   0.0230
#
#displacement restrain for movement on y axi
# P   DISP/CONEQ GLOBAL   NODE DOF VALUE  HIST
CONSTR PDISP     GLOBAL    1    5  6.26E-09  500
CONSTR PDISP     GLOBAL   11    5 -6.26E-09  600
#  mean             +        -        cycle number
#      1       6.26E-09  6.2     -4.2     3872046
#      2       6.26E-09  16.5   -14.5     628891
#      3       4.17E-08  1.8      0.2     379178
#      4       4.17E-08  3.3     -1.3     276920
```

#	5	-2.92E-08	-0.1	2.1	223829
#	6	4.17E-08	4.9	-2.9	114661
#	7	7.71E-08	1.4	0.6	62817
#	8	7.71E-08	3.1	-1.1	33529
#	9	6.26E-09	26.8	-24.8	23116
#	10	7.71E-08	3.9	-1.9	21535
#	11	7.71E-08	2.3	-0.3	20343
#	12	1.13E-07	1.3	0.7	15359
#	13	4.17E-08	6.4	-4.4	12548
#	14	-6.46E-08	0.5	1.5	7645
#	15	1.13E-07	3.0	-1.0	6869
#	16	7.71E-08	4.8	-2.8	5607
#	17	1.48E-07	1.2	0.8	4499
#	18	1.13E-07	3.6	-1.6	3013
#	19	7.71E-08	5.6	-3.6	2091
#	20	1.48E-07	3.0	-1.0	1981
#	21	1.13E-07	4.2	-2.2	1947
#	22	1.13E-07	2.4	-0.4	1742
#	23	1.83E-07	1.2	0.8	1280
#	24	-1.00E-07	0.7	1.3	1078
#	25	1.13E-07	4.7	-2.7	753
#	26	1.48E-07	3.4	-1.4	533
#	27	1.48E-07	2.5	-0.5	421
#	28	1.13E-07	1.9	0.1	397
#	29	6.26E-09	37.1	-35.1	389
#	30	4.17E-08	8.0	-6.0	379
#	31	2.19E-07	1.1	0.9	376
#	32	7.71E-08	7.3	-5.3	335
#	33	1.48E-07	3.8	-1.8	202
#	34	1.83E-07	2.2	-0.2	188
#	35	1.83E-07	2.9	-0.9	188
#	36	1.48E-07	1.7	0.3	168
#	37	7.71E-08	6.4	-4.4	168
#	38	1.13E-07	5.9	-3.9	168
#	39	2.54E-07	1.1	0.9	31
#	40	4.17E-08	9.5	-7.5	31
#	41	4.17E-08	11.1	-9.1	31
#	42	2.19E-07	2.9	-0.9	31
#	43	1.83E-07	3.6	-1.6	31
#	44	7.71E-08	8.1	-6.1	31
#	45	6.26E-09	57.7	-55.7	21
#	46	1.83E-07	3.3	-1.3	21
#	47	1.48E-07	4.7	-2.7	21
#	48	1.83E-07	4.0	-2.0	21
#	49	1.83E-07	5.0	-3.0	21
#	50	2.90E-07	1.1	0.9	10
#	51	-2.92E-08	-2.3	4.3	10
#	52	1.83E-07	1.5	0.5	10
#	53	2.19E-07	1.4	0.6	10
#	54	1.48E-07	2.1	-0.1	10
#	55	1.83E-07	2.6	-0.6	10
#	56	-2.92E-08	-11.2	13.2	10
#	57	2.90E-07	2.2	-0.2	10
#	58	1.48E-07	4.3	-2.3	10
#	59	2.19E-07	3.2	-1.2	10
#	60	2.54E-07	2.9	-0.9	10
#	61	2.19E-07	3.5	-1.5	10
#	62	2.54E-07	3.2	-1.2	10

```
#        63          1.83E-07  4.3      -2.3      10
#        64          2.54E-07  3.4      -1.4      10
#        65          1.13E-07  7.0      -5.0      10
#        66          1.48E-07  6.0      -4.0      10
#    HIST NO.  time      factor [-]
#    HIST NO.  LOAD time  VALUE [-]exper presure
THIST  100     0       0
              25      0
#    HIST NO.  LOAD time  VALUE [-]dry mass
THIST  200     0       1
              3       1
              5       1
              25      1
#
#    HIST NO.  LOAD time  VALUE [-]inner pressure
THIST  300     0       1
              5       1
              7       1
              13      1
              15      1
              25      1
#
#    HIST NO.  LOAD time  VALUE [-]mean tensile
THIST  400     0       0
              8       0
              9       1
              25      1
#    HIST NO.  LOAD time  VALUE [-]movement1
THIST  500     0       0
              10      0
              11      1
              12      1
              14.75   6.2
              20.25   -4.2
              23      1
              25      0
#    HIST NO.  time      factor [-]movement2
THIST  600     0       0
              10      0
              11      1
              12      1
              14.75   6.2
              20.25   -4.2
              23      1
              25      0
#      MNAME       TYPE    POISS DENSITY  TALFA TECOND HEATC EM       GM       ETRA
MATERIAL  CARCMAT     ELASTIC 0.30  7.70E+03 0.00  0.00   0.00   210.00E+09 80.00E+09 210.00E+09
MATERIAL  ZETAMAT     ELASTIC 0.30  7.86E+03 0.00  0.00   0.00   210.00E+09 80.00E+09 210.00E+09
MATERIAL  TENSMAT     ELASTIC 0.30  7.86E+03 0.00  0.00   0.00   210.00E+09 80.00E+09 210.00E+09
MATERIAL  THERMAT     ELASTIC 0.4203 1.80E+03 0.00  0.00   0.00   370.24E+06 80.00E+06 370.24E+06
#
MATERIAL nonlinear elastoplastic  1.0  0.3  7850.0  1.17e-5  50  800
#
# eps sigma ..1,n
0 0
3.000E-03 545.0E+06
5.000E-03 720.0E+06
8.000E-03 800.0E+06
```

a) BPOST

#BFPOSTfor BFlex POSTpro cessing
bfpost l01 1 10 1
bfpost l02 1 10 1
bfpost l03 1 10 1
bfpost l04 1 10 1
bfpost l05 1 10 1
bfpost l06 1 10 1
bfpost l07 1 10 1
bfpost l08 1 10 1
bfpost l09 1 10 1
bfpost l10 1 10 1
bfpost l11 1 10 1
bfpost l12 1 10 1
bfpost l13 1 10 1
bfpost l14 1 10 1
bfpost l15 1 10 1
bfpost l16 1 10 1
bfpost l17 1 10 1
bfpost l18 1 10 1
bfpost l19 1 10 1
bfpost l20 1 10 1
bfpost l21 1 10 1
bfpost l22 1 10 1
bfpost l23 1 10 1
bfpost l24 1 10 1
bfpost l25 1 10 1
bfpost l26 1 10 1
bfpost l27 1 10 1
bfpost l28 1 10 1
bfpost l29 1 10 1
bfpost l30 1 10 1
bfpost l31 1 10 1
bfpost l32 1 10 1
bfpost l33 1 10 1
bfpost l34 1 10 1
bfpost l35 1 10 1
bfpost l36 1 10 1
bfpost l37 1 10 1
bfpost l38 1 10 1

Rain flow counting in MATLAB

```
clear all;
clc
x  = load('test.txt');
tp = dat2tp(x,0,'Mw');
% figure (1)
% plot(x(:,1),x(:,2),tp(:,1),tp(:,2),'ro')
RFC=tp2rfc(tp);
range=RFC(:,2)-RFC(:,1);
minimum_r=min(range);
maximum_r=max(range);
N=10;%user define
range1=linspace(minimum_r,maximum_r,N);
for i=1:N-1
    meanrange1(i)=(range1(i)+range1(i+1))/2;
    numb(i)=max(size(find(range>range1(i)&range<range1(i+1))));
end
output=[meanrange1;numb]';
nn=max(size(output));
fid=fopen('output1.txt','w')
% fprintf(fid,'%10s %10s %10s\n',['meanrange','number','range'])
for j=1:nn
    fprintf(fid,'%4d %4d %4d\n',[output(j,1),output(j,2),range1(j)])
end
fprintf(fid,'%4d %4d %4d\n',[0.1,0.1,range1(nn+1)])
```